5-2014

Natural And Exogenous Genome Editing In Wiskott-Aldrich Syndrome Patient Cells

Tamara J. Laskowski

NATURAL AND EXOGENOUS GENOME EDITING IN WISKOTT-ALDRICH SYNDROME PATIENT CELLS

by

Tamara Jatoba Laskowski, B.S.

APPROVED:

_____
Brian R. Davis, Ph.D. - Supervisory Professor

_____
Phillip Carpenter, Ph.D.

_____
Gibert Cote, Ph.D.

_____
Laurence J.N. Cooper, M.D., Ph.D.

_____
Patrick Zweidler-McKay, M.D., Ph.D.

APPROVED:

_____
Dean, The University of Texas
Graduate School of Biomedical Sciences at Houston

NATURAL AND EXOGENOUS GENOME EDITING IN WISKOTT-ALDRICH SYNDROME PATIENT CELLS

A

DISSERTATION

Presented to the Faculty of
The University of Texas
Health Science Center at Houston
and
The University of Texas
MD Anderson Cancer Center
Graduate School of Biomedical Sciences
in Partial Fulfillment

of the Requirements

for the Degree of

DOCTOR OF PHILOSOPHY

by

Tamara Jatoba Laskowski, B.S.

Houston, Texas

May 2014

May 2014

DEDICATION

I would like to dedicate this work to my family. Their unconditional love and support and the many sacrifices they had to make made all the difference to me. I would like to especially dedicate this to my husband who has always believed in me, and has encouraged me to face and conquer any challenge. Lastly, I would like to dedicate this to my 18-month old son, who has an amazing power to make every difficult work day be easily forgotten when I walk through the front door and am greeted by his sweet smile and loving embrace.

ACKNOWLEDGEMENTS

I would like to begin by thanking my advisor, Dr. Brian Davis, for giving me an opportunity to work in his laboratory, for providing me with the resources necessary to excel in the completion of my PhD work, and for guiding and training me to be a successful scientist. I am grateful for the opportunities I was afforded during my work in the PhD Program to interact and collaborate with many scientists locally and internationally. These experiences not only contributed to enhance my knowledge and skill, but also taught me how to be an independent scientist.

I am fortunate to have had wonderful guidance and support from the faculty and staff of MD Anderson Cancer Center and University of Texas Health Science Center at Houston. I would like to thank the current and former faculty members of my advisory committee, who, through their support and commitment to education, taught me how to think as a scientist, and, most importantly, inspired me to apply all I have learned to the various obstacles and challenges that came up during the course of these six years. These are lessons that I will value throughout my career.

I am a member of the Human and Molecular Genetics Program at GSBS, and I would like to thank my fellow program students, as well as the program directors – Dr. Subrata Sen and Dr. Ann Killary – and the program manager, Mr. Bert Shaw for their continued support and friendship. HMG has served as a community of friends and colleagues who have helped me grow personally and professionally. I am very

fortunate to be associated with this wonderful group, and have made connections which I am certain will last a lifetime.

I would like to also acknowledge my fellow co-workers at the Center for Stem Cell and Regenerative Medicine and the Davis lab for their friendship and support throughout the six years I spent as a student in this department. I would like to specially highlight Wei Liao, Pooja Gandhi, Ana Crane, Amy Hazen, Shirley Li, and Qing Yan with whom I worked closely, and who, not only contributed to the work reported in this dissertation, but taught me new skills through the sharing of their knowledge and experience. On a personal note, I would like to also thank Colby Suire, Nathalie Brouard, Alexes Daquinag, Chieh Tseng, Yan Zhang, Philipp Kramer, Jacky Bui, Olga Sirin, and Mae Mao for the friendship and support, and for the many conversations we had, in which we exchanged knowledge and ideas about our work. A huge thank-you also to Isabel Alvarado, Veronica Quiceno, Stephanie Baca and Trina Bosley, our former and current administrative team, who work behind the scenes to ensure all of our needs are met, so we can focus on our work and the science.

Great science is never done in a vacuum; instead it is done with the help of many great professionals. I was fortunate to have wonderful collaborators who contributed their knowledge and resources so that I could successfully complete the projects described in this dissertation. I greatly appreciate Dr. Michael Holmes and Sangamo Biosciences for their generous gift to us, providing the Zinc-Finger nucleases used in the gene correction project. Dr. Dan Kaufman and his team from the University of Minnesota, especially David Knorr, Zhenya Ni, and Chao Ma who

so kindly provided to us their protocols for *in vitro* NK differentiation, and helped us establish this technology in our laboratory. Dr. Bart Vandekerkhove and Yasmine Van Caeneghen from Ghent University in Belgium have been instrumental to the *in vitro* generation of T-cells from our corrected iPSC, and I would like to thank them for their invaluable contributions to our work.

Finally, I would like to thank the people who most supported me over the past six years: My family, especially my dear husband Eric Laskowski, whose belief in me has served as a strong motivating force, encouraging me to face and conquer the challenges I encountered along the way. The unconditional love of my family and their support during the difficult times (and in the life of a PhD student, there sure are many difficult times!) were vital to my success in completing this work. Words are not enough to thank my parents, grandparents, brother, sister, and mother and father-in law who encouraged me through their words, prayers, and endless support all these years.

Above all, I thank God who gave me life, knowledge, and wisdom so that, through hard work and perseverance, I could accomplish this goal.

NATURAL AND EXOGENOUS GENOME EDITING IN WISKOTT-ALDRICH SYNDROME PATIENT CELLS

Tamara Jatoba Laskowski, B.S.

Advisory Professor: Brian R. Davis, Ph.D.

Wiskott-Aldrich syndrome (WAS) is an X-linked primary immunodeficiency disease characterized by thrombocytopenia, recurrent infections and increased autoimmunity. This disease is caused by mutations in the WAS gene (*WAS*) which encodes for the WAS protein (WASp), exclusively expressed in hematopoietic cells and required for proper platelet production and lymphoid cell function. Approximately 11% of patients with WAS exhibit a phenomenon called Somatic Revertant Mosaicism which is characterized by the presence of lymphocytes which naturally revert back to normal phenotype by restoring WASp expression. To date, the mechanisms of this naturally-occurring gene therapy remains poorly understood, and the full extent of the repertoire of revertant genotypes has not yet been elucidated. The remaining 89% of WAS patients require treatment early in life, or the disease leads to premature death. At present, cure for WAS can only be attained through allogeneic stem cell transplantation or lentiviral hematopoietic stem cell gene therapy.

In this work, we focused on both groups of WAS patients. In order to gain insight into the extent of the revertant repertoire in WAS revertant patients, we used next generation sequencing technology to analyze DNA from $WASp^+$ T-cells isolated from two revertant patients carrying the same germline mutation. We

identified over a hundred different revertant genotypes. In this report we describe those which directly reverted the original germline mutation, as well as those which are believed to provide a compensatory effect by inducing alternative splicing. Our findings represent, to our knowledge, the first report of ultra-deep analysis of somatic reversions in WAS patients.

In our study of non-revertant WAS patients, we investigated restoration of T- and NK-cell functionality following an *in vitro* virus-free zinc-finger nuclease (ZFN)-mediated genome editing strategy for correction of *WAS* mutations. We generated induced pluripotent stem cells (iPSC) from skin fibroblasts of a WAS patient carrying an insertional frame-shift mutation. Subsequently, a WAS-2A-eGFP transgene was targeted at the endogenous chromosomal location by homology-directed repair using ZFN, thereby correcting the gene defect and creating a GFP reporter for WASp expression. Hematopoietic progenitor cells were generated from WAS iPSC and gene-corrected iPSC (cWAS) *in vitro* via spin embryoid bodies. Human embryonic stem cell lines WA01 and WA09 were used as control. GFP expression was pronounced in all CD43+ hematopoietic lineages including myeloid, monocytic, lymphoid, erythroid and megakaryocytic lineages. Hematopoietic precursors were further cultured on OP9-DL1 to generate NK cells. NK cells were readily obtained from cWAS and WA01/WA09 progenitors, but to a far more limited extent from WAS progenitors. WAS-derived NK cells were unable to generate interferon-γ or tumor necrosis factor-α upon stimulation with K562. Cytokine production was restored in cWAS-derived NK cells.

Taken together these results indicate that targeted endogenous integration of

the WAS gene in WAS-iPSC results in restoration of the lymphoid defect observed in WAS-iPSC. Transplantation of gene-corrected iPSC-derived hematopoietic precursors may offer an alternative to lentiviral gene therapy which carries an inherent risk for insertional oncogenesis.

Table of Contents

List of Figures

List of Tables

CHAPTER 1: BACKGROUND AND INTRODUCTION

1.1 Wiskott-Aldrich Syndrome (WAS)

Wiskott-Aldrich Syndrome (WAS) is a monogenic X-linked primary immunodeficiency (PID) disorder characterized by microthrombocytopenia, severe eczma, recurrent infections, autoimmunity, and malignancies [1]. WAS was first described in 1937 by Alfred Wiskott though his evaluation of three brothers who presented with bloody diarrhea, eczema, microthrombocytopenia, episodes of fever, and recurrent ear infections. Because their sisters were not affected, Dr. Wiskott proposed the boys were afflicted with a novel hereditary thrombocytopenia [2]. In 1954, Robert Aldrich reported similar clinical findings in sixteen out of forty males, but not in any females, from a single family he studied over six generations. Through this study, he demonstrated the X-linked mode of inheritance of this disease [2, 3]. The disease was then named Wiskott-Aldrich Syndrome (WAS), after the two physicians who first described it.

The gene implicated in Wiskott-Aldrich Syndrome was identified much later, in 1994, through the work of Jonathan Derry, Hans Ochs, and Uta Francke [4]. Linkage analysis studies led to localization of the *WAS* gene at a region in Xp11.22-p11.23. Through the use of positional cloning strategies followed by evaluation of potential cDNA candidates, they were able to identify a sequence whose expression was detected only in cells of lymphocytic and megakaryocytic lineages, and was affected in patients diagnosed with WAS. Led by the identification of DNA

mutations in this sequence in four patients with classical WAS they postulated this newly-identified gene sequence was indeed the *WAS* gene [4].

The *WAS* gene is comprised 12 exons, which encode a 502-amino acid-long intracellular protein, expressed exclusively in cells of the hematopoietic system [4-6]. The WAS protein (WASp) has an intricate domain architecture comprised of WAS homology domain 1 (WH1), Cdc42/Rac GTPase binding domain (GBD), proline-rich domain, G-actin binding verprolin homology domain (V), cofilin homology domain (C), and a C-terminal acidic segment (A) [7]. The function of the WASp is not yet completely understood, however studies have reported it is associated with signal transduction pathways involved in actin polymerization and cytoskeletal reorganization [8-10] The VCA domains of WASp are described as the catalytic domains of the protein and interact with the Arp2/3 complex to activate actin nucleation (Figure 1), a process required for rearrangement of actin cytoskeleton, which is necessary to support various cellular functions, such as migration, vesicle trafficking, adhesion, and cell shape changes [10,11]. These cytoskeleton remodeling processes are essential for normal function of immune cells, including immunological synapse formation and activation of lymphocytes [7].

A.

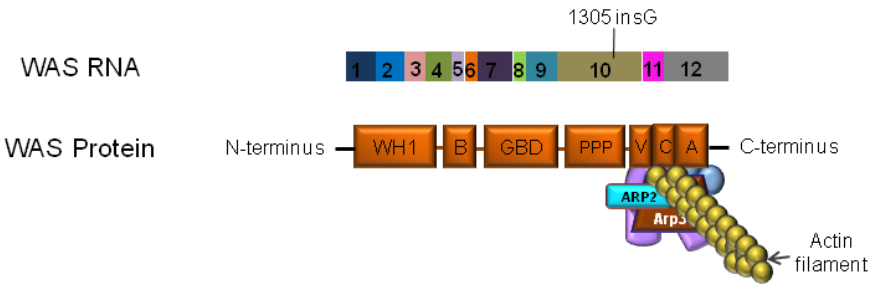
1305 insG
WAS RNA
1 2 3 4 5 6 7 8 9 10 11 12
WAS Protein
N-terminus
WH1
B
GBD
PPP
V
C
A
C-terminus
ARP2
Arp3
Actin filament

B.

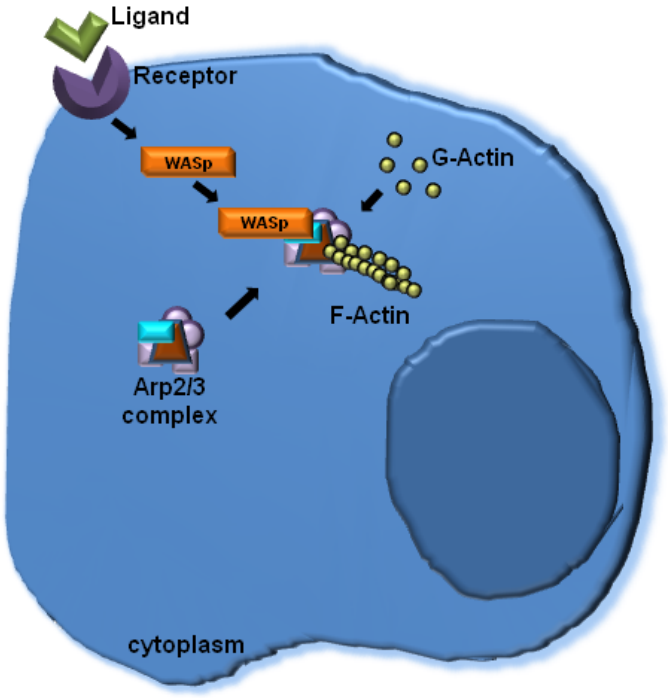
Ligand
Receptor
WASp
WASp
G-Actin
F-Actin
Arp2/3 complex
cytoplasm

Figure 1: **WASp plays a crucial role in activating the Arp2/3 complex and mediating the synthesis of actin filaments**. A. Organization of WASp domains and the exons associated with protein domains; B. Representation of WASp function in hematopoietic cell, interacting with Arp2/3 complex to mediate polymerization of actin filaments.

The absence of detectable WAS protein expression in hematopoietic cells is what confers the classical Wiskott-Aldrich Syndrome phenotype previously described. WASp deficiency can be caused by various possible mutations that may occur along the 12 exons of the gene. Hundreds of mutations have been mapped to the *WAS* gene [5, 12], and though classical WAS results in a severe clinical phenotype, there is a range of clinical severity, with some mutations causing decreased WASp expression, resulting in milder variants of WAS, typically referred to as X-linked thrombocytopenia (XLT) [12]. For both classical WAS and XLT, the mutations lead respectively to complete or partial loss of function of the gene. However, more recently, studies have shown that certain mutations which cause constitutive activation of WASp lead to X-linked Neutropenia (XLN) [13]. This disease appears to occur more rarely, with only 4 mutations reported to date: Leu270Pro, Ser270Pro, Ile276Ser, and Ile294Thr [12, 13].

The complications that result from the absence of WASp expression (giving rise to classical WAS phenotype) affect nearly all cells of hematopoietic lineage, and cause prominent immunologic impairments in both T-cell and B-cell function [14]. It has been shown that WASp-deficient T-cells are unable to reach optimal levels of activation through the T-cell receptor (TCR), and do not respond well to IL-2 stimulation [7,14-16]. Such impairments in T-cell function greatly contribute to the immunodeficiency seen in WAS patients. WAS-deficient B-cells have impaired ability to home to secondary lymphoid organs, therefore compromising the patient's humoral response [14]. In addition to defects in T- and B-cells, Orange and colleagues showed that in Natural-Killer (NK) cells harvested from WAS patients,

the absence of WASp expression correlated with significantly reduced cytolytic function in chromium-release killing assays [17] Furthermore, WASp deficiency has also been shown to affect the function of hematopoietic stem cells (HSCs). Lacout et.al.(2003) [18] reported data from competitive transplantation studies in mice suggesting that WASp plays a role in migration of HSCs, as well as engraftment of these cells in the bone marrow.

Cure for WAS can only be achieved by an allogeneic hematopoietic stem cell transplant (HSCT) from a genotypically-matched donor or by gene therapy. Though transplants are often the recommended treatment, challenges in finding suitable donors leave many patients with only the option to receive HSCT from mismatched related donors, thereby decreasing the efficacy of transplant, and increasing the risk of rejection [19].

1.2 Revertant Somatic Mosaicism in Wiskott-Aldrich Syndrome

Approximately 11% of WAS patients have been identified as having, in addition to immune cells which carry the inherited germ line mutation, cells which have undergone spontaneous genetic changes that resulted in reversion to normal phenotype. The presence of both phenotypically normal and abnormal cells *in vivo* is referred to as Revertant Somatic Mosaicism, and has been described in various disorders affecting the hematopoietic system, the liver, and the skin [20-23].

Revertant patients often present milder clinical symptomatology and may not require the more aggressive treatments that are commonly prescribed to non-revertant patients. A significant factor likely contributing to the observation of reversions in patients is the selective advantage *in vivo* for growth and proliferation of cells which carry the wild-type gene product. The fact that Revertant Somatic Mosaicism is reported in diseases affecting highly regenerative tissues capable of rapid and robust cell division may suggest that significant cell proliferation is also an important factor in supporting the origination of revertant cells [20,24].

The precise mechanisms whereby revertant cells emerge in WAS patients are not yet known. It is accepted that at least two events must occur: first, the emergence of molecular reversions in the *WAS* gene, and subsequently the *in vivo* selective expansion of these revertant cells [20]. Cells undergo random genetic changes throughout their lives, and it is possible that one of these changes may lead to partial or full restoration of expression of a gene product. These cells which have restored their phenotype have a better chance for growth and proliferation, thus accumulating in the patient over time [24]. Some studies of WAS have shown that second-site compensatory mutations, or point mutations directly affecting the mutant codon occurring during cell division may explain the origination of reversion in the patient [25, 26]. In WAS revertants, the predominance of WASp-expressing cells in some cell populations, such as T- and B-lympocytes confirms the selective advantage conferred to cells which carry reversions that partially or fully restore normal phenotype [27]. Furthermore, group demonstrated through clonal assay analysis of WAS-patient-derived T-cells *in vitro*, a selective proliferative advantage

in cells which revealed, by sequence analysis, base-pair changes in the *WAS* gene, which directly affected the mutated codon, or bypassed the mutation by inducing alternative splicing [23].

The collective data reported in these various studies led to our interest in establishing a methodology that allows for an in-depth investigation into the diversity of the revertant repertoire in WAS revertant patients'cells. We analyzed cells from a group of five WAS-revertant patients among whom there were three different germ line mutations. Our findings reported herein result from a comprehensive assessment of the various genotypic changes detected in the WASp-expressing ($WASp^+$) cells of these patients.

1.3 Gene Therapy for Wiskott-Aldrich Syndrome (WAS)

The vast majority of patients diagnosed with WAS present with the severe clinical symptomatology that is the hallmark of this disease. For these patients, the cure can only be achieved by an allogeneic hematopoietic stem cell transplant or gene therapy. Transplant from an HLA-matched donor has a very high success rate of conferring therapeutic benefit to the patient [28]. However, only one third of patients receive a matched transplant [28]. For patients without matched donors, gene therapy offers an alternative that can bring restoration of normal function in hematopoietic cells.

Autologous transplantation of *ex vivo* genetically corrected hematopoietic stem/progenitor cells (HSPCs) is a promising and attractive proposal for treatment of inherited primary immunodeficiencies such as WAS. This approach can confer upon the patient the clinical benefits of a transplant without the rejection risks associated with it. Virus-mediated approaches have been investigated as a feasible method to correct genetic mutations and rescue phenotype for several decades, and started with the use of retroviral vectors [29]. In the mid 1980s, Williams' and Dick's laboratories [30, 31] reported successful use of retrovirus for gene transfer into bone marrow-derived murine HSC. In light of these promising preliminary results, scientists became interested in applying this technology to treatment of inherited diseases [15, 16, 28,29]. The first gene therapy clinical trial, conducted at the National Institutes of Health (NIH), targeted T-lymphocytes of patients with Adenosine Deaminase-Deficient SCID [32]. One renowned gene therapy trial was conducted in Paris, France, and sought to treat patients with X-linked Severe Combined Immunodeficiency (X-linked SCID). In this trial, the patient's derived bone marrow HSCs were cultured *ex-vivo* and transduced by gammaretroviruses before autologous transplantation [23]. The results of this trial were astonishingly successful. Nine out of the ten patients treated showed rapid and vigorous T-lymphocyte production; however, four out of the nine patients developed T-cell leukemia 31-68 months after treatment ended [33,34]. Further investigations into the molecular mechanism responsible for this undesired effect revealed a vector-mediated integration adjacent to a known proto-oncogene (*LMO2)*, which trans-

activated the expression of this gene and led to the aberrant T-lymphocyte proliferation [34].

The SCID trial exposed one of the most significant concerns with gene therapies for treatment of human diseases: the potential oncogenic effects induced by transgene integration. Other, more recent trials for PID have reported aberrant clonal proliferation due to undesired integrations [35]. Because integration in the genome of the treated cells is a random process, there is an increased probability of genotoxic effects due to deregulation of gene expression, which may occur as a consequence of interactions between viruses and the human genome [36-38]. These concerns led to advances in the development of safer gene delivery vectors. New retroviral vectors were designed, now self-inactivating vectors (SIN-vectors), capable of safer and more efficient performance [39-42]. Their self-inactivating long-terminal repeats which reduce the potential for insertional activation of neighboring alleles, minimizing the potential for undesired effects. [43].

Further, lentiviral vectors were found to successfully transduce hematopoietic stem and progenitor cells (HSPCs), and in less time than gammaretroviruses [29 42, 44-45]. SIN versions of lentiviruses have also been designed and bring new hope for safer and more efficient gene therapy protocols [42]. Recently, Aiuti et.al. reported successful *ex vivo* correction of WAS defect in three WAS patients using SIN lentivirus-mediated gene transfer into HSPCs. This treatment conferred significant clinical improvement and restoration of immune function to patients, with no evidence of adverse effects, as reported in a 30-month follow-up [46]. Though results appear promising, integration site (IS) profiling analysis revealed an

estimated average vector copy number (VCN) of 2.3 in bulk-cultured $CD34^+$, and 2.6 VCN observed in T-cells. Integrations favored transcription unit sites and clustered in gene-rich regions, with a total of approximately 10,000 to 25,000 unique integrations per patient [46]. These data show that, even with the current state-of-the art approaches for viral-mediated gene therapy, there remains a risk of adverse side effects due to random transgene integration.

1.4 Site-specific genome editing

The extensive work accomplished in virus-mediated gene therapy studies contributed significantly to a greater understanding of the underlying biological events that cause potentially deleterious side effects in patients. Consequently, it motivated the field to develop new technologies and safer approaches. One such example is the emergence of site-specific genome editing strategies that utilize engineered nucleases to target a specific locus on the genome for correction, thus minimizing the risk of insertional mutagenesis. These nucleases are capable of mediating genomic changes by inducing a sequence-specific double-strand break (DSB), and thus stimulating the rapid non-homologous end-joining (NHEJ) repair mechanism, or by facilitating homology-directed repair when co-delivered with a custom homologous DNA template [47-50]. Currently there are three major custom nuclease systems available: Zinc-Finger nucleases (ZFNs), transcription activator-like effector nucleases (TALENs), and clustered regulatory interspaced short palindromic repeat (CRISPR)-Caspase system. [51,52]. All three systems have their

advantages and limitations. The major differences between them are related to specificity, efficiency, and design flexibility [50]. ZFN and TALENs are engineered endonucleases that contain sequence-specific DNA binding domains that are derived from zinc- finger and transcription activator-like effector (TALE) proteins. The versatility and programmability of DNA binding domains give ZFN and TALENs a level of flexibility that permits targeting of virtually any site in the genome [52]. TALE proteins originate from the plant pathogenic bacteria of the genus Xanthomonas, and their DNA recognition domains contain a series of 33-35-amino-acid repeat domains, each capable of recognizing a single base pair. Two hypervariable amino acids, known as the repeat-variable di-residues, determine the specificity of the TALE protein [52]. Multiple TALE repeats can be linked together to provide recognition to desired DNA sequences.

The CRISPR/Cas system has recently emerged as an alternative for use in genome editing strategies. This system offers a potentially simple and inexpensive option for inducing site-specific genetic modifications. CRISPRs are components of an adaptive immune system that exists in bacteria and archea and relies on small RNAs for sequence-specific detection and cleavage of invading foreign DNA [52, 53]. In the CRISPR/Cas system, short sequences from the invading DNA are integrated into the CRISPR genomic loci and subsequently transcribed and processed to generate crRNA. These, in turn, bind to trans-activating CRISPR RNA to form trcrRNA, which mediate the sequence-specific binding and cleavage of foreign DNA by Caspases [52]. This CRISPR/Cas system can presumably be redesigned to cleave any DNA sequence of interest by simply modifying the crRNA

[52]. A concern with the use of CRISPR/Cas system is the potential for off-site effects. More studies are required to evaluate whether this method affords the necessary level of recognition selectivity required for targeting a single specific site in more complex genomes [52].

ZFNs were the initial group of synthetic nucleases tested, and therefore are the most studied to date. These synthetic nucleases are designed in pairs, with each ZFN binding one strand of the DNA double-helix at a specific sequenced determined by zinc-finger protein (ZFP) recognition motifs [54-58]. As reviewed in Urnov et.al., these ZFPs contain a tandem assembly of Cys2-His2 fingers, each capable of recognizing 3bp of DNA. A series of ZFPs are linked together to provide for longer recognition sequences, typically ranging from 9bp on each strand (total of 18bp per cleavage site) to 18bp (total of 36bp per cleavage site), thus providing specificity for cleavage of unique sequences on the genome [54-58].

Several groups have reported successful targeting of human cells using ZFNs, in some cases introducing gene modifications to knock out a gene, and in other cases, correcting disease-causing mutations by targeted substitution or gene addition [47, 59-61]. Following a gene knock-out study in primary human T-cells, Perez et.al. reported successful targeting of the human CCR5 locus using ZFNs, and showed, by DNA sequencing analysis, that ZFNs are quite specific for their target. Only one other locus – the closely related CCR2 gene - was cleaved by the nucleases at a significant level, albeit still at much lower frequency than the target CCR5 locus [59]. Holt et.al. demonstrated this same locus could be targeted in human $CD34^{+}$ HSPCs using ZFNs, and that the engraftment and differentiation

potential of these cells were not impaired by ZFN activity [62]. Furthermore, Moehle et.al. demonstrated high efficiency site-specific integration of long extrachromosomal DNA donors via homology-directed repair in cells stimulated by ZFN-induced DSB, and, through this, established proof-of-principle for gene addition as a feasible approach for correction of mutation [47].

1.5 Genome Editing in induced pluripotent stem cells (iPSC)

The ability to genetically reprogram somatic cells to a pluripotent, undifferentiated state using specific factors was first described by Shinya Yamanaka's group in 2006 from studies in mouse fibroblasts [63]. The following year, both Shinya Yamanaka and James A. Thompson's group published reports describing that a combination of four factors was capable of inducing the reprogramming of human fibroblasts to pluripotent cells [64,120]. These reprogrammed cells, named induced pluripotent stem cells (iPSC), had embryonic-cell (ESC)-like morphology, and expressed the canonical ESC-specific cell surface markers. They also retained normal karyotype and demonstrated normal ESC-like pluripotent function by generating [64].

The advent of reprogramming technology broadened the opportunities for regenerative medicine and drug discovery. The possibility of deriving any tissue of interest from iPSC became an important aspect that inspired many scientists to look at these cells as a model for disease studies, especially in the case of rare disorders, for which patient samples are difficult to obtain. Genome editing in iPSC

quickly became an attractive strategy for therapies for monogenic diseases, such as WAS and other hematological disorders [65-68]. Many studies have coupled the iPSC technology with the use of tools for precise gene modification to generate reporter cell lines, correct disease-causing mutations, generate gene knock-out models, among many other applications, illustrating the vast utility of iPSC [60, 69-73]. Zou et.al. reported in 2011 the generation of iPSC from X-linked Chronic Granulomatous Disease (X-CGD) patient mesenchymal stem cells (MSC), and the subsequent genetic correction of these cells by ZFN-mediated HDR with a homologous DNA donor. They further differentiated the corrected cells into mature neutrophils and demonstrated restoration of normal function [60].

Similar to the work done for X-CGD correction, we generated iPSC from a WAS-patient's skin fibroblasts and corrected the defect by ZFN-mediated targeted gene addition in the endogenous WAS locus. Following *in vitro* differentiation of corrected WAS iPS (cWAS) into hematopoietic progenitor cells, we were able to demonstrate restoration of WASp expression, which correlated with functional restoration in Natural Killer (NK) cells derived from the corrected progenitors (Figure 2).

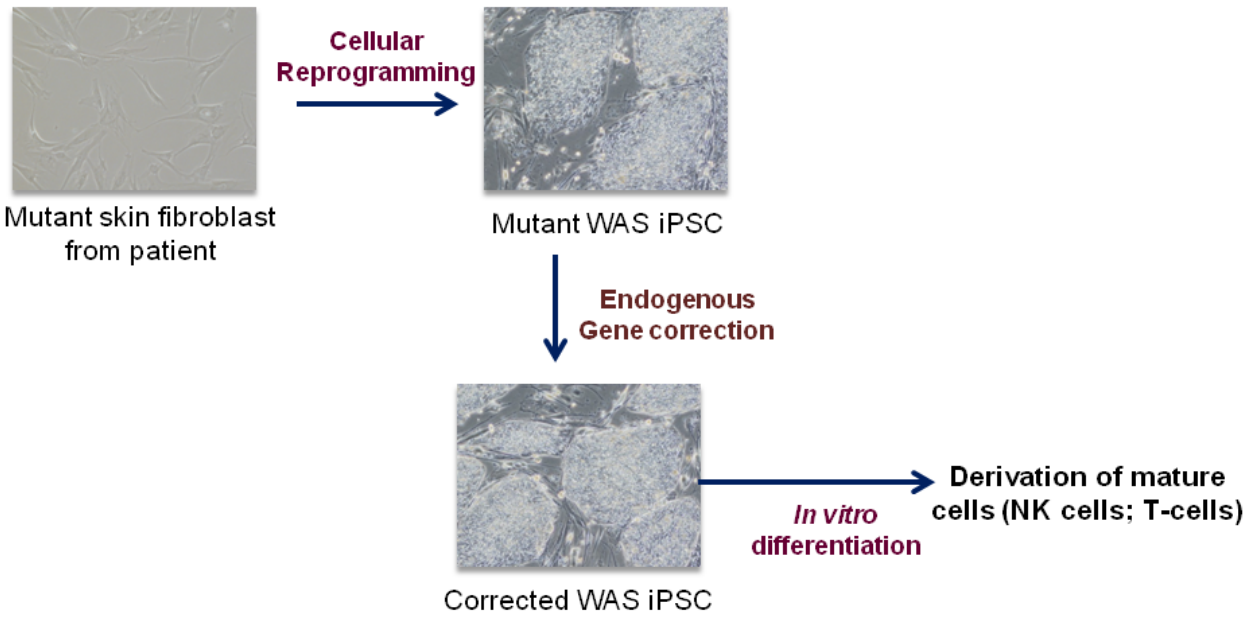

Figure 2: Schematic illustrating overall goal of gene correction project.

Reprogramming of WAS-patient fibroblasts followed by the subsequent correction of disease-causing mutation in iPSC provides a valuable tool for generation of disease-free hematopoietic cells.

CHAPTER 2: MATERIALS AND METHODS

2.1 Cell lines and culture

Skin fibroblasts from a WAS patient were obtained through Coriell Cell Repositories (Coriell # GM01598). WAS-fibroblasts and mouse embryonic fibroblasts (MEF; CF-1 mouse strain, Charles River) were maintained in DMEM supplemented with 10% fetal bovine serum (FBS), 2mM L-glutamine, and 2mM non-essential amino acids (NEAA), all from Invitrogen/Life Technologies.

Human embryonic stem cells (WA09) were maintained in hESC medium conditions, as outlined by the National Stem Cell Bank protocol SOP-CC-001C. Cells were maintained in DMEM-F12 (Invitrogen) supplemented with 20% Knock-out Serum Replacer (Invitrogen), 2mM L-glutamine (Invitrogen), 2mM NEAA (Invitrogen), 4ng/mL basic fibroblast growth factor (bFGF; Invitrogen), and 55μM 2-mercaptoethanol (Sigma). Medium changes occurred daily. WAS iPSC and cWAS iPSC cell lines were generated in our laboratory, and were cultured in the same hESC medium, but instead with 40ng/mL bFGF, with daily medium changes. All cells were cultured under humidified conditions at 37℃ and 5% CO_2 unless otherwise specified.

Both hESC and iPSC cells were passaged in clumps every 5-6 days, by first removing medium and washing twice with DPBS (+ Calcium,+ Magnesium; Invitrogen). Initial mild chemical detachment of colonies was induced by brief incubation (3-5 minutes) with Collagenase Type IV (Invitrogen), followed by two

washes with dPBS. Using a 5mL glass pipette tip, the well was scraped in vertical and horizontal motions to cut colonies into pieces, and collected by gentle pipetting. Cells were typically split at 1:6 to 1:12 ratio, and were subsequently plated onto 0.1%-gelatin (Sigma) coated 6-well cell culture plates (BD Biosciences) pre-seeded with approximately $2x10^5$ irradiated MEF (iMEF) feeders per well.

When performing single-cell adaptation, WA09 hESC and iPSC cells were first washed twice with DPBS, and 1mL of pre-warmed TrypLE reagent (Invitrogen) was added to each well, followed by incubation at 37℃ for 2 minutes. After thoroughly removing TrypLE by carefully aspirating from the side of the well, we added 1mL of hESC or iPSC medium, collected cells in a 50-mL conical vial, and filtered through a 70μm cell strainer (BD Biosciences). Cells were then plated onto 6-well plates pre-seeded with approximately $1.3x10^5$ iMEF per well. For the first two-three passages under single-cell dissociation, cells were plated at 1:1 to 1:2 ratio. Later passages were plated at 1:3 to1:6 ratios. Cells were passaged by this method 4-5 times before considered adapted to single-cell dissociation. Once a line was adapted, cells were expanded and cryopreserved in individual vials. Each adapted line was cultured for a maximum of 12-14 passages.

Murine bone-marrow stroma OP9 cells (provided to us by Naioki Nakayama), and OP9-DL1 cells (provided by Bart Vandekerckhove) were cultured in alpha-MEM medium supplemented with 20% FBS, 2mM L-glutamine, and 1X Pennicillin-Streptomycin (P/S; Invitrogen). Inactivation of these feeder cells, when necessary, was done by 3-hour incubation with 15μg/mL mitomycin C at 37℃ with 5% CO_2.

2.2 Derivation of WAS induced pluripotent stem cells (WAS-iPSC)

Patient skin fibroblasts were reprogrammed using pMXs-based retroviruses expressing the reprogramming factors OCT4, SOX2, KLF4, CMYC, AND NANOG. These reagents were provided by K. Plath and obtained through Addgene. For generation of pMXs-GFP construct, we obtained the ORF of eGFP by PCR amplification of CCR5-PGK-GFP construct provided by Michael Holmes (Sangamo Biosciences). Amplification introduced two novel enzyme sites – NotI and EcoRI – flanking the gene. The amplicon was then added to the pMXs vector backbone by directional cloning using NotI and EcoRI. For packaging the viruses, we adopted the protocol form Park and Daley [74] for VSV-G pseudotyped retroviral vectors. Two 150mm-plates were each seeded with approximately 7 million Plat-GFP Retrovirus Packaging Cell line (Cell Biolabs, Inc.) for each vector construct, including the GFP control. The following day, each plate was transfected with 6.25µg of the pMX retroviral vector backbone and 0.9µg of pCMV-VSV-G plasmid (obtained through Addgene). Each 15mm-plate of cells was maintained in 30mL of medium (DMEM, 10% FBS, 10µg/mL of Bastidcidin) containing 50µL of Fugene 6. Supernatant containing the virus was harvested 48 hours after transfection, and filtered through a 0.45µm filter into a polyallomer centrifuge tube. Material was centrifuged at 260000 rpm for 2 hrs in an ultracentrifuge (Beckman Coulter). Viral pellets were re-suspended in 600µL of DMEM-F12 and 100X concentrations of virus were generated. Infectious virus titer was determined by titration on human primary fibroblasts with pMXs-GFP virus, followed by flow-cytometric analysis for GFP expression.

For the reprogramming of patient skin fibroblasts, 10^5 cells were plated onto each well of a 6-well tissue culture plate on day 0. On the following two days, cells were transduced with the 5 reprogramming factors (OCT4, SOX2, KLF4, C-MYC, AND NANOG) by spinfection at a multiplicity of infection of 21.5 virus particles per cell, in fibroblast medium containing protamine sulfate (10µg/mL). Approximately 2.5 days after initial transduction, cells were trypsinized and replated at a 1:1 ratio onto gelatin-coated plates seeded with iMEF. The following day, the medium was removed and hESC medium containing 40ng/mL bFGF was added, initiating pluripotent stem cell culture conditions. Starting at day 12 of culture, hESC medium pre-conditioned on iMEFs was used, and medium changes occurred daily. At approximately day 16 post-transduction, individual iPSC-like colonies began to emerge, and initial detection was done based on morphology. Live-cell staining for known pluripotent stem cell surface marker - TRA-1-60 – was done (anti-TRA-1-60 mouse IgM monoclonal antibody, Stemgent, 1:200 dilution, followed by Alexa488-conjugated anti-mouse IgM seconday antibody, 1:250 dilution; both from Invitrogen) and iPSC colonies were confirmed. Each iPSC clone was subsequently cut into smaller fragments with a glass, end-closed pipette, and transferred – one colony per well - into a 12-well tissue culture plate pre-seeded with iMEF. Plating medium used was hESC medium supplemented with 10µg Y-27632 (Alexis Biochemicals). Once plated, cells were allowed to expand, and upon successful expansion, they were further passaged in a 1:2 to 1:4 ratio in subsequent passages. Once clones were established, they were characterized, expanded, and cryopreserved.

2.3 Characterization of iPSC

Each clone was analyzed first for expression of known pluripotency markers. Expression of TRA-1-81 surface marker was analyzed by live-cell immunostaining (anti-TRA-1-81 mouse IgM, 1:200 dilution, Millipore). Moreover, following Wicell protocol (SOP-CH-102B) co-expression of SSEA-4 surface protein and OCT4 transcription factor by flow cytometry was assessed on BD LSRII running BD FACSDiva software (Becton Dickinson). We considered detection of ≥90% $OCT4^{+}SSEA4^{+}$ cells to be a population of pluripotent cells with minimal spontaneous differentiation. Alkaline phosphatase activity was assessed by VECTASTAIN ABC-AP Kit (Vector laboratories) by first fixing iPSC with 2% paraformaldehyde in DBPS for approximately 30 minutes. Following incubation, paraformaldehyde was removed and the substrate solution 123 was added to each well. Cells were allowed to incubate in the substrate solution in the dark, as per manufacturer protocol. Following a 5-minute wash with DBPS containing 0.1% Tween-20, cells were observed under microscoscope. Karyotype analysis of WAS iPSC was performed at Texas Children's Hospital Clinical and Research Cytogenetic Laboratory where approximately 20 metaphase cells were analyzed per line.

Pluripotent function of each iPSC line was assessed by teratoma formation assay. iPSC were cultured on 30% Matrigel with daily medium changes using mTESR (Stem Cell Technologies) to remove residual iMEF. Approximately 2-3 million iPSC were injected into the kidney capsule or the testis of six-week old Fox Chase SCID beige mice (Charles River), and monitored weekly for emergence of

tumor. A total of 3 mice were prepared for each cell line. Tumors were removed 6-8 weeks post injection, paraffin-embedded, and prepared for histological analysis by hematoxylin adeosin (Applied Stem Cell Inc.).

Pluripotency gene expression was assessed by quantitative RT-PCR. The goal of this analysis was to confirm silencing of retroviral transgenes used in the process of reprogramming. Total RNA was isolated from iPSC and control hESC WA09 (RNeasy kit, Qiagen), and synthesized cDNA by reverse transcription using Improm-II Reverse Transcription System (Promega). The levels of expression of pluripotency genes were assessed by SYBR Green incorporation. By using specific primers we were able to distinguish endogenous gene expression from total gene expression for each of the reprogramming factors (each primer set included one primer designed to bind sequences that include the 3'UTR) (Table1).

PLURIPOTENCY GENE EXPRESSION ANALYSIS PRIMERS		
Purpose	**Primer Sequence -F**	**Primer Sequence -R**
Total OCT4 expression	CAGTGCCCGAAACCCACAC	GGAGACCCAGCAGCCTCAAA
Endogenous OCT4 expression	TTCGCAAGCCCTCATTTC	CCATCACCTCCACCACCT
Total SOX2 expression	CAAGATGCACAACTCGGAGA	GCTTAGCCTCGTCGATGAAC
Endogenous SOX2 expression	TGCTGCCTCTTTAAGACTAGG	CCTGGGGCTCAAACTTCTCT
Total KLF4 expression	GGGAGAAGACACTGCGTCA	GGAAGCACTGGGGGAAGT
Endogenous KLF4 expression	GACCACCTCGCCTTACACAT	TTCTGGCAGTGTGGGTCATA
Total c-MYC expression	AGCGACTCTGAGGAGGAACA	CTCTGACCTTTTGCCAGGAG
Endogenous c-MYC expression	GCTGCTTAGACGCTGGATTT	TAACGTTGAGGGGCATCG
Total NANOG expression	TCTCCAACATCCTGAACCTCA	TTGCTATTCTTCGGCCAGTT
Endogenous NANOG expression	TTGGAAGCTGCTGGGGAAG	GATGGGAGGAGGGGAGAGGA

Table 1: List of Primers used for pluripotency gene expression analysis. Primers used for qRT-PCR analysis of expression of pluripotency-associated genes in iPSCs generated from patient fibroblasts as well as WA09 hESC normal control.

RT-PCR analysis was performed in duplicates for each cell line using an ABI7900 instrument. Expression levels were normalized to that of house-keeping gene GAPDH, and the profile obtained for iPSC lines was compared to the one obtained for the WA09 hESC control cell line.

Southern Blot analysis of genomic DNA from WAS iPSC and cWAS iPSC was performed with the goal to verify the number of donor integrations present in the targeted-corrected cWAS iPSC. Genomic DNA was first digested with PvuII and ScaI restriction enzymes. A 2.3kb long probe encompassing the pgk-Puro-TK selection cassette was used to detect integration sites in puromycin-resistant clones. We expected the probe would hybridize with a 3.8kb long genomic DNA band that resulted from initial enzyme digestion.

2.4 Assessment of ZFN activity

Two pairs of zinc-finger nucleases targeting the *WAS* gene – S1 and S4 - were engineered by Sangamo Biosciences, and provided to us as a gift through a collaboration. S1 ZFN plasmids (pVAX-C2A-3FN-Fok11914 and pVAX-N2A-3FN 11916-Fok) and S4 ZFN plasmids (pVax15755 and pVax15724)) were first tested in K562 erythroleukemia cells. Using Amaxa Nucleofection cell line kit V (Lonza), ZFN expression plasmids were delivered to K562 cells as per protocol instructions, at doses ranging from 1ug to 5µg per ZFN (2µg to 10µ total ZFN plasmid). Following manufacturer's protocol, we used Nucleofection kit V (Lonza) and electroporated $1x10^6$ K562 cells per reaction. Immediately following electroporation, cells were

gently transferred from cuvette to a 6-well tissue culture plate containing K562 medium – PRMI1640 (Hyclone, Fisher Scientific), 10%FBS (Hyclone, Fisher Scientific), 2mM L-glutamine (Invitrogen), 1X P/S (Invitrogen). Cells were cultured for 7 days in incubator at 37℃, 5% CO_2. Cell proliferation was assessed by counting every 2 days in a hemacytometer. Cell viability was evaluated by Trypan Blue staining (Life Technologies).

In experiments with iPSC we transfected $2x10^6$ dissociated cells by Amaxa Nucleofection (Stem cell kit 1, Lonza). ZFN expression plamids or *in situ* generated RNA were delivered. In order to generate RNA for each ZFN, 1µg of plasmid DNA was first linearized by *XbaI* digestion. Following linearization, capped RNA was synthesized using MessageMAX^{TM}T7 ARCA-Capped Message Transcription Kit (CellScript, Inc.) as per protocol. This product was then treated with DNaseI, and subsequently, a poly(A) tail was added using Poly(A) Polymerase Tailing Kit (Epicentre). This material was purified by MegaClear Kit (Ambion), and analyzed on Agilent Bioanalyzer for assessment of size, concentration, and quality.

Following transfection, cells were plated in a gelatin-coated well of a 6-well plate pre-seeded with approximately $2.5x10^6$ iMEF per well, and cultured in iPSC medium - DMEM-F12 (Invitrogen) supplemented with 20% Knock-out Serum Replacer (Invitrogen), 2mM L-glutamine (Invitrogen), 2mM NEAA (Invitrogen), 40 ng/mL basic fibroblast growth factor (bFGF; Invitrogen), 55µM 2-mercaptoethanol (Sigma), and supplemented with rock inhibitor Y-27632 (Alexis Biochemicals) only for the first day. Medium was changed daily. Approximately 3-5 days from initial transfection, we harvested DNA from bulk culture, and a 253-bp region flanking the

ZFN cleavage site (Table 2) was amplified by PCR (AccuPrime High fidelity taq polymerease, Invitrogen).

Purpose	Primer name	Primer sequence (5'to 3')
CEL1 at S1 site (exon 1)	WAS-1F	CCAGAGAAGACAAGGGCAGAA
	WAS-1R	GATGGAGAGGGAAAGGAGGAG
CEL1 at S4 site (intron 1)	WAS-4F	CACCGTTTCTTCCTCTTCCTC
	WAS-4R	ACTCCACTGACCCCTGCTTT
Donor homology	WAS E1-2 Flg	ATGGCAGTGGAAATAAATGAA
	WAS E1-2 Rlg	CCACACCCTTAGACACCAACTC
InFusion_WAS-2A-GFP	WAS infusion_F	TCTGACCTCTTCTCTTCCTCCCACAGGA
	WAS-2A-Infusion_R	CGTCCCCGCATGTTAGAAGACTTCCCCTGCCCTCGGCTCTGTCATCCCATTCATCATCT
	2A-GFP_Infusion_F	CTTCTAACATGCGGGGACGTGGAGGAAAATCCCGGGCCCATGGTGAGCAAGGGCGAGGA
	GFP-Infusion_R	CTGGTTCTTTCCGCCTCAGAAGCCATAGAGCCCACCGC
Infusion cloning PuroTK	Infusion-PuroTK_F	ATGAGGCAGGAAGGACCAGGTCCTAGGATAACTTCGTATAG
	Infusion-PuroTK_F	AGGTCTTGGAGCCAGACCTGGTCCTAGGATAACTTCGTATAA
Target Integration	S4-pgk-GFP-Donor-F	TCTGAGCCAGTCAGAAGGAGAT
	S4-pgk-GFP-Donor-R	CCTAGAAAGTTCAGGTCAGGGG
RT-PCR	WAS-ex9	GTGCGGCAGGAGATGAGGCG
RT-PCR	WAS-ex10-11junction	GGGCCCCAGGGGTCTTGTTCA
RT-PCR	RT-11-12junction	ATCCACTCCTCCGACGAAGG
RT-PCR	RT-GFP	GATGCCGTTCTTCTGCTTGTC
RT-PCR	endogenous-F	GATGCACGTGATGCAGAAGAGAA
RT-PCR	endogenous-R	AGCACAGGGCAGCAAGTAACTCA

Table 2: List of Primers.

ZFN activity in pools of cells was determined by using the CEL-1 /Surveyor nuclease assay (Transgenomics) [59, 61]. CEL-1 recognizes allelic mismatches resulting from the rapid but imperfect Non-Homologous End-Joining (NHEJ)-mediated repair of double-strand break induced by ZFN (Figure 3).

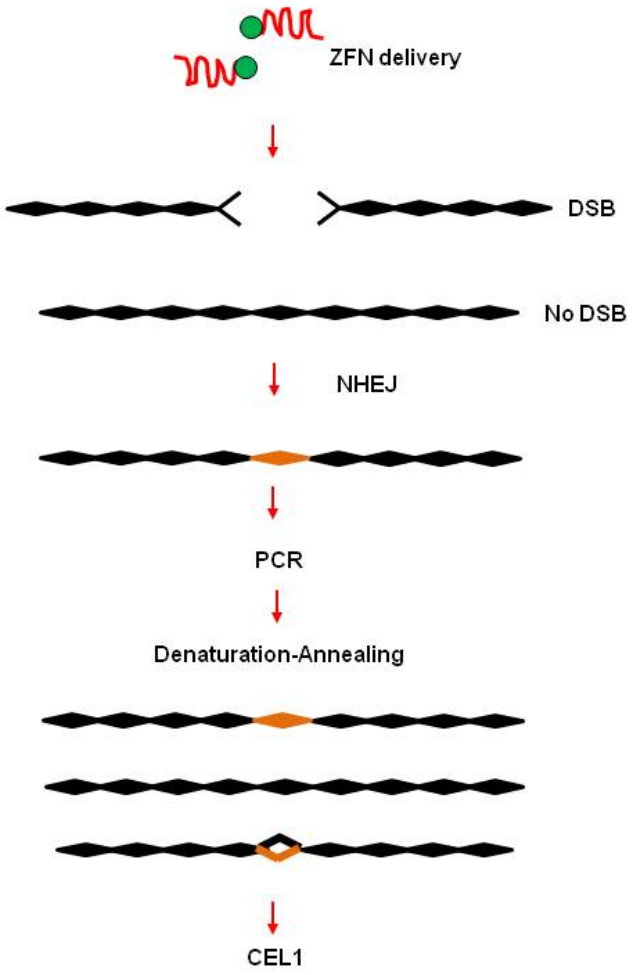

Figure 3: Schematic illustrating method applied for determination of ZFN activity analysis. This schematic describes ZFN activity when delivered without donor molecule. Subsequent to cleavage, dsDNA break is repaired by NHEJ, and an indirect measure of ZFN activity is obtained by treatment of DNA with CEL-1 nuclease.

PCR amplification of bulk-transfected cells generates a mixture of wild-type (WT) and mutant amplicons. By denaturing and slowly reannealing this product (95℃ incubation for 10 minutes; cool to 85℃ at -2℃/sec, and cool to 25℃ at -1℃/sec), homoduplexes originate (either from two WT strands or two mutant strands) as well as heteroduplexes (formed when a WT strand reanneals to a mutant strand), in which case a DNA "bubble" is formed as a consequence of base-pair mismatches. These mismatch sites are cleaved by CEL-1, and subsequently resolved on a 10% polyacrylamide gel. Through densitrometry quantitation using Sybr Gold (Life Technologies) we were able to compare the intensity of the cleaved heteroduplexes to that of the parental band and determine the level of CEL-1 activity, which was calculated using the equation: %CEL-1= (1-(√parental fraction))x100. This value, in turn, is an indirect measure of the frequency of endogenous target sequences that underwent NHEJ repair subsequent to ZFN-mediated cleavage.

2.5 Generation of Donor template

We initially amplified from wild-type K562 cells a 1.6kb-long region of WAS sequences encompassing exons 1 and 2, and spanning the ZFN-cleavage site in intron 1. These sequences were cloned into the pSC-B–amp/kan vector (Agilent Technologies), generating our WAS-homology donor arms. Subsequently, by site-directed mutagenesis, we introduced an NsiI endonuclease site in intron 1, near the

ZFN cleavage site, leaving 751bp of WAS-homology sequences to the right of the enzyme site, and 815bp to the left (Figure 4).

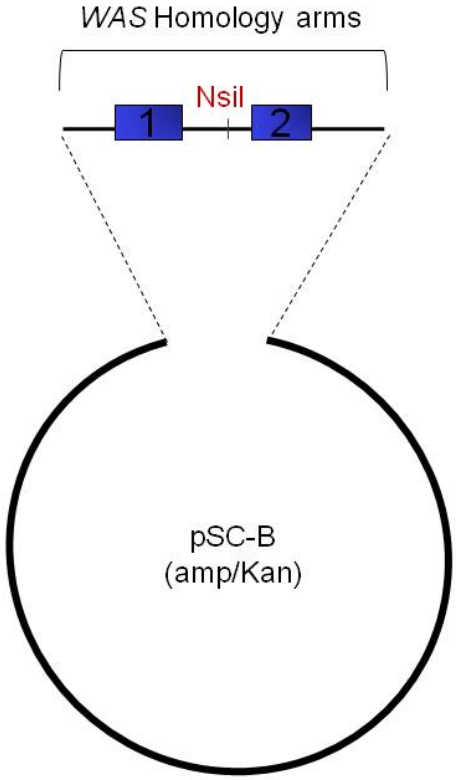

Figure 4: Generation of donor homology arms. Approximately 1.6kb of WAS sequences flanking the ZFN cleavage site were used to generate the homology arms necessary for HDR-mediated integration into the WAS locus.

For generation of our first donor, we cloned a 43-bp oligonucleotide sequence containing a BamHI enzyme site directly into the NsiI site of pSC-B homology donor vector. The resulting construct was named “patch donor”. For our next donor molecule, we used PCR amplification to extract the sequences for PGK-GFP-pA from the CCR5-Patch-hPGK-GFP-pA-DonorTOPO plasmid obtained from our collaborators at Sangamo Biosciences. Both the forward and reverse primers contained NsiI sites, and amplicon was cloned by ligation into the NsiI site in the pSCB plasmid. The resulting plasmid contained PGK-GFP-pA sequences flanked by WAS-homology arms.

In order to build our correction donor, we purchased a vector encoding the WAS cDNA sequences. By site-directed mutagenesis, we introduced a base-pair change (C→A) at position 995 in exon 10 (QuickChange Lightening Site-Directed Mutagenesis kit, Agilent Technologies). We then extracted exons 2-12 sequences using custom-designed fusion primers containing splice acceptor sequences on the 5’→3’ forward primer (table 2). The reverse primer included WAS exon 12 sequences and approximately half of the 2A sequences. A second set of primers was used to amplify eGFP from our PGK-GFP donor plasmid (table 2). The forward primer in this set contained the remaining sequences necessary for completion of the 2A peptide sequences linking WAS and GFP (table 2). These amplicons were generated in such a way as to work as “puzzle pieces” that fit together in the order WAS-2A-GFP. We cloned the two pieces in one single reaction by In-Fusion cloning (In-Fusion® HD Cloning Kit, Clontech Laboratories) into the donor homology plasmid vector. Our next step was to add the selection cassette to the WAS-2A-GFP donor.

Using In-Fusion primers, we PCR-amplified the loxP-pgk-PuroTK-loxP sequences from pPthc-Oct3/4 plasmid (received from Dr. Naioki Nakayama). This cassette allowed us to include the puromycin resistance gene, as well as the thymidine kinase "suicide" gene for negative selection. This double selection feature was instrumental in obtaining our final targeted clones. We cloned the selection cassette in the SexAI enzyme site using In-Fusion technology (In-Fusion® HD Cloning, Clontech Laboratories).

2.6 Target Integration in WAS iPSC

We had previously determined that delivery of 2μg of each ZFN in the form of RNA was sufficient to induce good level of activity without cytotoxic side-effects. ZFN and/or donor plasmid were delivered by Amaxa Nucleofection using the Human Stem Cell Nucleofector Kit 1 (Lonza). For each reaction, $2x10^6$ iPSC were first dissociated to single-cell suspension by Accutase treatment for 2-3 minutes at 37℃ (STEMCELL Technologies). This brief treatment resulted in most iMEF detaching from the well, leaving the iPSC still slightly attached to the plate. This facilitated removal of iMEF during careful aspiration of Accutase. We then mechanically dissociated iPSC by adding PBS and gently pipetting. Cells were subsequently centrifuged in 1.5mL micotubes at 200g for 5 minutes. Following removal of supernatant, cell pellets were resuspended in 100μL of nucleofector solution (provided in the kit). Each cells suspension was then mixed with ZFN and donor reagents. For each experiment, a minimum of 3 samples were prepared: 1)

ZFN-only control (2µg of ZFN-RNA and $2x10^6$ iPSC), 2) Donor only (4µg or 8µg of donor plasmid), and 3) ZFN+Donor (2µg of ZFN-RNA and 4µg or 8µg of donor plasmid). Each mixture was placed in a cuvette and electroporated in nucleofector, under Amaxa program A23. Following nucleofection, we used 500µL of iPSC medium supplemented with 10µM Y-27632 to gently transfer cells from cuvette to a gelatin-coated 6-well tissue culture plate pre-seeded with puromycin-resistant iMEF. The contents of each cuvette were divided into 2 wells. Starting on the following day, culture medium was changed daily. Puromycin selection (by feeding cells with medium containing 0.5µg/mL of puromycin) started at day 4 post transfection, and approximately 2-5 days later, puromycin-resistant colonies were mechanically picked and transferred to a new 6-well plate for expansion (about 3 to 4 additional passages under puromycin selection).

Following expansion in puromycin-containing medium, each remaining clone was analyzed by target-integration PCR (TI-PCR) with primers spanning the integration site (Table 2). In order to ensure successful amplificatioin of a long product (if targeted integration occurred), we used the Expand Long Template PCR system (Roche Applied Science), as per manufacturer protocol. PCR product was resolved by agarose gel electrophoresis.

2.7 Generation of hematopoietic progenitor cells from iPSC

We used a spin embryoid body (EB)/ OP9 co-culture method for generation of $CD34^+CD43^+$ hematopoietic progenitor cells from pluripotent stem cell lines: WAS,

cWAS, WA01, and WA09. For EB generation, we slightly adapted the Ng et.al. protocol [75]. EBs were generated from single-cell adapted iPSC in expansion phase. All cultures had undergone 6 to 8 passages under TrypLE selection. When using cryopreserved cells, we first thawed and cultured cells on low-density iMEF – coated 6 well plates for two passages prior to experiment.

On the day of experiment, we washed cells twice with DPBS (Invitrogen). We then added 1mL of pre-warmed TrypLE (Invitrogen) into each well and incubated at 37℃ for 2 minutes. This short incubation was sufficient to dissociate the colonies and detach iMEF feeders. Following incubation, we carefully removed TrypLE, and with it most of the iMEF. We added 1mL of hESC medium containing 10μM Y-27632, collected cells by gentle pipetting, and filtered cell solution through a 70μm strainer (BD Biosciences). We counted cells, and aliquotted the necessary number of cells for preparing 4 to 6 96-well plates containing 1 spin EB per well – typically 5000 WA09 cells per EB, and 7000 WAS iPSC or cWAS iPSC per EB. Once the appropriate number of cells was obtained, vials were centrifuged at 430g for 3 minutes at 4℃. Supernatant was removed, and cells were resuspended in hematopoietic differentiation medium – STEMdiff APEL medium (STEM CELL Technologies) supplemented with Stem Cell Factor (SCF; Peprotech), Vascular Endothelial Growth Factor (VEGF; Peprotech), Bone Morphogenic Protein 4 (BMP4; Peprotech), and Y-27632 (Alexis Biochemicals). Table 3 lists the specific amounts of each of these factors required for our iPSC and WA09 hESC lines.

Hematopoietic Differentiation: Spin EB generation					
Cell line	# of cells/EB	SCF (ng/mL)	VEGF (ng/mL)	BMP4 (ng/mL)	Y-27632 (μM)
WA09 hESC	5000	40	20	5	10
WAS iPSC	7000	40	20	10	20
cWAS iPSC	7000	40	20	5	10

Table 3: Optimal cell number and cytokine conditions for hematopoietic differentiation. Both cell number and cytokine levels were empirically determined for each cell line. Table shows optimal conditions used in hematopoietic differentiation experiments.

Using a multichannel pipette and a sterile reservoir, we quickly dispensed 100µL of solution containing the appropriate number of cells into each well of a low-attachment U-bottom 96-well plate (BD Biosciences), such that one EB would be generated per well. Plates were centrifuged at 480g for 7 minutes, at room temperature. Following centrifugation, we verified by microscopy that each well contained the same size cluster of cells centered at the bottom of the well. Plates were placed in incubator at 37℃ with 5%CO_2 and remained in culture for 4 to 5 days. Medium was not changed during this time, with the goal to keep EB undisturbed.

Throughout this initial period in culture, EBs developed significantly, adopting a compact, three-dimensional spherical structure, and growing in size. Four to five days after plating, we harvested EBs by carefully pipetting each EB out of the well using a P1000 pipette. We transferred 16 EBs into each well of a 6-well plate, pre-seeded with $2x10^5$ mitomycin-C –treated murine OP9 bone marrow stromal cells per well. Prior to transfer, each well was washed twice with PBS (Hyclone, Thermo Scientific). EB/OP9 co-culture was maintained for 8 to 9 days in STEMdiff APEL medium supplemented with SCF, VEGF, and BMP4 as previously described. At day 4 post transfer, we refreshed medium by adding 1mL fresh STEMdiff APEL containing the three factors and rock inhibitor into each well.

Subsequent to transfer onto OP9 stroma, we observed the EBs quickly attached to the feeders (typically about 4-6 hours after transfer). On the following 2 to 3 days, EB-generated stromal cells began to spread to the immediate vicinity of the EB. Between days 3 and 4, we observed the emergence of “bubble-like”

vesicles expanding outward from the EB, and, inside these structures, hundreds of small, round, hematopoietic-like cells appeared. Over the next couple of days, more of these cells emerged, and they were released into the stroma. We hypothesized this event indicated the start of hematopoietic differentiation. In order to better capture this dynamic process, we observed one well for 2 days (from day 4 to day 5), by live imaging. Time lapse images were acquired at 20-minute intervals with an Andor IXon3 885 EMCCD camera (Andor) on an Olympus IX-81 (Olympus) microscope fitted with a microscope enclosure (Precision Plastics) maintained at 37℃ with 5% CO2. A final compilation of images resulted in a movie recapitulating the emergence and progression of hematopoietic cell development in the EB/OP9 co-culture.

On day 8 to 9 post transfer, we observed a lot of hematopoietic-like cells floating in culture, and clusters of these cells spread throughout the well. We harvested supernatant, and added 1mL pre-warmed TrypLE into each well. Plates were incubated for 3 minutes, and EBs were collected by adding 1mL of STEMdiff APEL medium into each well, and pipetting vigorously. Subsequently, EBs were pooled and transferred into a 50-mL conical vial (BD Biosciences). We mechanically dissociated EBs by repeatedly passing them through first a 20-gauge needle (3 to 4 times), followed by a 25-gauge needle in a 5-mL syringe (3 to 4 times). Once EB were completely dissociated, solution was filtered through a 70μM cell strainer, and filtered cells were centrifuged at 350g for 5 minutes. We subsequently washed cells once with PBS, resuspended in PBS, and filtered through a 45μM cell strainer, and counted by Trypan Blue exclusion method.

2.8 Flow Cytometric Isolation of $CD34^+CD43^+$ hematopoietic progenitor cells

Progenitors derived from each line – WAS iPSC, cWAS iPSC, and WA09 hESC– were collected after PBS wash, and stained, following manufacturer's protocol, for known hematopoietic surface markers CD34 (Allophycocyanin-conjugated mouse IgG1,κ clone 8G12, BD Biosciences), CD43 (Brilliant Violet 421-conjugated mouse IgG1,κ clone 1G10, BD Horizon), and CD45 (Phycoerythrin-conjugated mouse IgG1,κ clone HI30, BD Pharmingen). Respective isotype controls were also generated for each fluorophore used in the panel. Samples were incubated on ice for 30 minutes, and subsequently washed twice with 1mL FACS buffer (PBS, 2%FBS). After second wash, samples were resuspended in 400µL of FACS buffer per $1x10^6$ cells. Flow cytometric analysis was performed using BDFACS Aria II instrument (BD Biosciences), and we sorted the $CD34^+CD43^+$ hematopoietic progenitor population from each cell line. We observed that, for cWAS-derived progenitors, the sorted population expressed GFP.

2.9 Flow Cytometric Analysis of WASp expression in $CD34^+CD43^+$ hematopoietic progenitor cells

In order to allow for cell receptor turnover to eliminate from the cell surface residual antibodies used for sorting, we cultured sorted $CD34^+CD43^+$ hematopoietic progenitor cells for approximately 36 hours prior to immunostaining. During this time, cells were maintained in STEMdiff APEL medium supplemented with SCF, VEGF, and BMP4, as described in the previous section.

WASp is an intracellular protein, and, in order to assess WASp expression in sorted $CD34^+CD43^+$ hematopoietic progenitor cells, we first centrifuged approximately $5x10^5$ cells from each line, for each condition. We aspirated supernatant and vortexed each tube to dislodge the pellets. Cells were resuspended in 100µL of fixation medium (Reagent A, Invitrogen Fix & Perm kit) and incubated at room temperature for 15 minutes. Following incubation, cells were washed with 2mL of PBS supplemented with 5%FBS, and subsequently centrifuged at 300g for 5 minutes. Again cell pellets were dislodged by vortexing, and resuspended in 100µL (final volume) of permeabilization medium (Reagent B, Invitrogen Fix & Perm kit) containing either 20µL mouse monoclonal anti-WASp-APC B-9 IgG_{2a} antibody (Santa Cruz Biotechnology), or the respective isotype control. Following 20-minute incubation at room temperature, cells were washed with PBS/5%FBS and re-suspended in 300µL of FACS buffer. Cells were analyzed on BDFACS Aria II instrument (BD Biosciences).

2.10 Colony-Forming Assay

Through flow cytometry sorting, we obtained total $CD34^+$ cells from day 14 differentiation of WAS, CWAS, and WA09. We centrifuged $1.5x10^5$ cells per line at 350g for 5 minutes. We resuspended each cell pellet in 1.5mL of PBS. To each vial of cell solution, we added hSCF (100ng/mL), hFlt3L (100ng/mL), hMGDF/TPO (100ng/mL), hIL-6 (10ng/mL), hIL-3 (10ng/mL), hGM-CSF (10ng/mL), hG-CSF (10ng/mL), and EPO (4units/mL) (all from Peprotech).

In a 50-mL falcon tube, we prepared colony assay medium by mixing together Methyl Cellulose (STEMCELL Technologies) + 1% BSA (Sigma) + 30% FBS (Hyclone, Thermo Scientific) using a 5mL syringe. We then added each cell-growth factor mixture to 4.5mL of methyl Cellulose colony assay medium, and vortexed vigorously to mix the contents well. Using a clean 5mL syringe, we transferred approximately 1.5mL of mixture into each of 3 35mm sterile tissue culture plates. Subsequently, plates were incubated in humidifier chamber at 37℃ with 5% CO_2 for 14 days. We performed two experiments, each in triplicate.

2.11 Reverse Transcription PCR (RT-PCR) analysis

We performed RT-PCR analysis of RNA isolated from sorted $CD34^+CD43^+$ hematopoietic progenitor cells for detection of WASp mRNA and GFP mRNA in the cells derived from cWAS iPSC. First, we isolated total RNA from iPSC and control hESC WA09 (RNeasy kit, Qiagen) lines, and synthesized cDNA by reverse transcription using Improm-II Reverse Transcription System (Promega). We quantified RNA in a Nanodrop spectrophotometer. Approximately 150ng of cDNA was added into a PCR reaction for specific amplification of WAS mRNA using primers binding to exon 9 (forward primer) and the exon junctions between exons 10 and 11 (Table 2), yielding a 445bp-long amplicon. For detection of GFP mRNA, we seeded approximately 150ng of cDNA into each PCR reaction and using primers binding the exon 11-12 junction of the *WAS* gene and GFP, yielding a 613-bp long amplicon. All RT-PCR reactions were performed using Platinum Taq High Fidelity

Polymerase (Invitrogen) utilizing 1X Enhancer (Invitrogen) and, in both cases, cDNA was amplified for 30 cycles, and then subsequently resolved by agarose gel electrophoresis. Negative-control reactions were performed using material generated in a minus-RT reverse transcription reaction (RNA material which did not undergo reverse-transcription due to absence of Reverse Transcriptase enzyme in the reaction). In the case of GFP mRNA analysis, DNA isolated from cWAS iPSC was used as a positive control for amplification.

Subsequent to PCR-amplification, material generated for analysis of WASp mRNA was purified by a spin-column system (NucleoSpin® Gel and PCR Clean-Up, Clontech) and submitted for Sanger sequencing analysis to LoneStar Sequencing (Houston, TX). We utilized the same forward and reverse PCR primers for bi-direction sequencing of purified material. We analyzed sequencing results using Lasergene SeqMan analysis software.

2.12 Generation of Natural Killer (NK) cells

Immediately following flow cytometric analysis and cell sorting, we initiated NK differentiation of $CD34^{+}CD43^{+}$ progenitors derived from each of our lines – WAS, cWAS, and WA09. In order to accomplish that, two days prior to sorting, we seeded 24-well plates (BD Biosciences) with $5x10^{4}$ live OP9-DL1 murine stromal cells that express the Notch ligand Delta –like 1. Cells were incubated overnight at 37℃ with 5% CO_2 in alpha-MEM medium supplemented with 20% FBS, 2mM L-glutamine, and 1X Pennicillin-Streptomycin (P/S; Invitrogen). The following day, each well

was washed twice with PBS, and seeded with $3x10^4$ to $5x10^4$ sorted $CD34^+CD43^+$ progenitors per well and kept in NK cell differentiation medium containing: 56.6% DMEM-high glucose, 28.3% HAMS/F12 (Invitrogen), 15% heat-inactivated human AB serum (Valley Biomedical), 2 mM L-glutamine (Invitrogen), 1 uM β-mercaptoethanol (Sigma), 5 ng/mL sodium selenite (Sigma), 50 uM ethanolamine (MP Biomedicals), 20 mg/L ascorbic acid (Sigma), 1% P/S (Invitrogen), 20 ng/mL SCF, 20 ng/mL IL-7 (PeproTech), 10 ng/mL IL-15 (PeproTech), 10ng/mL Flt3 ligand (Flt3L) (PeproTech), and 5 ng/mL IL-3 (first week only) (PeproTech) [76]. Medium was prepared fresh on the day of experiment. Cells were cultured in this system for 28-32 days, with half-medium changes occurring every 3-4 days. Umbilical cord blood (UCB)-derived $CD34^+$ cells were plated under the same conditions and used as NK differentiation control.

NK cells were also generated (unintentionally) as a by-product of a T-cell differentiation protocol, as described in Timmermans et.al. [77]. Day 12 spin EBs were first dissociated as previously described [77] and cells were resuspended in MEM-α medium supplemented with 20% FBS, SCF (10 ng/ml), fms-like tyrosine kinases 3 receptor (Flt3-L: 5 ng/ml; Peprotech) and rhIL-7 (5 ng/ml; R&D Systems). Cells were transferred onto subconfluent OP9-DL1 cultures. Every 3 days, medium was refreshed by half-medium changes, and every 5-7 days, cells were transferred onto a fresh OP9-DL1 monolayer. Progenitors were kept in this culture system for a period of 6-weeks.

2.13 Flow Cytometric Isolation of NK cells and analysis of NK phenotype

At the end of 28 days of differentiation in OP9-DL1 co-culture, cells were harvested by removing the supernatant first, followed by brief dissociation in TrypLE to dislodge hematopoietic cells that remained attached to stroma (500µL of TrypLE reagent was added into each well, and plates were incubated at 37℃ for 2 minutes). Following TrypLE dissociation, each well was washed twice with NK differentiation. Cells were collected, filtered through a 70µM strainer, and centrifuged at 350g for 5 minutes. We aspirated supernatant, resuspended cells in PBS by vigorous pipetting, and filtered through a 45µM cell strainer. This material was centrifuged again at 350g for 5 minutes, and cells were finally re-suspended in FACS buffer. Mature $CD45^{+}CD56^{+}$ NK cells were phenotyped by flow cytometric analysis at day 28-30 (CD56-AF647 and CD45-PE antibodies, BD Pharmingen). Individual reactions for analysis of NK-specific receptors CD16, NKG2D, CD94, and CD117, were prepared using the following antibodies: CD16-PE, NKG2D-PE,CD94-APC, and CD117-PerCP-Cy5.5 (all from BD Biosciences). Analysis was performed on BDFACS Aria I instrument (BD Biosciences).

2..14 Immunological analysis of NK-cell effector function

In order to detect restoration of proper immune response by NK cells derived in our differentiation experiments when in the presence of K562 leukemia cells, we examined the secretion of Inerferon-gamma (IFN-γ) and Tumor-necrosis factor alpha (TNF-α) when NK cells were co-cultured overnight with K562 at 1:1 effector-

target ratio. Upregulatioin of cytotoxic cytokine levels was analyzed utilizing the Cytometric Bead Array (CBA) microbead capture system (BD Biosciences).

2.15 Western Blot Analysis for detection of WASp

Approximately $1.5x10^6$ to $3x10^6$ sorted $CD34^+$ progenitor cells or $CD56^+$ NK cells from each line were collected by centrifugation at 350g for 5 minutes at room temperature. Supernatant was removed and cells were washed once with PBS. Following centrifugation and removal of PBS, working on ice, we resuspended cells in 100µL to 200µL of RIPA buffer containing 1 protease inhibitor cocktail tablet (cOmplete Protease Inhibitor Cockail tablet, Roche Applied Science) and transferred cells to a 1.5mL-eppendorf microtube. We cells lysed for 30 to 60 minutes on ice. Following lysis, tubes were spun down at 13,000rpm for 10 minutes at 4℃. Protein supernatant was subsequently removed, and cell debris discarded in the pellet. We added 5µL of each lysate to 95µL of dH_2O to generate 20x dilutions, and measured protein concentration by Bradford Colorimentric Assay (Pierce BCA™ Protein Assay Kit, Thermo Scientific). Our standards were generated from bovine serum albumin (BSA) dilutions as indicated in manufacturer's protocol (Bio-Rad Protein Assay Standard II).

Each sample was prepared by taking 10µg of total protein and adding 1X Reducing agent (novex NuPAGE Sample Reducing Buffer (10X); Life Technologies). We then added 1X novex NuPAGE LSD sample buffer (4X) (Life Technologies) to each sample. Using RIPA buffer, we adjusted the final volume to

70µL. We pre-washed NuPAGE 7% Tris-Acetate gel (Life Technologies) 3 to 4 times with dH_2O to remove gel debris and bubbles. We then placed gel in the electrophoresis apparatus. After locking it in position, we filled the inner chamber with 20X Tris-Acetate SDS Running Buffer (Life Technologies) containing 500µL Antioxidant (Invitrogen NuPAGE) for each 200mL of running buffer. The outer chamber was filled with 1X Tris-Acetate SDS Running Buffer. We finally loaded each sample into a well of the gel. We loaded 8µL of protein standard solution molecular weight marker (Precision Plus Protein Standard, BioRad). We ran the gel for approximately 1 hour, at 100V for the first 10 to 15 minutes, and 150V for the remainder of the time). In order to prepare for gel transfer, we soaked the nitrocellulose transfer membrane (Amersham Biosciences Hybond-C Extra Pore size 0.45µm), Whatman filter paper, and sponges in 1X Transfer Buffer (Invitrogen NuPAGE) containing 10% methanol. We assembled the transfer "sandwich" (using the soaked sponges, filter paper, and membrane) closed the chamber, and placed it in the electrophoresis apparatus. We ran transfer for 2.5 hours at 45V, on ice.

Following transfer, we blocked non-specific binding by incubating membrane in Blotto blocking buffer (5% solution of non-fat milk in Tris-buffered saline, Thermo Scientific) for 30 minutes at room temperature with gentle shaking. We subsequently incubated the membrane in a 1:1000 dilution of anti-human WASp antibody clone 5A5 (mouse monoclonal IgG2a,κ; BD Biosciences) in TBS buffer overnight at 4℃. On the following day, we washed the membrane with approximately 10mL of TBS buffer (enough to completely cover membrane) for 7 minutes with gentle shaking. We washed 4 times, for a total of 30 minutes.

Following the washes, we diluted an HRP-conjugated secondary antibody (anti-mouse IgG; Cell Signaling Technologies) 1:5000 in blocking buffer, and incubated membrane in secondary antibody dilution for 1 hour at room temperature on an orbital shaker. We then washed the membrane with TBS buffer four times, as described above in this section.

Detection of target protein was obtained by mixing Reagent A (Luminol Ehancer solution), and Reagent B (Peroxide solution) (both from Amersham ECL Prime Western Blotting Detection Reagent kit) at a 1:1 ratio to a final volume of 1mL, sufficient to cover the membrane. We then mixed reagents well, and pipette the solution over the membrane, allowing it to incubate for 1 to 3 minutes. After draining the excess liquid, we transferred the membrane onto a piece of clear plastic wrap, and wrapped it carefully, avoiding airl bubbles. We placed the protein blot side-up on a photo cassette, and exposed negatives (Amersham Hyperfilm) onto membrane and developed the films to obtain final Western results.

2.16 Comparative Genomic Hybridization Analysis

We isolated DNA from WAS iPSC and cWAS iPSC, and 8ug of each purified material was sent to WiCell for comparative genomic hybridization and Single-nucleotide polymorphism (SNP) analyses. Samples were analyzed using the Agilent SurePrint G3 Human Genome CGH+SNP Microarray. This array analysis is capable of detecting copy number gains and losses, copy neutral aberrations, and mosaicism. Data analysis was also done by WiCell.

2.17 Cell preparation and flow cytometric sorting of WASp^{+} revertant cells

Peripheral blood mononuclear cells (PBMCs) were isolated by Ficoll-Hypaque density gradient (GE Healthcare) for both patient samples and normal controls. Immediately following isolation, cells were sub-fractionated into distinct lymphocyte populations by magnetic bead separation (Dynalbeads, Invitrogen).

Cells were initially stained for cell surface antigens using FITC-conjugated anti-CD4 antibody and Phycoerythrin (PE)-conjugated anti-CD8 antibody (BD Biosciences) for T-cells, APC-conjugated anti-CD45RO (BD Biosciences) for distinguishing between memory and naïve T-cells. Subsequently, cells were washed, then fixed and permeabilized with Caltag Fix & Perm kit (Invitrogen), and further stained with anti-hWASP mouse monoclonal antibody (clone B9, Santa Cruz), or purified mouse IgG for 30 min at 4℃. Stained cells were analyzed and sorted by FACS Aria flow cytometer and analyzed using DIVA software (Becton Dickinson). Positive and negative cell populations were obtained by fluorescence cell sorting.

2.18 DNA Isolation and PCR assay

Sorted cells were lysed by incubation with a detergent solution containing protein K for 2 hours at 42℃. Following lysis, DNA was amplified using fusion primers spanning the region of interest. Fusion primers were designed based upon recommendations from Roche 454 for generation of product suitable for next generation sequencing. Primer sequences: forward 5'→3'gaggctcagaagaaatcaatg,

and reverse 5'→3' agctactggacgttctgga. Each primer carries an identifier sequence (MID) and an adaptor sequence determined by Roche 454, and selected for each cell type. Utilizing these primers, each population was amplified in two rounds of 30 cycles each with a unique MID, in order to allow for amplicon origin identification after sequencing. Appropriate PCR product was confirmed by gel electrophoreises and purified using Agencourt AmPure XP PCR purification kit (Beckman Coulter). The integrity of purified PCR was further verified by bioanalysis using the 2100 Bioanalyzer (Agilent Technologies).

2.19 Next-Generation Sequencing

Purified PCR product was submitted to Family Tree DNA in Houston, Texas. Each amplicon pool was subjected to emulsion PCR and subsequent bi-directional sequencing using Roche 454 GS Titanium Sequencing kit. Sequences were obtained and analyzed using Roche GS Amplicon Variant Analyzer software. Since each lymphocyte population from WAS 4 and WASJ patients were amplified using primers carrying different multiplex identifier (MID) sequences, individual populations were separated based on the presence of said MIDs, as listed in table 4 below. Analysis was then performed on each population separately, and each genotypic variant identified was catalogued. The total number of forward and reverse sequence reads carrying the same variant was also obtained for each genotypic variant identified, and the percentages of each group of forward and

reverse reads were obtained. The final percentage was determined by taking the mean of the individual percentages obtained for forward and reverse reads.

CHAPTER 3: RESULTS

3.1 Generation and characterization of WAS-patient derived induced pluripotent stem cells (WAS-iPSC)

We obtained skin fibroblasts from a WAS patient through Coriell Cell Repositories (Corielle # GM01598). Initial Sanger sequencing analysis identified the patient's germ line mutation as an insertion of a G at position 1305 in exon 10 of the *WAS* gene. This insertion leads to a frame-shift at amino acid 424 of WASp, resulting in an aberrant amino acid sequence throughout the C-terminal VCA domains of WASp and premature truncation, which is believed to lead to degradation of protein. This region of the protein contains a common acting monomer-binding motif and an acidic region which activates the actin-related protein (Arp2/3) complex known to be a key player in polymerization of G-actin [8]. Thus, the C-terminus of WASp plays a crucial role in WASp-dependent signaling necessary for proper actin polymerization and cytoskeleton reorganization in hematopoietic cells, as illustrated in Figure 1.

Using retroviral vector-mediated gene delivery, we transduced WAS fibroblasts with five transcription factors previously reported to induce reprogramming: OCT4, SOX2, KLF4, CMYC, AND NANOG [63, 64]. Approximately 2 weeks following transduction, we observed the emergence of human embryonic stem cell (hESC)-like colonies. We isolated and further expanded 11 clones in culture, all of which continued to display both the morphology and proliferation properties consistent

with those of hESC. We isolated these cells for characterization. First, we confirmed cells maintained normal karyotype (Figure 5C) and carried the 1305insG germline mutation in the WAS locus (Figure 5A). Subsequently, cells were analyzed through immunofluorescence staining and flow cytometry, and shown to express the characteristic markers of undifferentiated human pluripotent stem cells -TRA1-81, SSEA-A and Oct4 - and exhibited alkaline phosphatase activity consistent with hESC-like phenotype (Figure 5B). Lastly, teratoma formation assays provided final confirmation of pluripotent function of WAS iPSC (Figure 5).

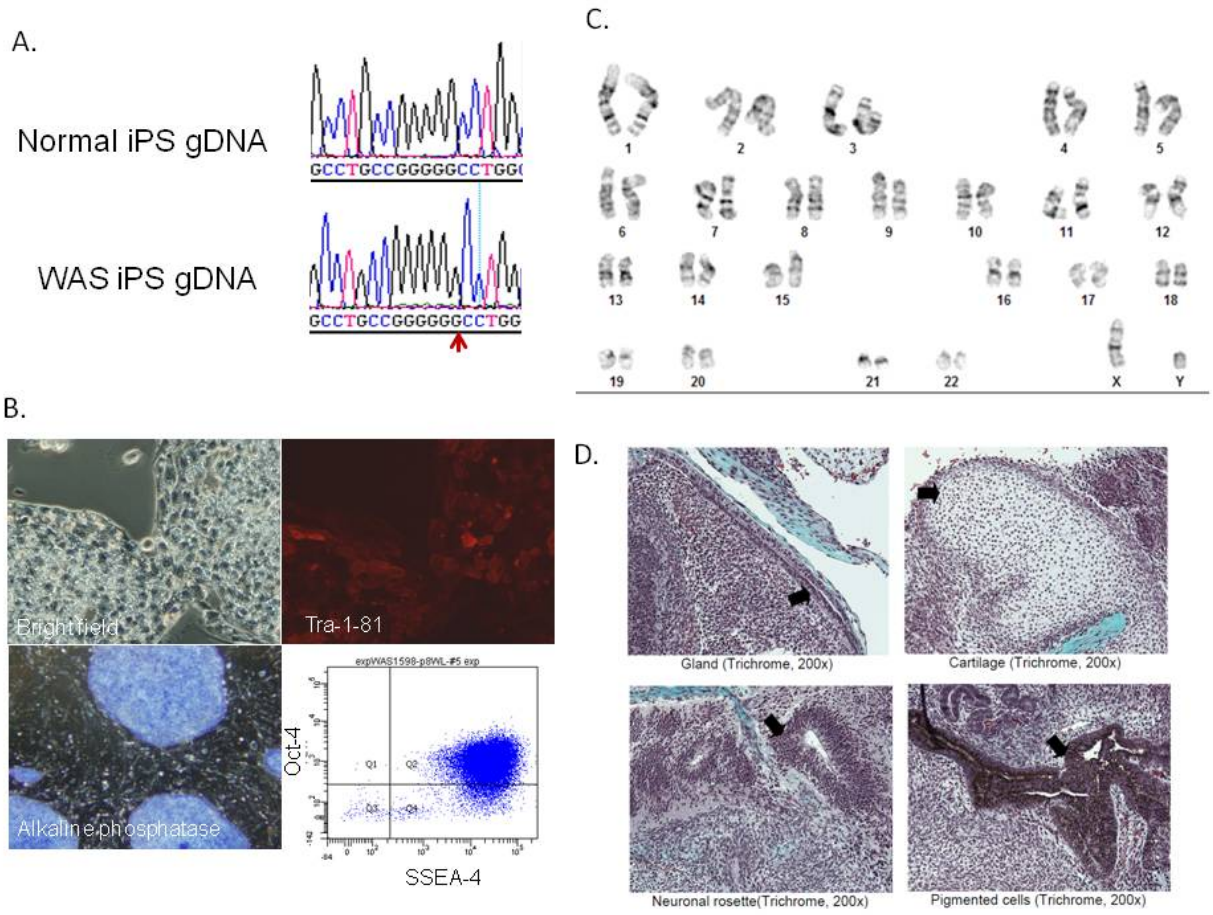

Figure 5: WAS iPSC characterization. A. Sequencing analysis shows 1305insG in WAS iPSC; B. Expression of pluripotent markers, TRA1-81 and SSEA-4 surface antigens and Oct4 transcription factor, and alkaline phosphatase activity; C. Karyotype analysis shows normal, male karyotype. D. Teratoma formation assay - tissues from all germ layers originated from WAS iPSC demonstrating pluripotent activity.

Additionally, we assessed pluripotency gene expression in WAS iPSC by quantitative reverse-transcription PCR (qRT-PCR), and demonstrated expression levels in patient-specific iPSC were comparable to those seen in WA09 human embryonic stem cells (hESC), used as control in this experiment. (Figure 6).

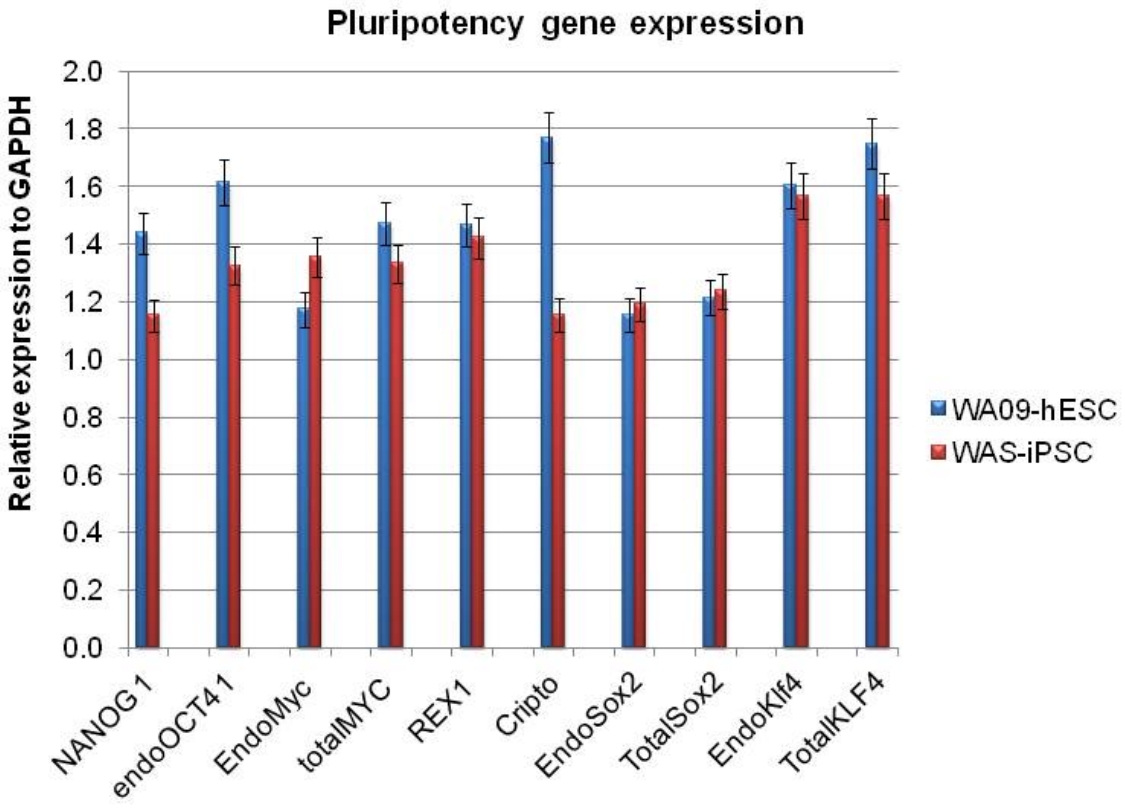

Figure 6: Expression of pluripotency genes in WAS iPSC compared to normal WA09 hESC.

3.2 Analysis and optimization of Zinc-Finger nuclease (ZFN) activity

In order to identify high-efficiency ZFNs for targeting the WAS locus, we analyzed two sets of ZFN plasmids – S1 ZFN and S4 ZFN – recognizing sequences in exon 1 and intron 1 respectively. These proprietary reagents were provided to us as a generous gift through collaboration with Sangamo Biosciences.

We initially tested the efficiency of the WAS-ZFN by delivering the nucleases to K562 cells by Amaxa electroporation. This erythroleukemia cell line was derived from a female patient, thus carrying two copies of the *WAS* gene, one on each X-chromosome [78]. Three days following transfection, we sampled the cultures for DNA analysis by PCR utilizing primers flanking the cleavage site (Figure 7).

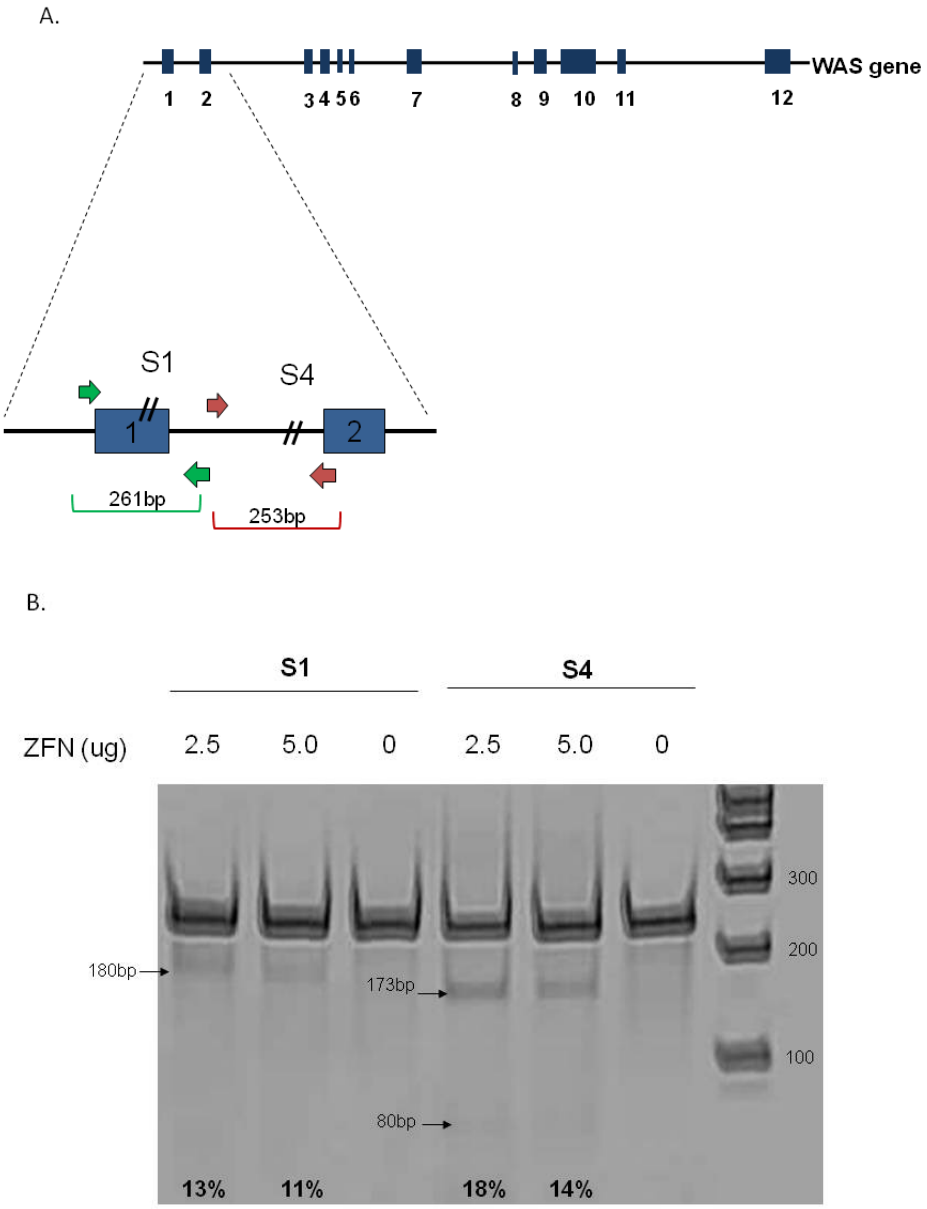

Figure 7: Assessment of ZFN activity on the WAS locus by CEL-1 assay. A. Schematic illustrating ZFN cutting sites and amplification strategy for CEL-1 analysis. B. CEL-1 digestion of material derived from K562 cells treated with S1 or S4 ZF

Following a denaturation-annealing cycle, the product was digested using CEL-1 nuclease for detection of allelic mismatches due to NHEJ error-prone DSB repair, as previously illustrated in Figure 3. The digested bands were resolved by gel electrophoresis, and by comparing their relative intensity to that of the parental band, a measure of CEL1 activity at the mismatch sites was obtained using the equation: %CEL-1= (1-(√parental fraction))x100 (Figure 7B). This value reflects the level of ZFN-mediated cleavage that induced NHEJ repair in treated cells [56]. We continued culture of treated cells for an additional 4 days, and observed signs of toxicity in S1-treated cells in the subsequent days following ZFN-treatment. Cells looked unhealthy, lost viability, and did not proliferate as well as S4-treated cells. S4-treated cells survived and proliferated at the same rate as no-ZFN control cells, indicating no toxicity due to either intron-targeting by ZFN or potential off-target effects.

3.3 Targeted Endogenous Integration in K562 cells

Once we established efficient ZFN activity in K562 cells, we proceeded to test our ability to target the WAS locus in these cells. We chose to move forward with S4-ZFN, and constructed donor molecules which contained approximately 750bp of WAS-homologous sequences on either side of the cleavage site. Our first donor template consisted of only a small 45-bp DNA patch containing a *BamHI* endonuclease recognition site (Figure 8).

A.

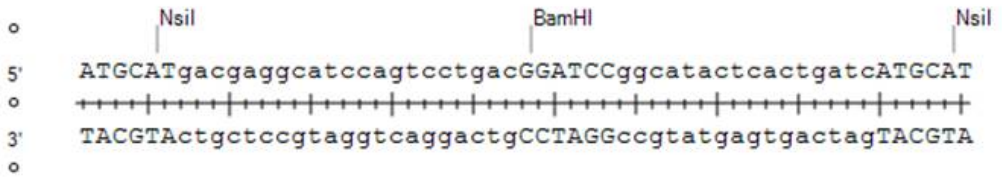

B.

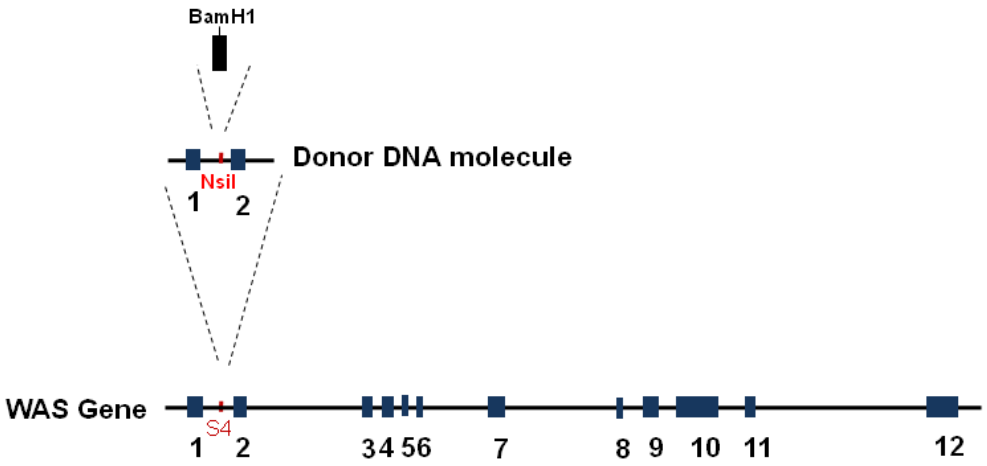

Figure 8: Patch Donor DNA construction. A. Sequence of oligonucleotide patch containing *BamHI* restriction enzyme site. B. Schematic illustrating strategy for targeting homologous donor molecule to S4 site on *WAS* gene.

This enzyme is not present in the endogenous sequence, thus providing us with a tool for detection of integration. Using Amaxa nucleofection, we delivered ZFN and donor template at different doses and identified a combination of ZFN-donor (2.5μg and 20μg, respectively) that resulted in the highest level of targeted integration, as assessed by *BamHI* digestion (Figure 9), with 23% efficiency, as calculated by the ratio of the sum of fluorescence intensities from both digested bands over the total (taking into account the base-pair length of each band).

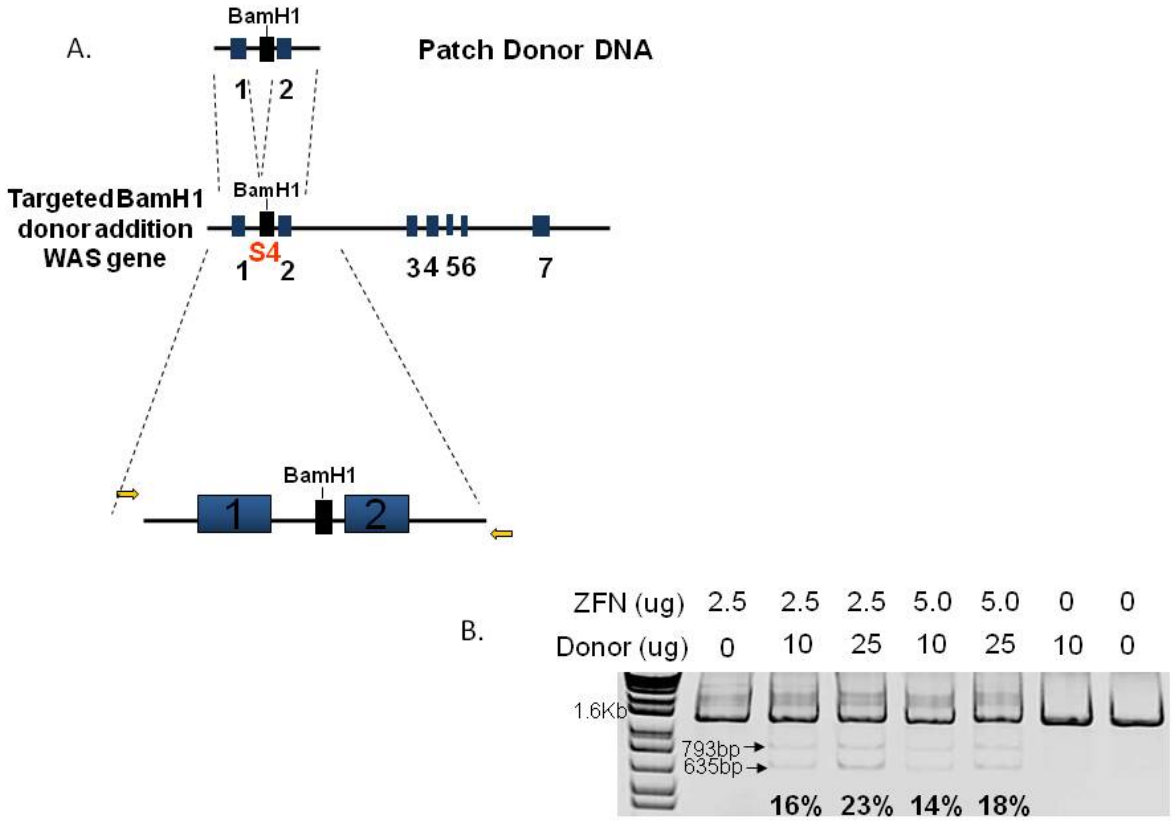

Figure 9: Detection of Patch donor integration in K562 cells. A. Schematic illustrating PCR strategy for detection of donor integration. B. *BamHI* restriction enzyme digestion of material derived from K562 cells treated with donor and ZFN at different doses, as outlined above gel image.

Because the efficiency of homology-directed repair decreases with larger donor templates [47], we built a 1.6kbp-long GFP reporter construct targeted for insertion in the endogenous WAS locus. This donor comprised a GFP reporter gene driven by the human phosphoglycerate kinase (PGK) promoter flanked by the same homology arms as the previous *BamHI* donor. We nucleofected K562 cells with ZFN+donor as well as donor-only to account for any potential off-site integrations that can occur due to spontaneous DSB. We detected GFP^+ cells within 48-72 hours following transfection, and at day 7 we sorted the GFP^+ population from both conditions. We subsequently expanded the sorted cells in culture for a period of three weeks, and extracted DNA for PCR analysis. As illustrated in Figure 10A, targeting at the intended site in intron 1 of the WAS gene could be easily identified by a PCR assay. Utilizing primers placed on the left homologous arm of the donor molecule (forward primer in schematic), and in the endogenous *WAS* gene intronic sequence (reverse primer in schematic), a 3kb-long band indicating successful targeting at S4 site (as shown in Figure 10B). A smaller band of 1.4kb in size was also identified, representing the proportion of alleles in which no integration of donor sequences occurred. We observed targeted endogenous integration in only the GFP^+ cells which received both ZFN and donor, at an efficiency of 30%, as estimated by densitometry analysis (Figure 10C) in the same manner as calculated for the *BamHI* donor integration experiment previously described in this section.

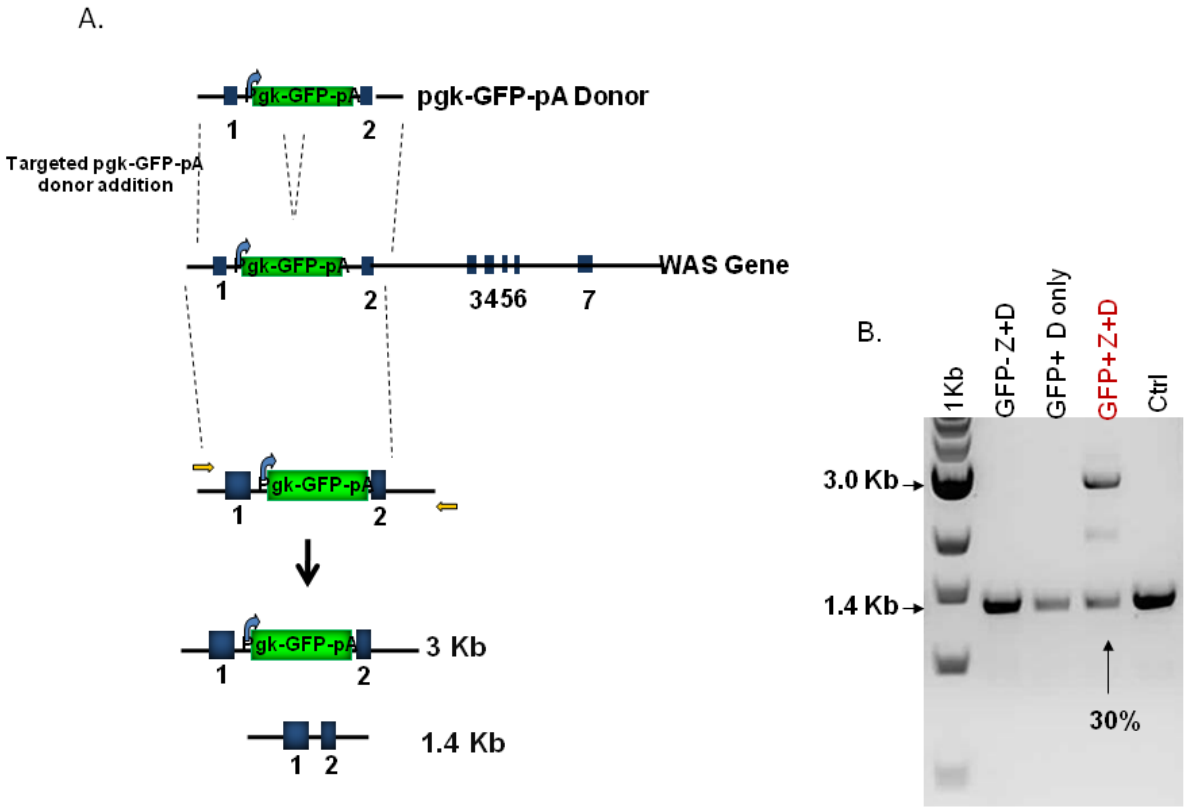

Figure 10: Targeted endogenous integration of PGK-GFP donor in K562 cells.

A. Schematic illustrating targeted integration and expected sizes for PCR products.

B. Agarose gel electrophoresis analysis of PCR product showing targeted integration (3.0kb band) in GFP^+ K562 cells treated with ZFN and donor.

3.4 Targeted Endogenous Integration in WAS-iPSC for correction of WAS mutations

Unlike other monogenic diseases for which there is only one single causative mutation, different mutations on the *WAS* gene can lead to undetectable WASp expression and thus cause the WAS phenotype observed in patients. No single mutation has been reported as predominant in patients. Therefore, a correction approach needs to repair most of the reported mutations [5] in order to be applicable to most patients. Taking this into account, we built a donor molecule designed for use with S4-ZFNs with the goal of integration in intron 1 of the *WAS* gene. This donor consists of wild-type WAS cDNA sequences for exons 2 through 12 (WAS_{2-12}), thus covering almost all the possible exonic disease-causing mutations that have been reported. We introduced a silent point-mutation at position 995 of exon 10 sequence by replacing the wild-type cytosine (C) with an adenine (A). This change modifies the existing XhoI restriction enzyme recognition sequence (CTC*GAG) to an XbaI recognition sequence (TCTA*GA), while still encoding for the same amino acid, Arginine. This silent modification gives us a valuable tool for distinguishing between mutant and corrected mRNA material.

The WAS_{2-12} cDNA was preceded by splice acceptor sequences and, together, these were linked to a green-fluorescent protein (GFP) reporter gene via 2A peptide sequences to generate a bicistronic reporter donor molecule. The 2A sequences are a short peptide (20 amino acids long) and are derived from a group of virus named *Aphthoviruses*, an example of which is the *Foot-and-mouth disease virus*. These short peptides have been shown to induce a novel “cleavage” event, by

acting co-translationally and preventing the formation of a normal peptide bond between the glycine and the last proline which, in turn, causes the ribosome to skip to the next codon, and the subsequent cleavage between the glycine and the proline. This results in the release of discrete protein products in stoichiometric proportions, with most of the 2A peptide fused to the upstream protein [79, 80].

In order to allow for selection of successfully-targeted iPS clones, we subsequently cloned in a selection cassette containing a murine phosphoglycerate kinase (pgk) promoter-driven Puromycin-Thymidine Kinase selection markers. The repair template along with the selection cassette were flanked by approximately 750bp-long WAS-gene-homology arms on either side, yielding the final homologous donor molecule utilized for targeted correction in WAS iPSC (Figure 11).

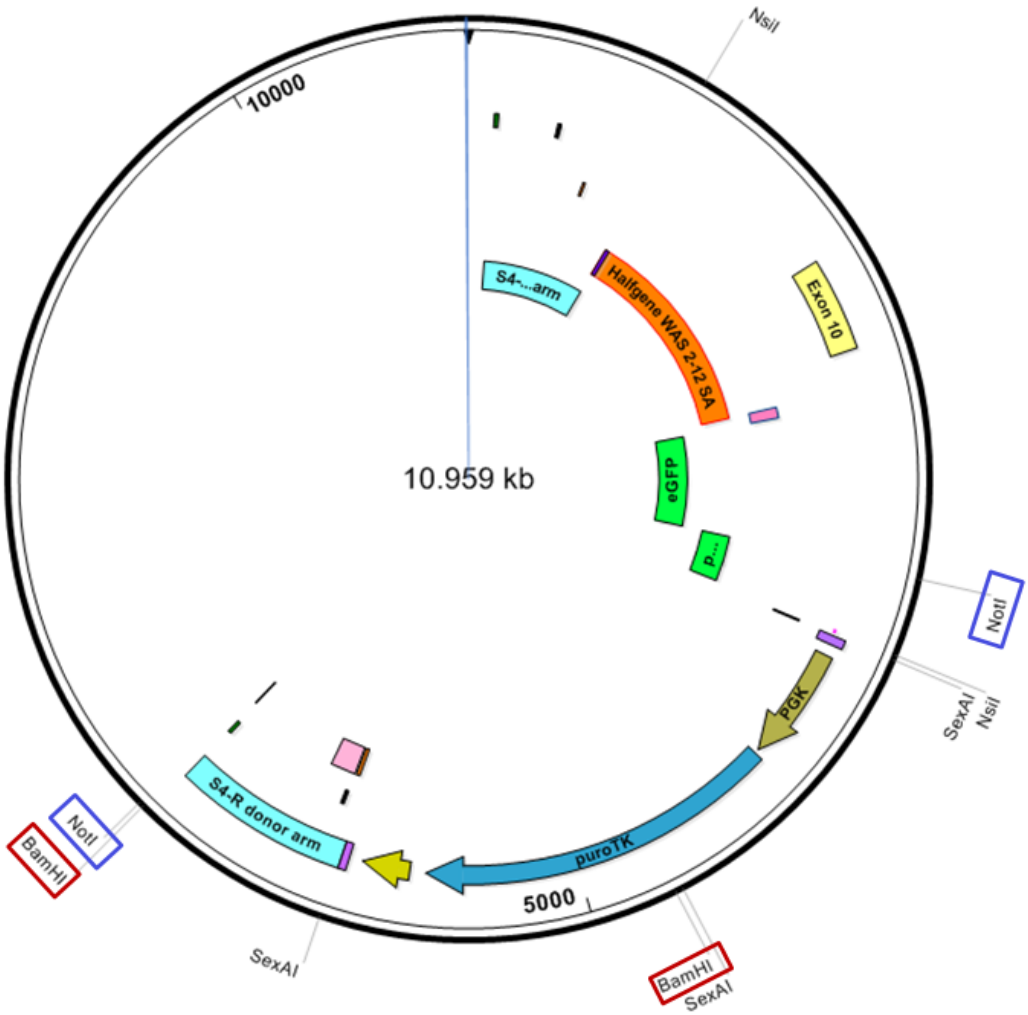

Figure 11: Donor template for correction of WAS. Final donor construct, containing flanking homology arms, corrective WAS sequences, GFP reporter gene, and selection cassette. Marked in blue and red boxes are the enzyme selections used for initial confirmation of successful cloning.

We confirmed successful cloning by PCR analysis using the same fusion primers (initially used for cloning) for the amplification of the insert, and detected 5 clones out of 18 which had the expected insert (Figure 12A). We further evaluated clones 1, 2, 9, and 10 for correct assembly by digestion with BamHI and NotI restriction enzymes. Based on the plasmid map we constructed (Figure 11), we expected each enzyme to cleave the donor plasmid in two separate places, yielding two digested bands in each case (BamHI→ 2.2kb and 8.8kb; NotI→ 3.7kb, and 7.2kb) (Figure 12B).

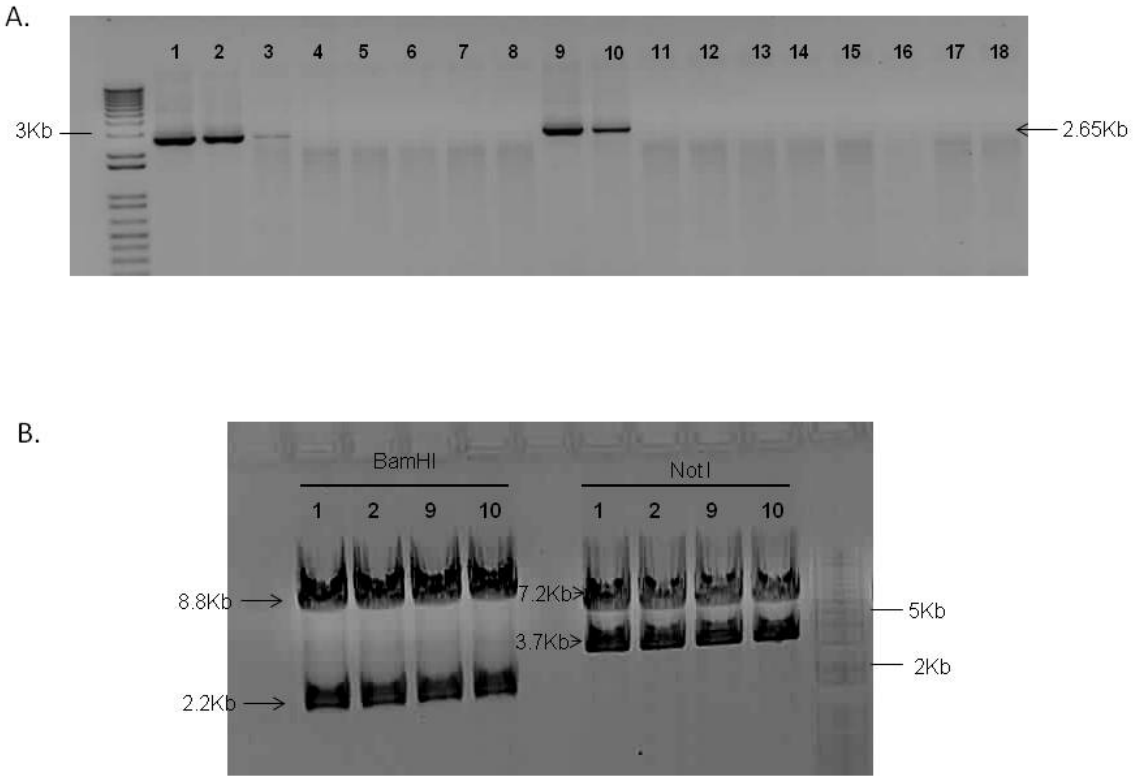

Figure 12: Validation of donor construction by PCR and restriction endonuclease digestion. A. PCR amplification of insert resulted in detection of 5 potentially correct clones. B. Further assessment by *BamHI* and *NotI* restriction enzyme digestion confirms correct clones.

We co-delivered S4-ZNFs and the $WAS_{2\text{-}12}$-2A-GFP donor construct to WAS-iPSC by Amaxa nucleofection. Three days later, DNA was isolated from ZFN-only control, and ZFN activity was determined to be 16% in iPSC using CEL-1 Assay (Figure 13A). Following subsequent culture under puromycin selection, the 7 surviving clones were analyzed by Targeted Integration PCR assay (TI-PCR) utilizing primers placed in the endogenous WAS sequences flanking the donor homology arms. This analysis revealed 6 clones had the desired integration in intron 1 of the *WAS* gene (Figure 13B).

A.

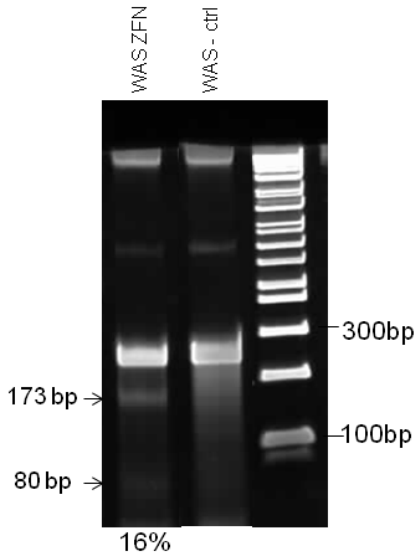
WAS ZFN
WAS - ctrl
300bp
100bp
173 bp
80 bp
16%

B.

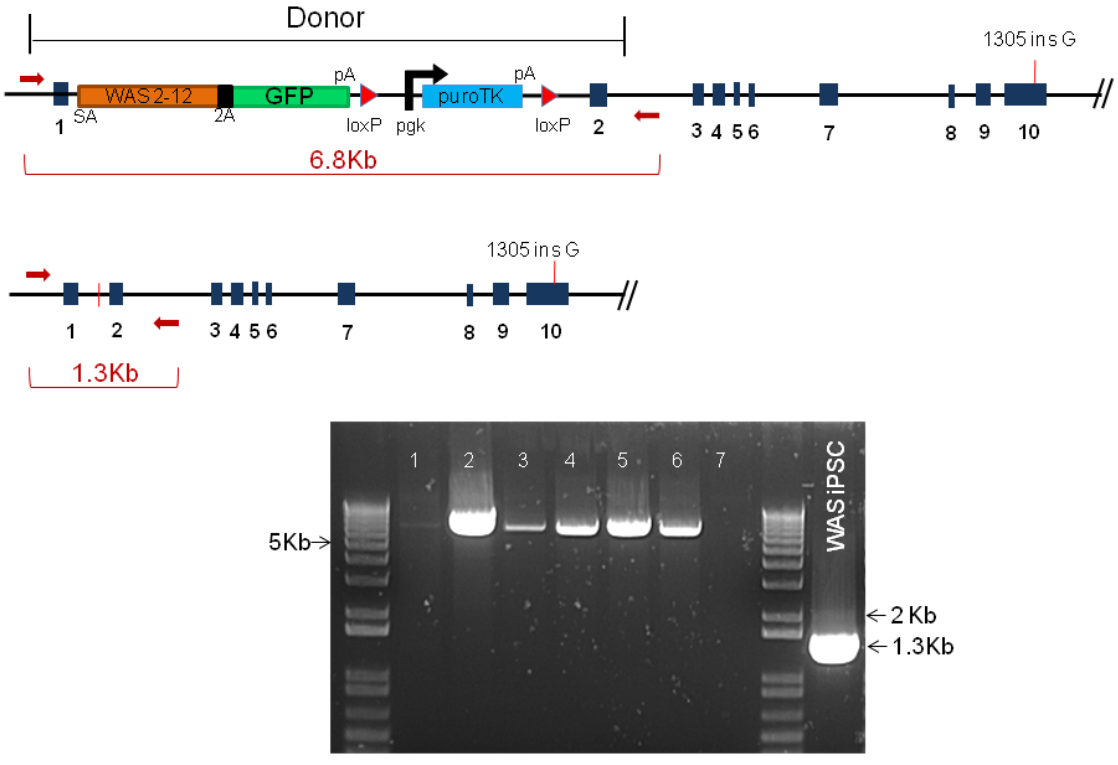
Donor
1305 ins G
pA
pA
WAS 2-12
GFP
puroTK
1
SA
2A
loxP
pgk
loxP
2
3 4 5 6
7
8
9
10
6.8Kb
1305 ins G
1
2
3 4 5 6
7
8
9
10
1.3Kb
1
2
3
4
5
6
7
WAS iPSC
5Kb
2 Kb
1.3Kb

Figure 13: CEL-1 activity and Targeted endogenous integration in WAS iPSC. A. ZFN efficiency in WAS iPSC determined by CEL-1 assay. B. Schematic illustrating PCR strategy for detection of targeted clones. PCR amplification of puromycin-resistant clones was resolved by gel electrophoreisis and shows the intended targeting at the *WAS* locus in 6 out of 7 clones.

In a control experiment, we delivered ZFNs only to iPSC, and determined cleavage efficiency by CEL-1 assay to be 16% (Figure 13A). Based on clone stability in culture over several passages (i.e. retaining undifferentiated hESC-like morphology), we selected clone 5 for further characterization. In order to confirm integration of our transgene occurred only once in the cellular genome, and at the intended site, we performed Southern Blot analysis of cWAS clone 5. By digesting DNA material from targeted and mutant iPSCs with enzymes (*PvuII* and *ScaI*) which cleaved in a pattern that allowed for detection of on and off-site integrations, the results showed only the desired WAS-intron 1 integration was present (Figure 14).

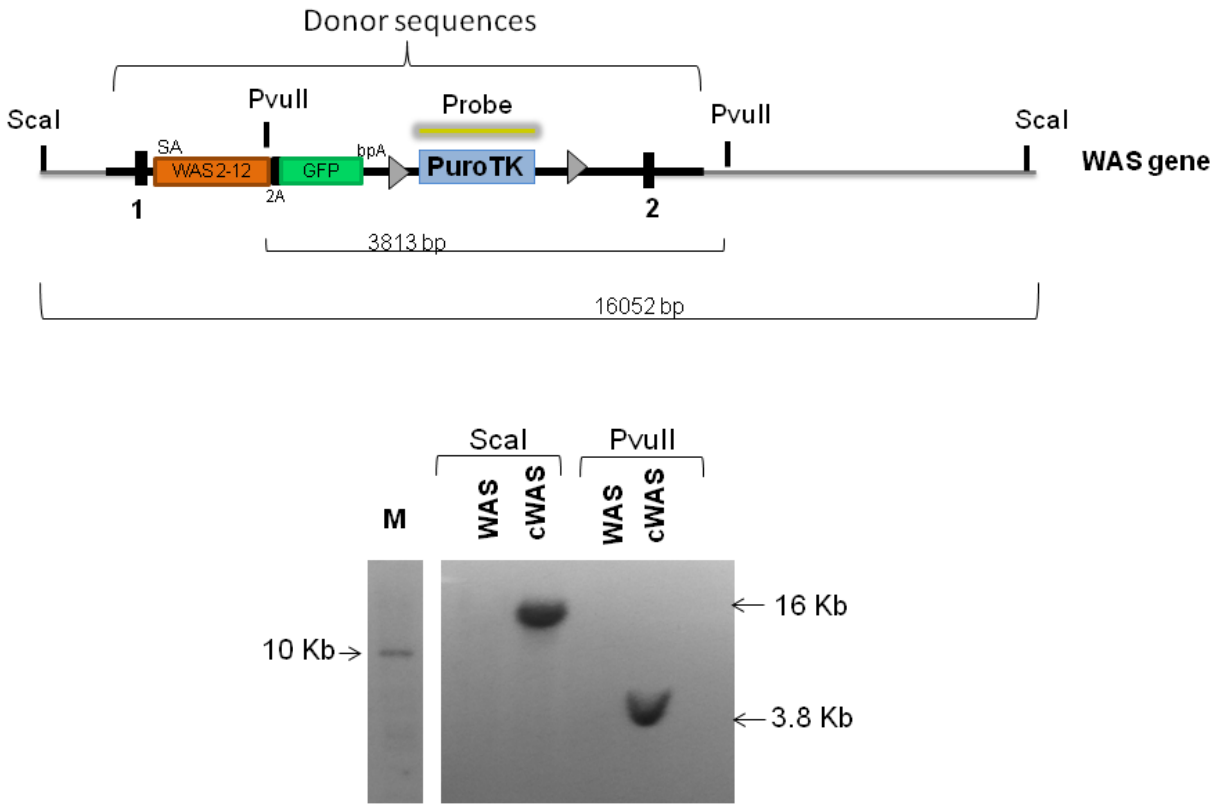

Figure 14: Southern Blot analysis of targeted WAS iPSC clone (cWAS). Schematic illustrates strategy used for detection of the intended integration on the WAS gene, as well as potential off-site integrations.

Both WAS mutant and corrected iPSC lines were evaluated by comparative genomic hybridization array (array CGH) analysis for the presence of potentially deleterious genetic changes. This analysis resulted in detection of a total of 32 changes. Of these, 25 were shared between the mutant and corrected lines, indicating they did not occur as a consequence of the genomic manipulations that occurred during the process of correction. The remaining 7 unique changes were distributed between the two lines – 3 appeared in the mutant, and 4 in the corrected (Table 4). We do not, at this time, know whether any of the 4 unique changes found in cWAS arose as a consequence of the process of genetic correction.

Class	Chr	Cytoband	Size(bp)	Start	Stop	Type	p-Value / LOH Score	WAS	cWAS
CGH	1	q21.1	143611	145,655,992	145,799,602	DEL	3.95E-16		
CGH	2	p11.2	159607	89,141,608	89,301,214	AMP	2.03E-39		
CGH	3	q13.31	184015	116,691,055	116,875,069	DEL	6.25E-24		
CGH	4	q13.2	90702	69,392,576	69,483,277	AMP	3.23E-15		
CGH	6	p25.3	102973	259,318	362,290	DEL	1.38E-34		
SNP	7	p21.3 - p21.2	2480335	11,664,329	14,144,663	LOH	6.642396		
CGH	8	p11.22	122621	39,258,894	39,381,514	AMP	NA		
CGH	8	p12	412790	32,196,359	32,609,148	DEL	NA		
CGH	8	p22	58286	15,952,011	16,010,296	AMP	5.42E-15		
CGH	8	p23.1	583097	7,169,490	7,752,586	DEL	2.26E-23		
CGH	8	q23.1	572546	106,670,876	107,243,421	AMP	NA		
CGH	10	q11.21	112557	45,218,780	45,331,336	DEL	1.31E-12		
CGH	11	p15.5	485	2,016,675	2,017,159	AMP	6.40E-31		
CGH	14	q32.33	132778	106,405,703	106,538,480	AMP	NA		
CGH	14	q32.33	321250	106,636,701	106,957,950	AMP	3.17E-24		
CGH	14	q32.33	147132	107,134,803	107,281,934	DEL	3.17E-15		
CGH	15	q11.1 - q11.2	2077055	20,481,702	22,558,756	AMP	NA		
CGH	16	p11.2	1838301	31,934,834	33,773,134	DEL	1.73E-14		
CGH	22	q11.22	171922	23,056,562	23,228,483	AMP	NA		
CGH	X	p11.23	61838	48,317,353	48,379,190	AMP	NA		
CGH	X	p11.23	551	48,759,648	48,760,198	AMP	6.35E-14		
CGH	X	p22.33	2630127	60,701	2,690,827	AMP	NA		
CGH	X	q28	184649	152,987,955	153,172,603	AMP	NA		
CGH	X	q28	206750	153,576,890	153,783,639	AMP	NA		
CGH	X	q28	288442	154,944,466	155,232,907	AMP	NA		
CGH	2	p21	534675	44,637,720	45,172,394	AMP	5.55E-18		
SNP	7	q21.13 - q21.3	3492774	89,792,465	93,285,238	LOH	6.1204314		
CGH	1	q31.3	54582	196,744,721	196,799,302	DEL	3.67E-10		
CGH	17	q21.31	88566	44,188,441	44,277,006	AMP	2.99E-10		
CGH	3	p26.1	63993	4,070,291	4,134,283	AMP	7.89E-11		
SNP	11	q12.3 - q13.3	6883527	62,032,068	68,915,594	LOH	6.3685884		
CGH	22	q13.31	206671	46,997,715	47,204,385	AMP	1.67E-16		

Table 4: Array CGH analysis results for WAS and cWAS. Most variants were seen in both lines. Seven unique changes were detected. Shaded blocks indicate positive identification, whereas white blocks mean variant was not detected in those cells.

We subsequently treated the targeted clone 5 with Cre-recombinase, and assayed for the removal of the loxP-flanked Puromycin-Thymidine kinase selection cassette. Any cells which did not undergo proper excision and retained the selection cassette would be rendered sensitive to Thymidine kinase-induced “suicide” when treated with Ganciclovir. After negative selection, we obtained 8 targeted corrected WAS iPSC (cWAS) clones, containing the endogenous integration of $WAS_{2\text{-}12}$ -2A-GFP and one residual loxP site, as illustrated in Figure 15.

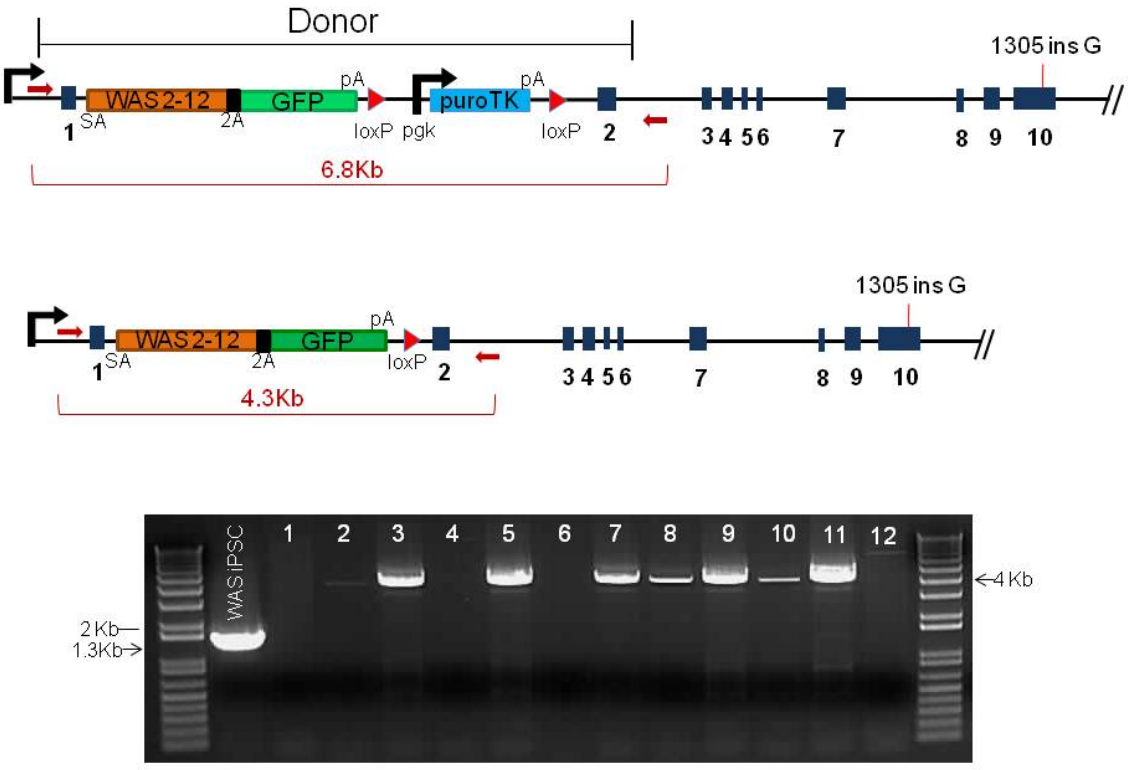

Figure 15: Excision of selection cassette by expression of CRE-recombinase. Schematic illustrates the expected outcome if successful excision occurred. Removal of selection cassette was successful in 10 out of 12 cWAS clones. WAS iPSC DNA was used as control.

Following targeted correction and CRE-recombinase excision of selection cassette, corrected iPSC were evaluated for pluripotency by teratoma formation assay. As shown in Figure 16, targeted-corrected WAS iPSC (cWAS) formed a teratoma when injected in a mouse, and gave rise to tissues from all three germ layers, confirming maintenance of pluripotent state, and thus showing no evidence that either ZFN activity or targeted integration at the *WAS* locus impaired pluripotent function.

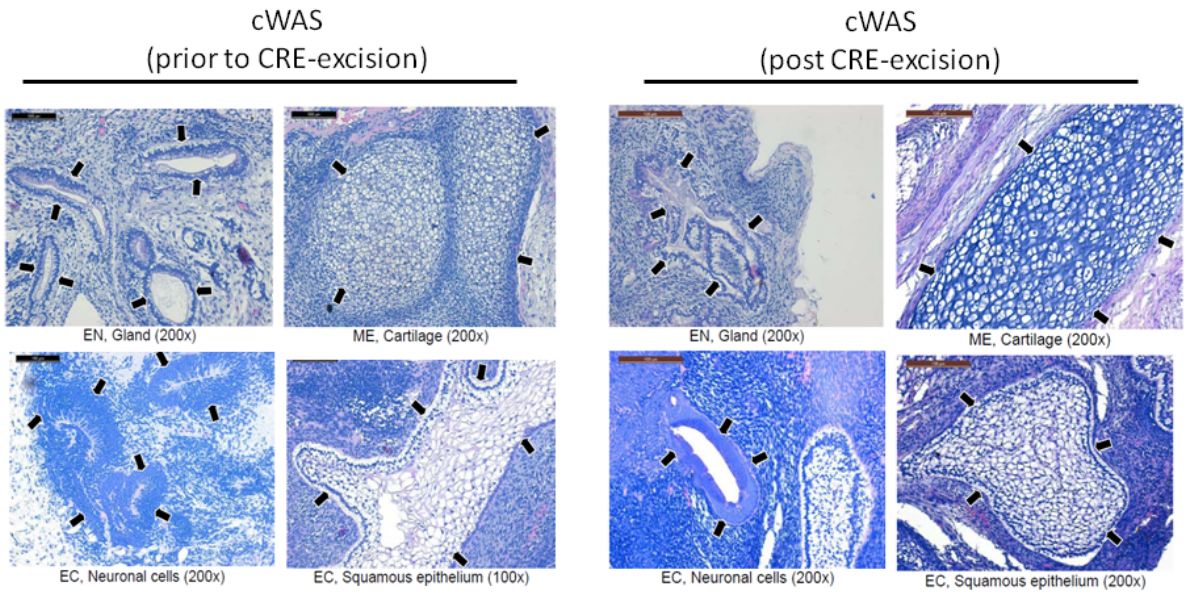

Figure 16: Evaluation of pluripotency of cWAS iPSC by Teratoma formation assay. Teratoma formation analysis was done at both stages of iPSC generation, after targeted integration at the WAS locus, and also following CRE-recombinase-mediated excision of selection cassette.

3.5 Generation of hematopoietic progenitors from human pluripotent stem cells

Wiskott-Aldrich Syndrome is a hematological disorder that affects the function of various cells in the immune system. Abnormal cell function results from the absence of WASp expression. This protein functions exclusively in hematopoietic cells, and plays a critical role in cellular function, as previously described. In order to assess whether our correction strategy resulted in restoration of WASp expression, we proceeded to derive hematopoietic cells from our corrected WAS-patient derived iPSC (cWAS), alongside mutant WAS iPSC and WA01 or WA09 hESC.

In order to induce hematopoietic differentiation, we first adapted each of our cell lines to a single-cell passaging method over the course of 5 weeks, as described in Chapter 2. Once cells were adapted, we obtained single-cell preparations of each of our lines – WAS iPSC, cWAS iPSC, WA01, and WA09 human embryonic stem cell (HESC)- and plated 5000-7000 cells per well of a 96-well plate for generation of spin embryoid bodies (EB). These were then cultured for 5 days in stem cell differentiation medium under stimulation of stem cell factor (SCF), vascular endothelial growth factor (VEGF), and bone morphogenic protein 4 (BMP4) at levels optimized for each cell line. (Approximately 36hrs after initial culture, we observed cell clusters acquired a three-dimensional, spherical morphology characteristic of embryoid bodies. At the end of 5-days in spin EB conditions, 16 EBs were transferred to each well of a 6-well plate pre-seeded with Mitomycin C-inactivated murine bone marrow OP9 cells and cultured for an additional 9 days (Figure 17).

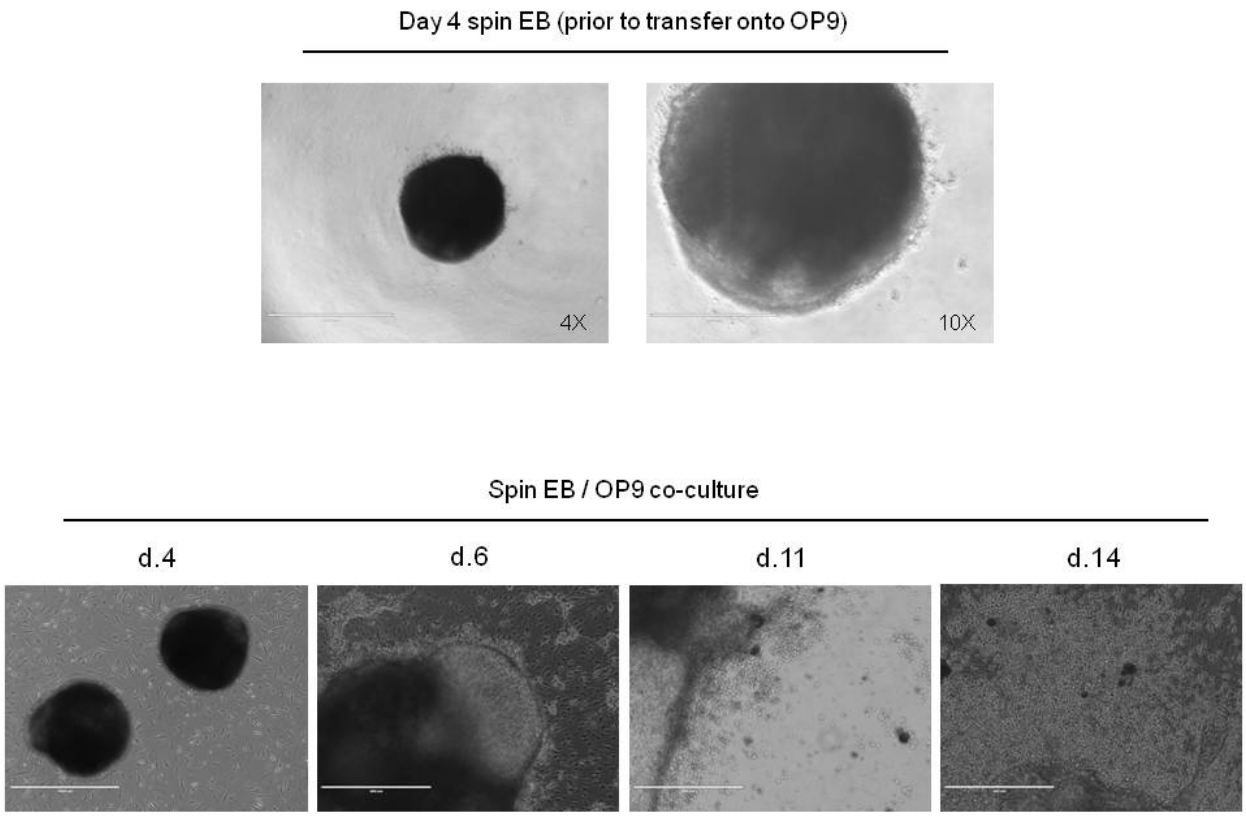

Figure 17: Spin EB in OP9-co-culture. Images capture EB changes over time in *in vitro* hematopoietic differentiation culture. At day 4, post transfer to OP9 stroma, EBs remain in suspension, but after 2-4 hours begin to attach to feeders. In the following 10 days of co-culture, EBs begin to expand and release hematopoietic cells onto the well.

Within the first 24 hours, EBs attached to the feeder layer, and, utilizing time-lapse live cell imaging, we could observe that, during days 3-5 in co-culture, spin-EB–derived stroma spreaded out onto the well, and large fluid-filled vesicles protruded from EBs. Within a few days, small, round cells formed inside these vesicles, and erupted to form small distal cell clusters. By day 12-14 (total days of culture), we observed vast cell proliferation and a significant number of cells floating in suspension, no longer attached to the feeders (Figure 18).

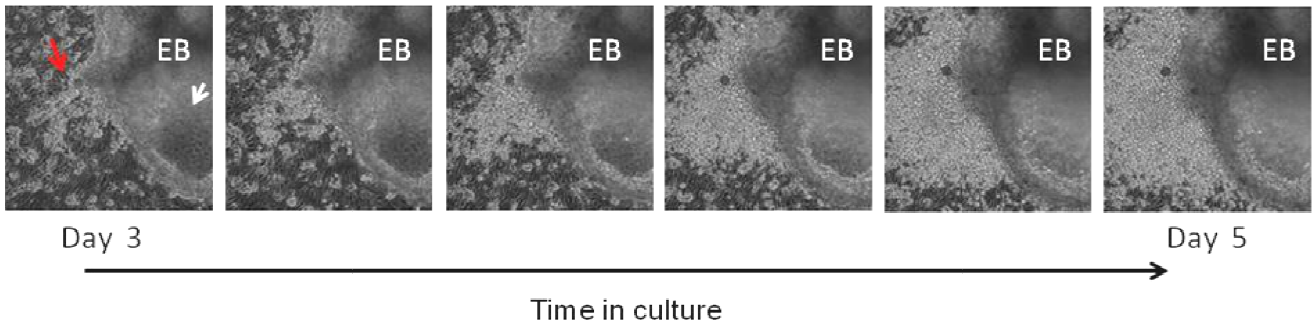

Figure 18: Time-lapse imaging of spin EB in co-culture. Images show hematopoietic differentiation of spin EB in OP9 co-culture over time. Red arrow marks release and proliferation of hematopoietic cells originated from EB. White arrow marks the vesicle where most hematopoietic cells seem to grow and proliferate prior to extravasation.

At this time, we harvested cells from supernatant, and disrupted EBs to collect all remaining cells still trapped inside. Once cell preparation was filtered and mostly free of OP9 feeders, cells were counted, stained for known hematopoietic progenitor surface markers CD34, CD43, and CD45, and analyzed by flow cytometry. Flow Cytometric analysis revealed all three lines (WAS, cWAS, and WA09) were capable of efficiently generating hematopoietic cells, and the hematopoietic progenitor cells ($CD34^+CD43^+$ and $CD34^+CD43^+CD45^+$) derived from the targeted-corrected cWAS iPS line expressed GFP, as expected, providing us with the first evidence of expression of the integrated transgenes (Figure19).

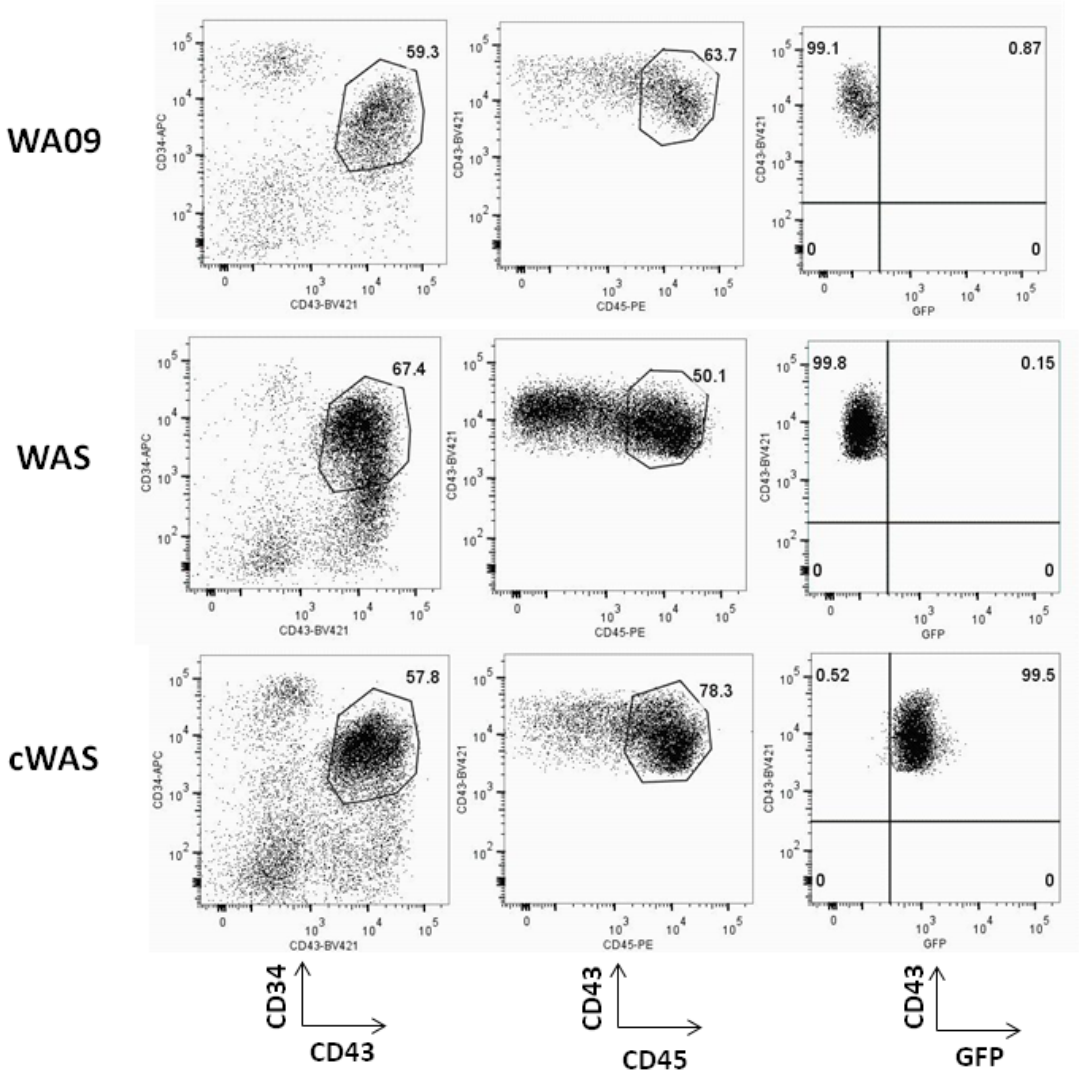

Figure 19: Flow cytometric detection of hematopoietic progenitor cells. First column shows $CD34^{+}CD43^{+}$ hematopoietic progenitor cells derived from both corrected and mutant iPSC, as well as from WA09 hESC control. Second column highlights the percentage of these cells that also express CD45. Third column shows GFP detection in cWAS-derived progenitors.

We also analyzed our *in vitro* hematopoietic differentiation cultures for the presence of lineage-specific progenitor cells, and identified cells expressing markers of myeloid, erythroid, and megakaryocytic hematopoietic lineages (Figure 20).

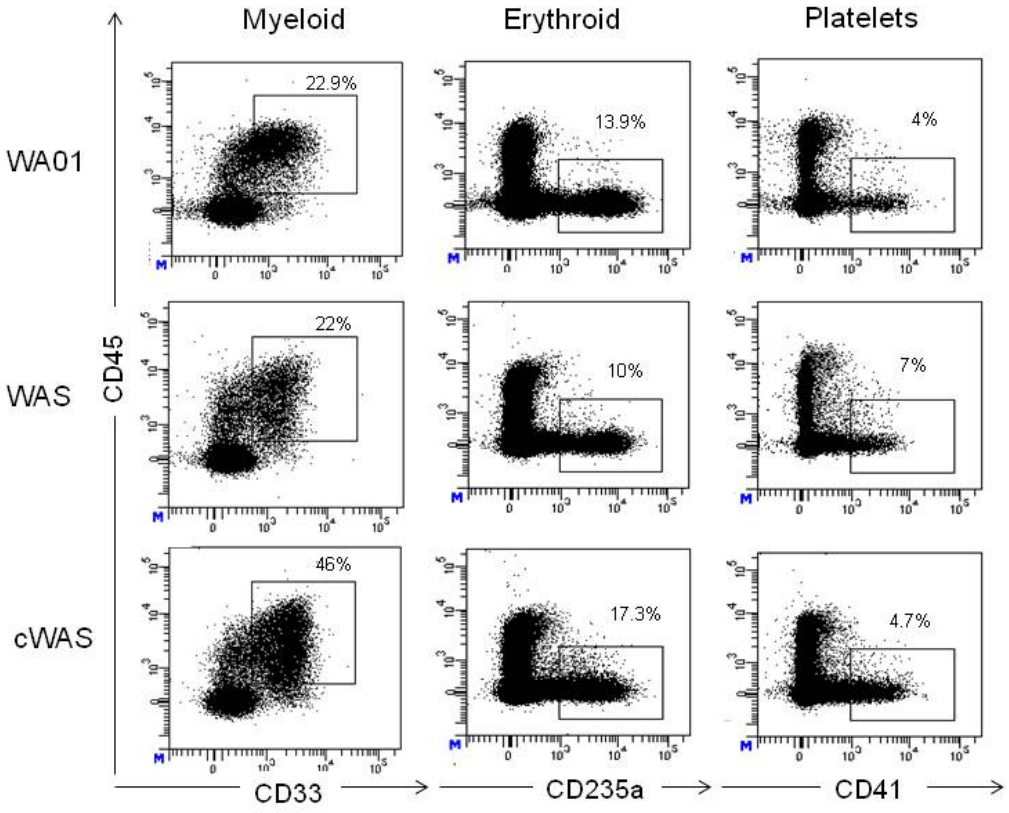

Figure 20: Derivation of myeloid, erythroid, and megakaryocytic cells from WAS, cWAS, and hESC-derived progenitors.

Moreover, when assayed for GFP expression, these myeloid, erythroid, and megakaryocytic cells expressed GFP at a similar level to that observed for $CD34^{+}CD43^{+}CD45^{+}$ hematopoietic cells. Endothelial cells, which are $CD43^{-}CD45^{-}$ did not express GFP, as expected, and were used as negative control in this experiment (Figure 21).

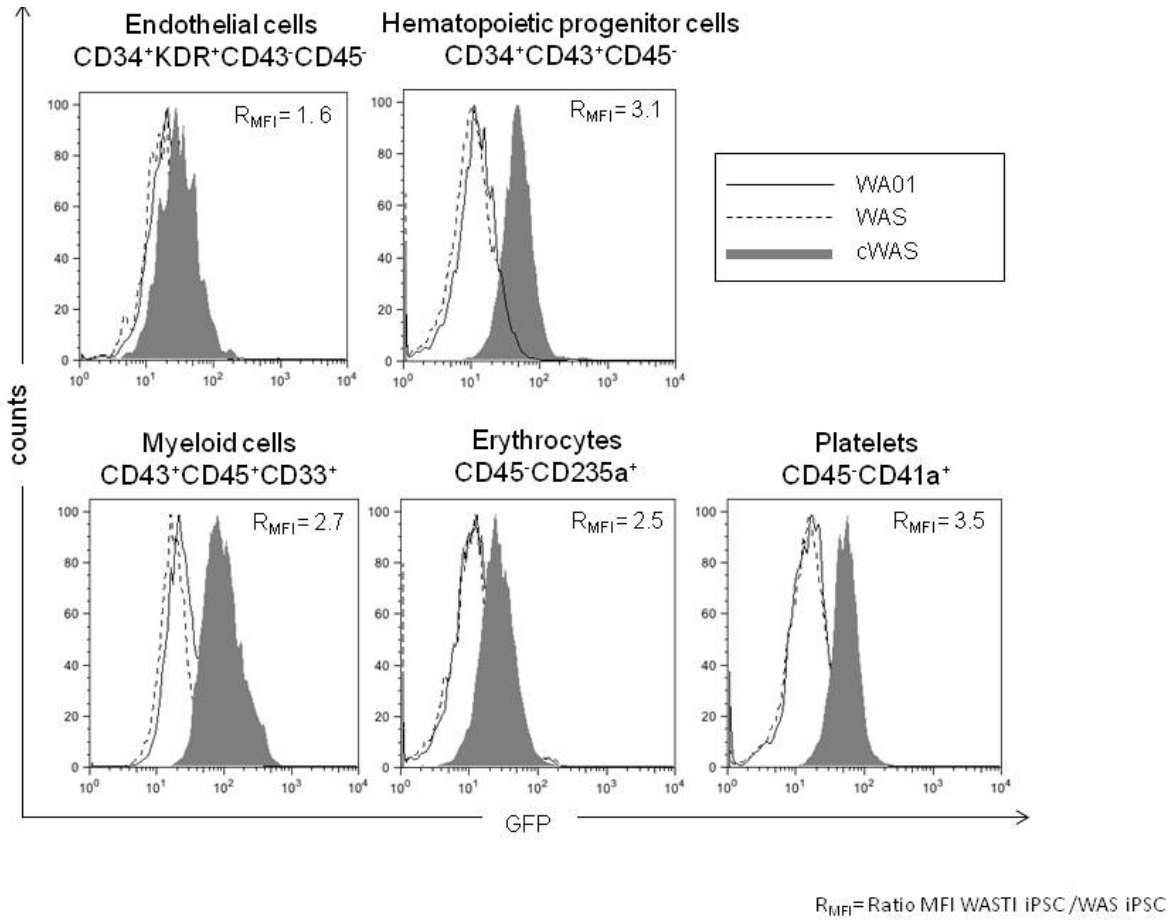

Figure 21: GFP expression in hematopoietic cells derived from cWAS. GFP expression derived from our integrated reporter transgene is observed in myeloid cells, erythrocytes, and platelets, demonstrating WAS-promoter activation.

In addition to characterization of progenitor immunophenotype, we also performed colony-forming assays from total $CD34^+$ cells derived from WAS, cWAS, and WA09 in order to evaluate the *in vitro* differentiation potential of these cells. Our progenitors derived from both mutant and corrected iPSC lines showed similar CFC potential to the control WA09-derived $CD34^+$ cells. We observed predominantly granulocyte and macrophage colonies emerging from progenitors from all three cells lines (Figure 22A). All colonies resulting from cWAS were GFP^+, demonstrating sustained expression of our transgene reporter (Figures 22B).

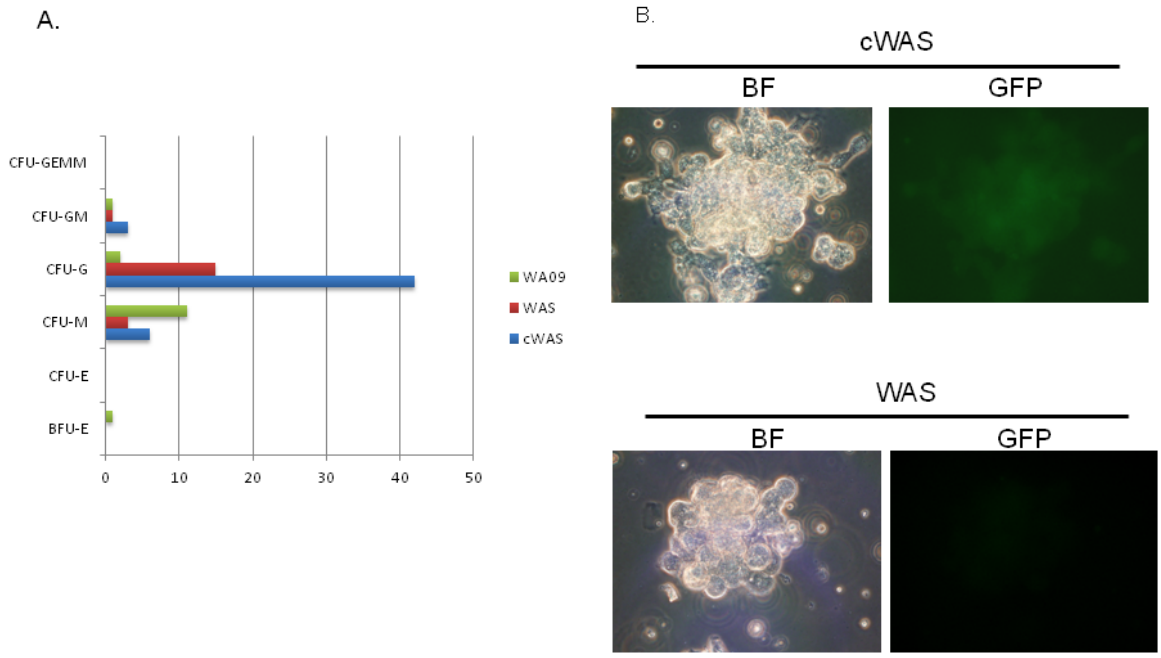

Figure 22: Colony-forming assays for differentiation of hematopoietic progenitors. A. Average numbers of colonies obtained from each line. Two experiments were done, each in triplicates. B. Images of colonies derived from WAS and cWAS progenitor cells. GFP expression detected in cWAS colonies.

3.6 Detection of WASp and GFP expression in $CD34^+CD43^+$ hematopoietic progenitor cells derived from cWAS

The *WAS* gene promoter is only active in hematopoietic cells. Detection of GFP expressing cells in cWAS iPS-derived progenitors was the first step in determining successful targeted integration, as described above in Figure 18. To further confirm proper transgene expression, we analyzed sorted $CD34^+CD43^+$ cells by Reverse Transcription PCR utilizing two sets of primers- one specific for WAS and the other anchored on both WAS and GFP (primers listed in Table 2).

As previously described, our WAS-mutant cells carry a germ line insertion of a G at position 1305 in exon 10 of the *WAS* gene. In our repair donor template, the exon 10 sequences are wild-type, thus absent of the additional G. Furthermore, as mentioned earlier in this section, we also introduced a silent base-pair change earlier in exon 10 of our donor, which replaced the existing *XhoI* site with an *XbaI* restriction enzyme site. Therefore, a simple endonuclease digestion would facilitate detection of correct mRNA from mutant mRNA.

RNA was harvested from progenitor cells derived from all three lines (WAS, cWAS, and WA09) and subsequent to reverse-transcription, cDNA was amplified in an RT-PCR assay (Figure 23A).

A.

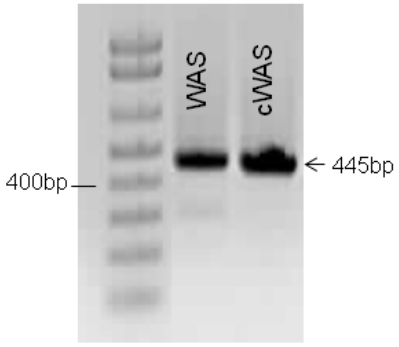
WAS
cWAS
400bp
445bp

B.

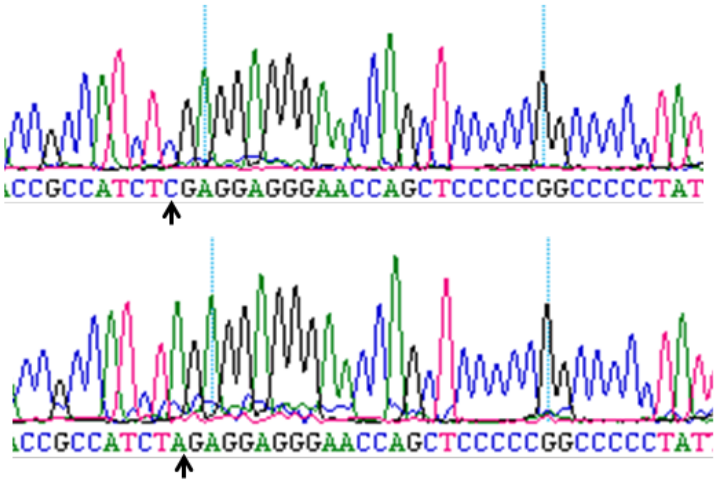
WAS
CCGCCATCTCGAGGAGGGAACCAGCTCCCCCGGCCCCCTAT
cWAS
CCGCCATCTAGAGGAGGGAACCAGCTCCCCCGGCCCCCTAT

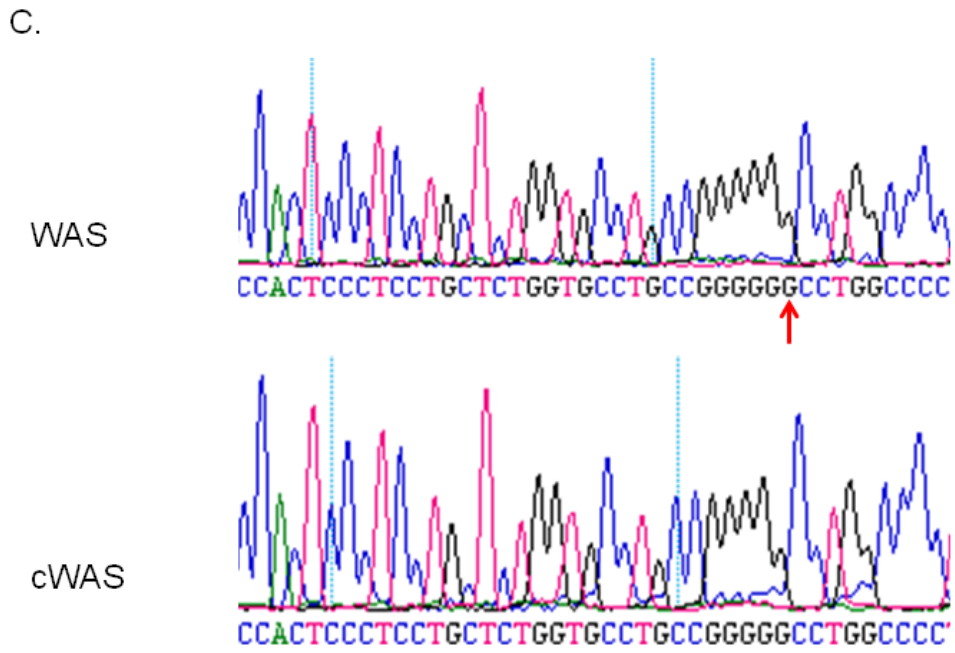

Figure 22: Expression of corrected WAS mRNA in cWAS-derived progenitor cells. A. Detection of WAS mRNA expression through RT-PCR amplification of cDNA from both WAS and cWAS hematopoietic progenitor cells. B. Sequencing of PCR product shows base-pair changed introduced in donor sequence (995C→A), which results in loss of *XhoI* site and gain of *XbaI* site in corrected cells. C. Sequencing exon 10 (1305 position) from RT-PCR material derived from WAS and cWAS progenitors show restoration of wild-type sequence in corrected cells, as evidenced by the loss of additional G.

In order to assay the RT-PCR product for the changes introduced in the donor molecule, we performed Sanger Sequencing analysis, and demonstrated that mRNA resulting from cWAS carried the silent point mutation (C→A) at position 995 and carried the wild-type sequence at exon 10 (absent of insertion G mutation) (Figures 23B and 23C). Taken together, these data confirmed proper splicing from endogenous exon 1 to the integrated transgene and generation of mRNA from transgenic *WAS*.

We also assessed expression of *WAS* and GFP transgenes in mutant and corrected progenitors by real-time quantitative RT-PCR (qRT-PCR). Using primers anchored on both WAS and GFP, we again observed WAS mRNA and GFP mRNA expression in corrected cells. Furthermore, in order to detect residual endogenous mRNA that may potentially be transcribed in the corrected cells, we included in our qRT-PCR analysis primers binding to exon 11 of WAS and the 3'UTR. The results showed no evidence for mRNA derived from the endogenous mutant locus in corrected cells (Figure 24).

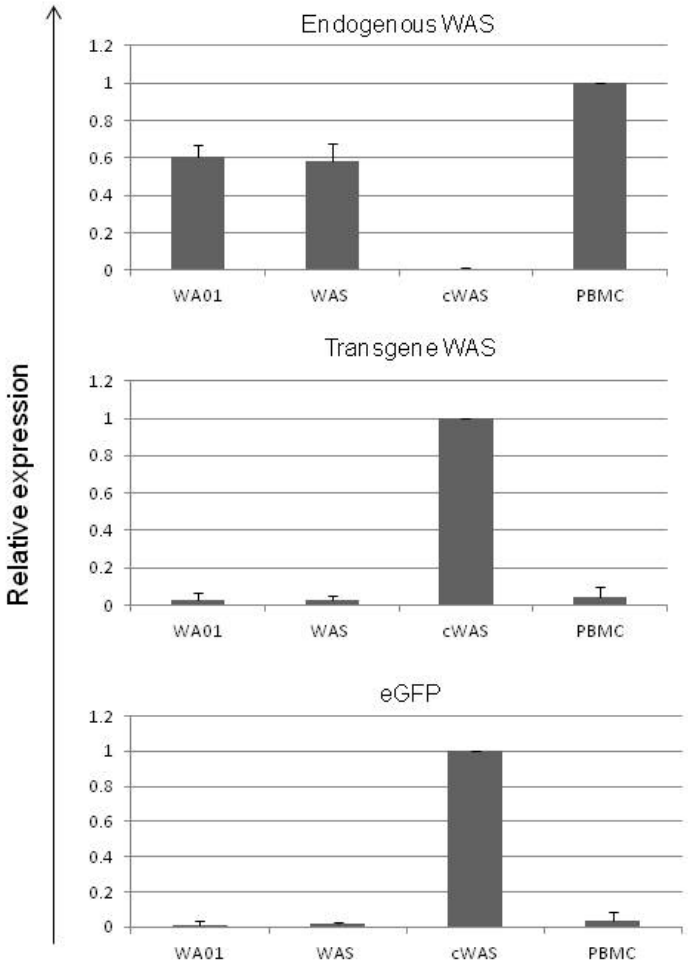

Figure 24: qRT-PCR analysis of WAS and cWAS progenitors for detection of WAS and GFP mRNA expression. Top panel shows levels of endogenous WAS mRNA expression. No endogenous WAS mRNA is detected in cWAS-derived progenitors. Middle panel shows expression of transgene WAS (detected using primers in both WAS and GFP) in cWAS-derived progenitors. Bottom panel shows the corresponding expression of integrated GFP reporter transgene.

Driven by the encouraging results from mRNA analysis, we proceeded to assay our cWAS progenitors for WAS protein expression. GFP expression observed in corrected progenitor cells by flow cytometry provided the first evidence suggesting proper function of transgene in generating protein. Determining expression of transgenic WASp was the next step to confirm correction. Sorted $CD34^{+}CD43^{+}$ progenitor cells were fixed and permeabilized and stained for WASp. Flow cytometric analysis results revealed WASp expression in both cWAS and WA09-derived progenitors when compared to isotype (Figure 25). We observed a shift in the mean fluorescence intensity (MFI) value for cWAS-progenitors when compared to the isotype control. This shift was also similar to that observed for WA09-derived normal progenitor cells. A small shift was detected in mutant progenitor cells. Because the antibody used for WASp detection may have a low level of cross-reaction to a close family member, N-WASp, we believe this small shift may have resulted from binding to N-WASp.

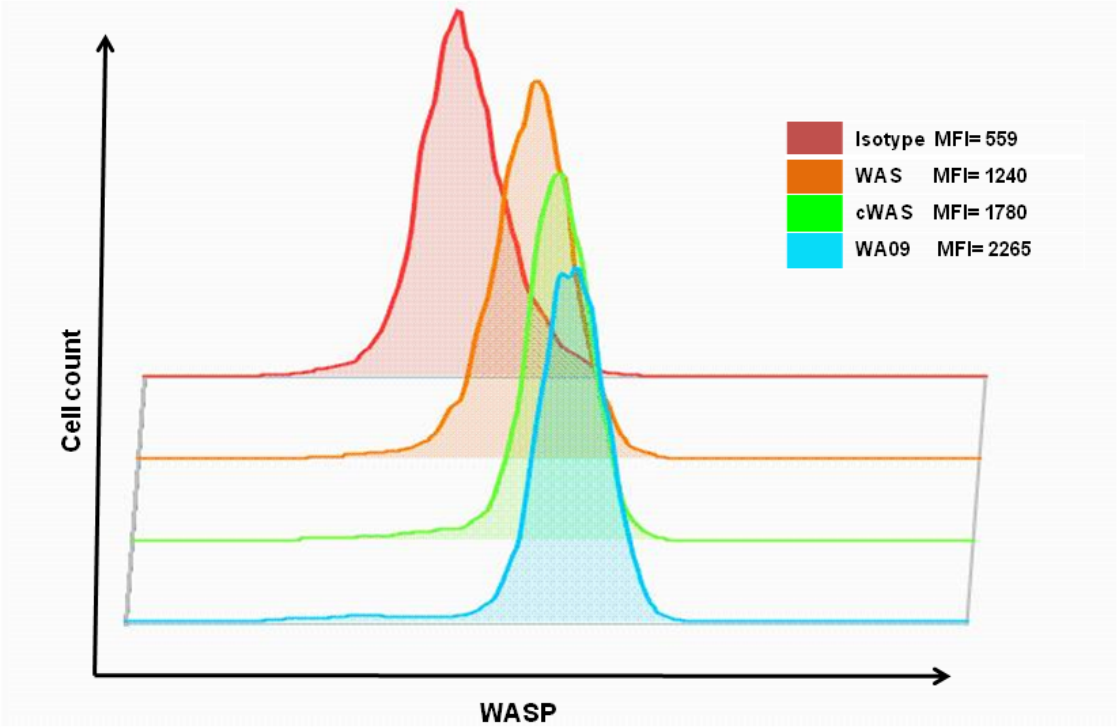

Figure 25: Detection of WASp by intracellular immunostaining and FACS analysis. Hematopoietic progenitors derived from WAS, cWAS, and WA09 hESC were assayed for expression of WASp. Histograms were overlayed for comparison.

For a final confirmation of WASp expression we assayed protein lysates by Western Blotting. This analysis showed restoration of protein expression in our gene-corrected hematopoietic cells, and also demonstrated absence of WASp in our patient-derived WAS progenitors, as expected (Figure 26).

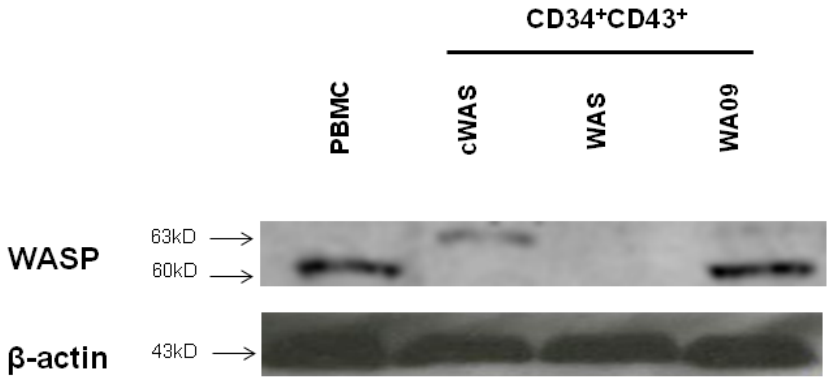

Figure 26: Western Blot analysis of hematopoietic progenitor cells for detection of WASp. Shift in size of WASp expressed in cWAS progenitors is due to fusion with residual 19 amino acids from “2A tag”.

We also observed that the WASp band detected in cWAS-derived progenitors appeared at a higher molecular weight (approximately 63kD, instead of the expected 60kD). This is consistent with what has been reported for constructs linked by a 2A peptide. During translation, after ribosome skipping and subsequent cleavage at the 2A site, approximately 19 amino acids from the peptide remain attached to the upstream protein, which explains the shift in size [80].

3.7 Natural Killer (NK) cell differentiation from iPSC-derived $CD34^+CD43^+$ progenitor cells

Natural Killer (NK) cells are part of the innate lymphoid system, and play an important role in immune defense against viral infection and cancer [81]. These cells comprise 10-20% of all mononuclear cells, and, unlike T-cells, NK cells lack T-cell receptor (TCR), and kill a wide range of targets in a manner that is independent of human leukocyte antigen (HLA)- recognition [82,83]. In WAS patients, NK cells lack WASp expression and display impaired cytotoxic function, which contributes to immunedeficiency in these patients [17].

In order to demonstrate restoration of immune function as a consequence of WAS correction, we derived NK cells from $CD34^+CD43^+$ progenitors from WAS and cWAS iPSC, and WA09 hESC in a well-established NK-specific co-culture-based assay reported to give rise to cytotoxic, mature cells capable of killing tumor cell targets [84,85] (Figure 27).

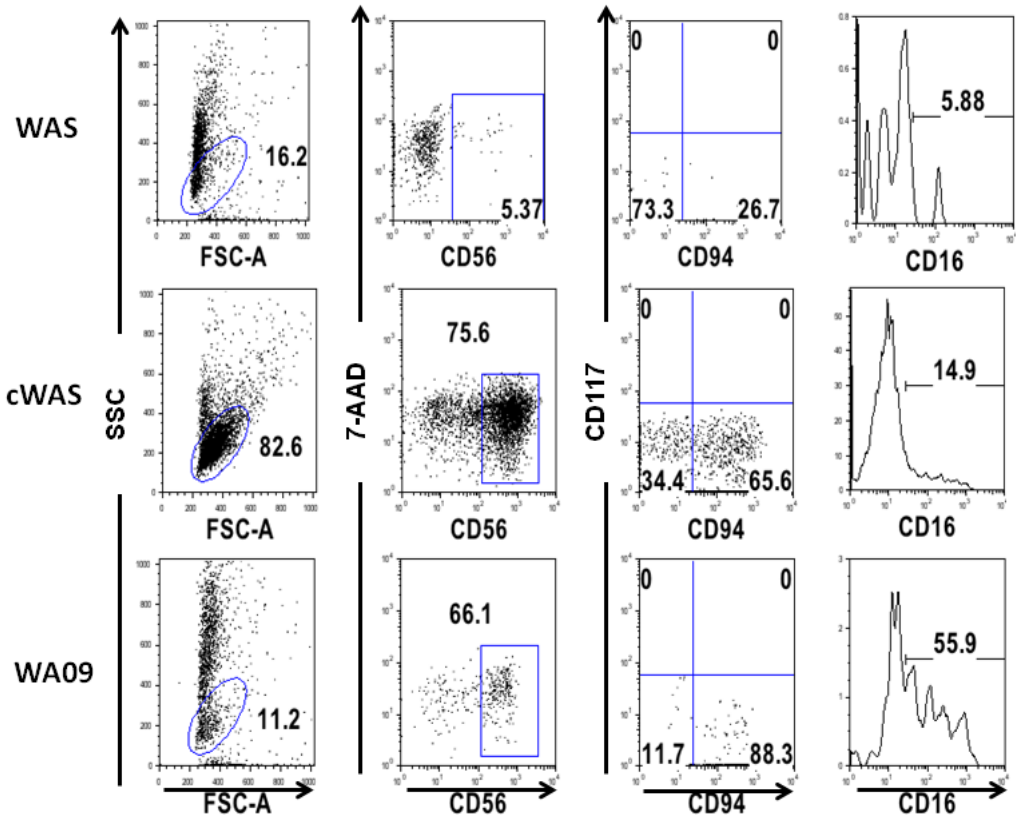

Figure 27: *In vitro* Generation of NK cells. Panels show expression of NK-specific markers. A noticeable deficit in generation of NK cells is shown for WAS-derived progenitor cells in the second column, where the low percentage of $CD56^{+}$ cells is highlighted.

At the end of approximately 30 days, flow cytometric analysis showed robust generation of a distinct $CD56^{+}$ population from both WA09 and cWAS progenitors, consistent with NK phenotype (Figure 27). Furthermore, these cells expressed NK receptors CD16, and CD94. Our mutant progenitors, however, differentiated very poorly in 3 separate experiments, generating a very low number of NK cells. This result was obtained irrespective of whether OP9-DL1 or OP9-DL4 stromal feeders were used for the differentiation process.

We confirmed WASp expression in cWAS-derived NK cells by Western Blotting. Due to the very low number of NK cells obtained through in vitro differentiation, there were not enough cells for Western Blot analysis. As seen with the progenitors, we observed the WASp band appeared at a higher molecular weight, consistent with the shift we expect for a WASp-2A fusion (Figure 28).

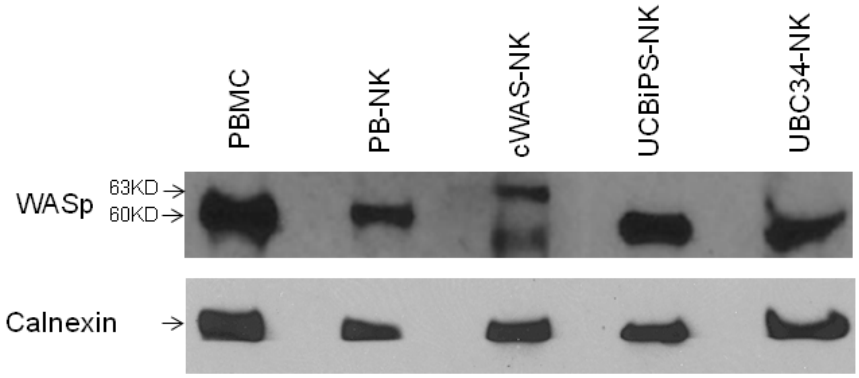

Figure 28: Western Blot analysis of WASp in NK cells. Lane 1 shows WASp expression in total PBMC; Lane 2 shows WASp expression in NK cells isolated from peripheral blood of normal donor; Lanes 3-5 show expression of WASp in *in vitro* differentiated NK cells (respectively, from cWAS iPSC-derived progenitors, umbilical cord blood-derived iPSC-derived progenitors, and from primary $CD34^+$ hematopoietic progenitors obtained from umbilical cord blood).

A lower-molecular weight band was detected in NK cells derived from cWAS progenitors. We do not yet have knowledge of what it may be. Sanger sequencing analysis of RT-PCR product from corrected NK cells revealed transcription of only the transgenic *WAS* RNA, carrying both the C→A change at base-pair position 995 in exon 10, and the corrected, wild-type sequence at position 1305 (where original germline insertion of G occurred) (Figure 29). These data suggest the lower band observed in Western Blot does not result from mutant protein, which is consistent with our findings that neither *WAS* mRNA nor WASp is detected in the mutant $CD34^{+}CD43^{+}$ progenitor cells, as shown in Figures 28 and 29.

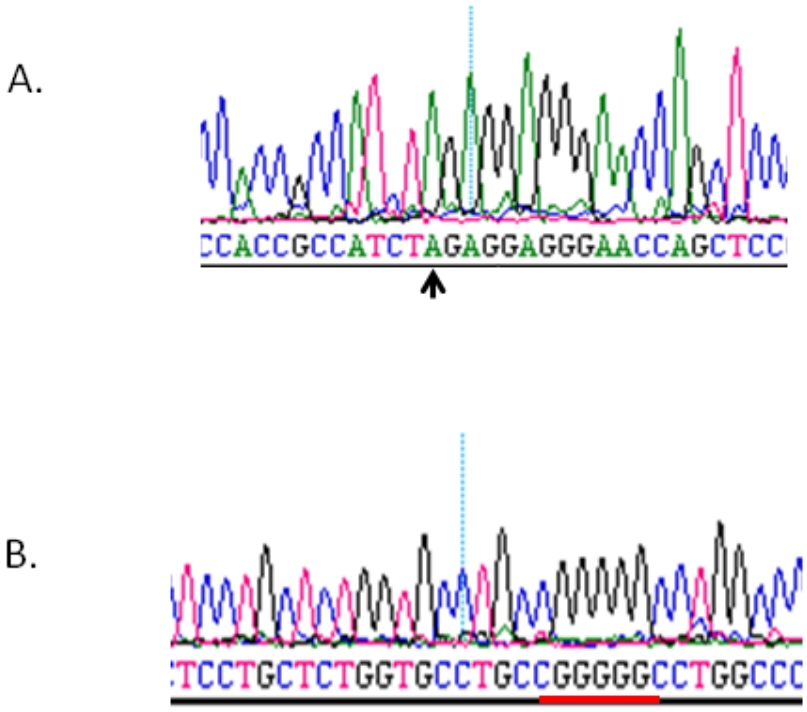

Figure 29: RT-PCR analysis of *WAS* gene expression in corrected NK cells. Figure A shows silent base-pair change at position 995 (C→A) indicated with back arrow. Figure B shows normal, wild-type sequence only present in RNA, absent of insG mutation (underlined in red).

In order to assay restoration of function in corrected NK cells, we evaluated the ability of *in vitro* generated NK cells to respond to K562 erythroleukemia cells in co-culture assays and detected a remarkable difference in the expression levels of pro-inflammatory cytokines interferon gamma (IFNγ) and tumor necrosis factor alpha (TNFα) between mutant and corrected NK cells. Mutant NK cells were deficient in their ability to respond to K562 cells (Figure 30), while cWAS-derived NK cells showed an upregulation in the levels of both IFNγ and TNFα cytokines, demonstrating restored function.

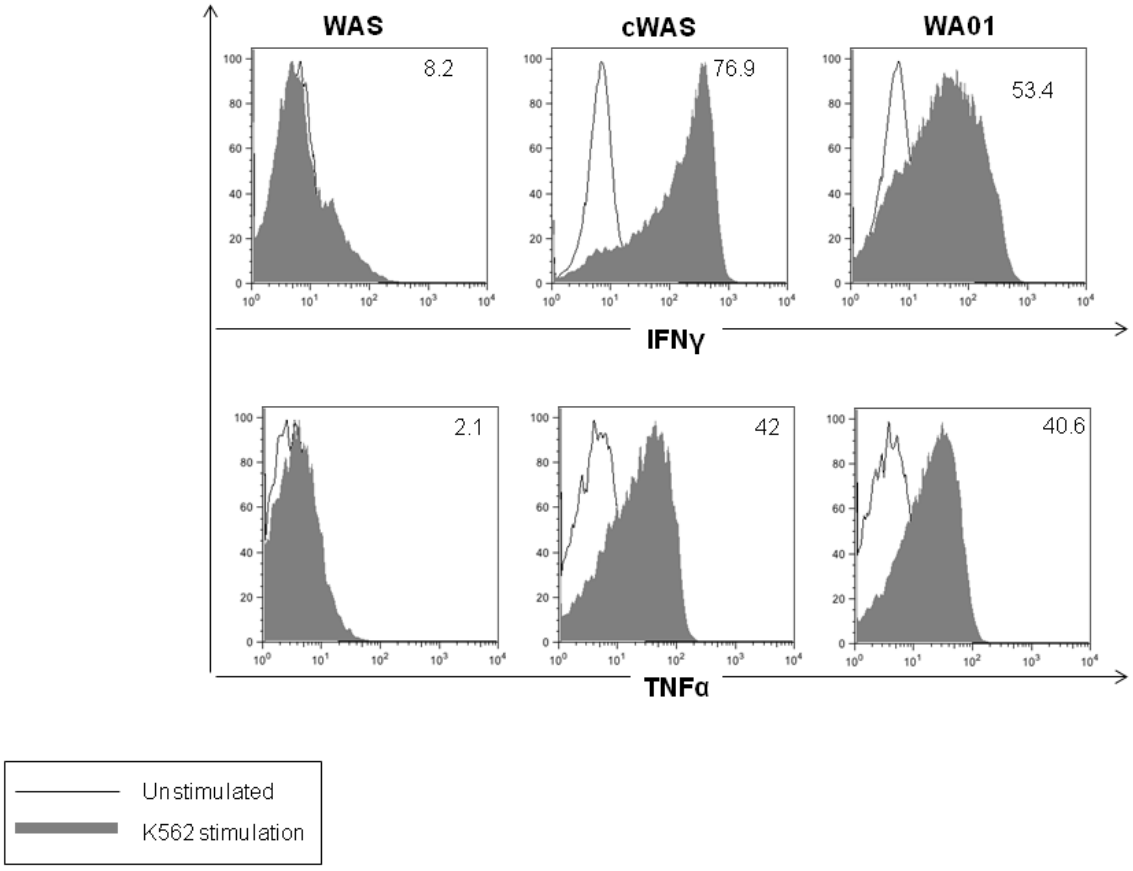

Figure 30: Upregulation of IFNγ and TNFα cytokine responses upon co-culture with K562 cells. Upregulation of cytokines associated with NK cell cytotoxic function.

3.8 Isolation of purified Revertant lymphocyte populations from WAS-revertant patient's peripheral blood mononuclear cells (PBMC)

We obtained whole blood samples from two WAS-revertant patients, namely WAS4 and WASJ. Both patients are known to carry the same WAS germline mutation: a base-pair change at position 995 of exon 10 (C995T) which results in a premature stop codon, and the loss of the original arginine amino acid at this position on the WAS protein. Consequently, a truncated protein is produced, which lacks the catalytic VCA domains necessary for proper function.

In order to detect revertant cells in different lymphocyte populations, we first performed a negative isolation utilizing antibody-bound magnetic beads to obtain purified lymphocyte populations. Subsequent to magnetic isolation, we analyzed cells by immunostaining and flow cytometry to isolate specific subpopulations: $CD4^+$, $CD8^+$, $CD4^+CD45Ro^+$, $CD8^+CD45Ro^+$, and $CD8^+CD45Ro^-$. We identified $WASp^+$ and $WASp^-$ populations within each of these groups (Figure 31).

A.

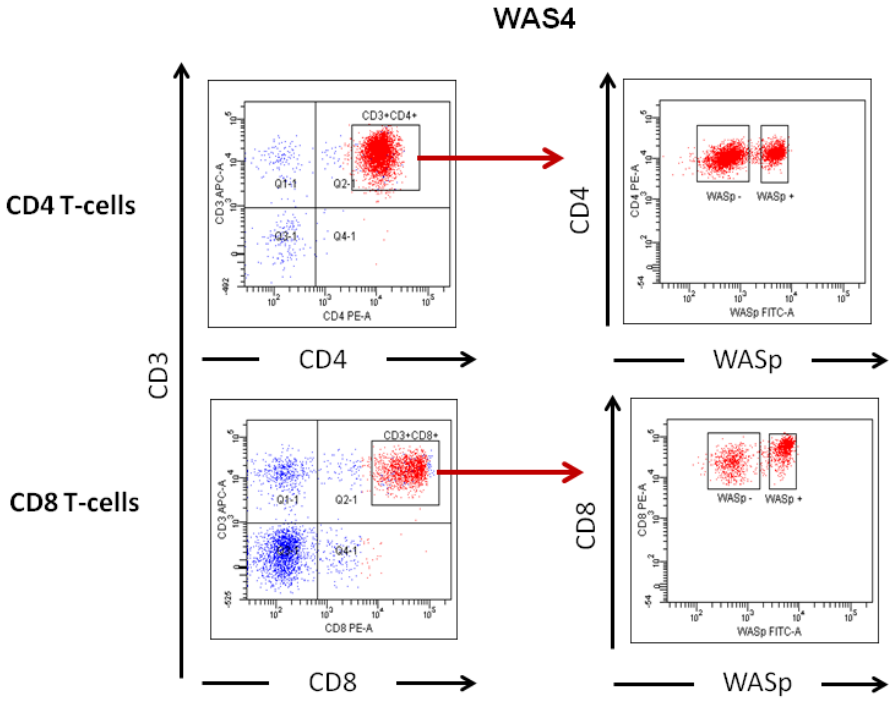
WAS4
CD4 T-cells
CD8 T-cells
CD3
CD4
CD8
WASp
CD3+CD4+
CD3+CD8+
Q1-1
Q2-1
Q3-1
Q4-1
CD3 APC-A
CD4 PE-A
CD8 PE-A
WASp FITC-A
WASp -
WASp +

B.

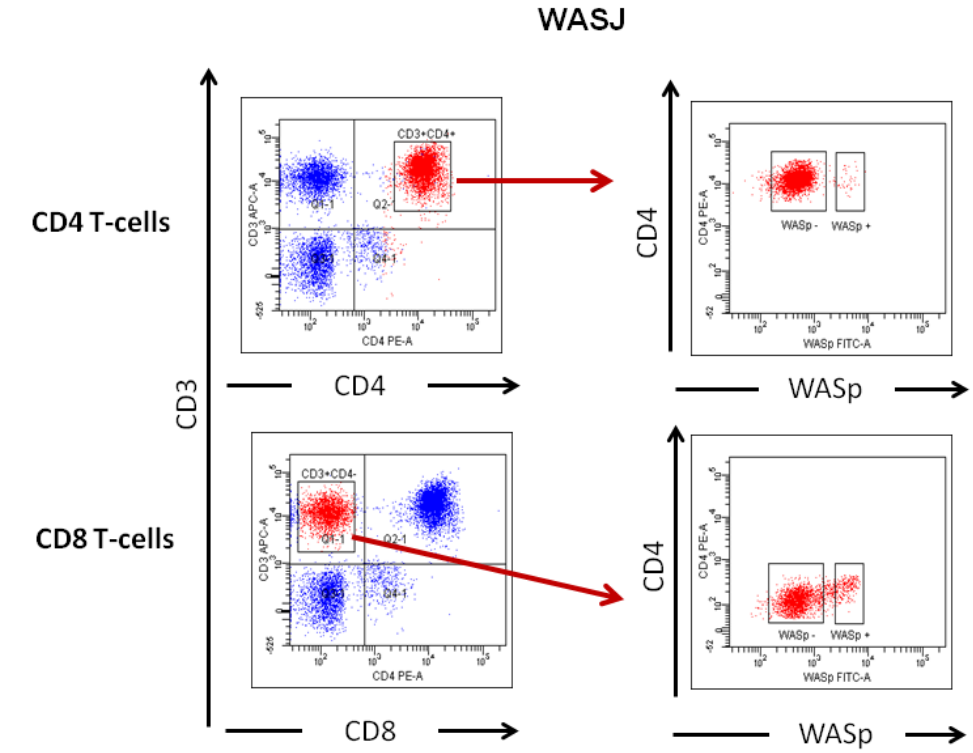
WASJ
CD4 T-cells
CD8 T-cells
CD3
CD4
CD8
WASp
CD3+CD4+
CD3+CD4-
Q1-1
Q2-1
Q3-1
Q4-1
CD3 APC-A
CD4 PE-A
WASp FITC-A
WASp -
WASp +

C.

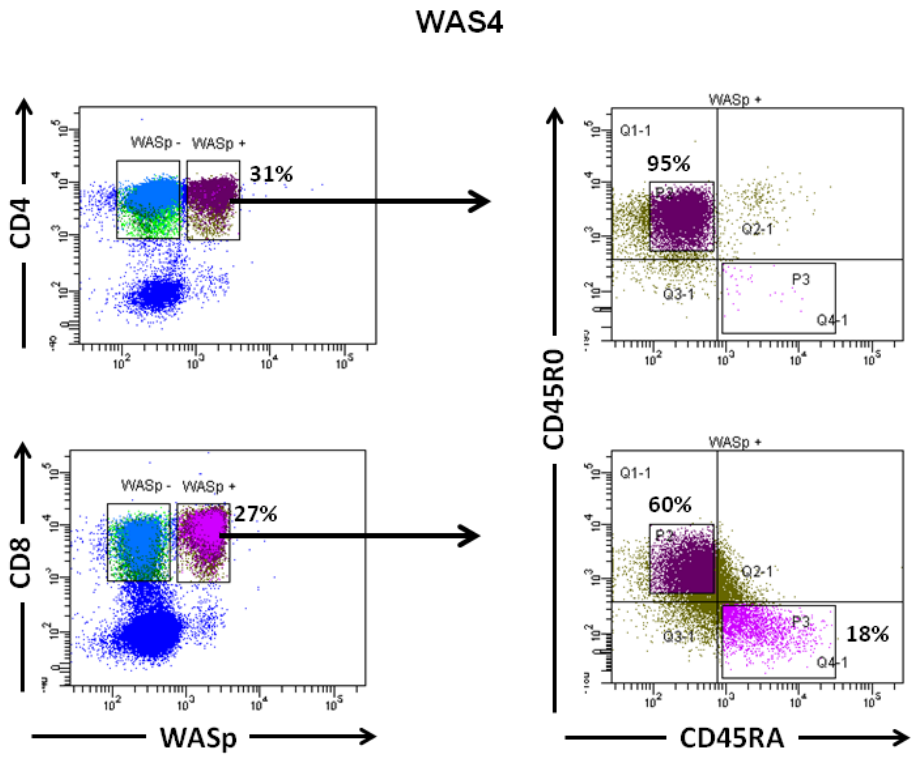

Figure 31: Flow Cytometric analysis and detection of WASp$^+$ lymphocytes in PBMC samples isolated from WAS4 and WASJ revertant patients. Panel A shows detection of WASp$^+$ CD4$^+$ and CD8$^+$ T-cells in patient WAS4. Panel B shows detection of WASp$^+$ CD4$^+$ and CD8$^+$ T-cells in patient WASJ. Panel C shows analysis of CD4$^+$ and CD8$^+$ T-cells for the presence of memory (CD45R0) and naïve (CD45RA) WASp-expressing cells.

Each sorted population was subsequently lysed and a 260bp-region neighboring the germline mutation site was amplified using primers labeled with specific identifier sequences for each cell population (Figure 32 and Table 5). Purified PCR material was subsequently prepared for 454 sequencing analysis.

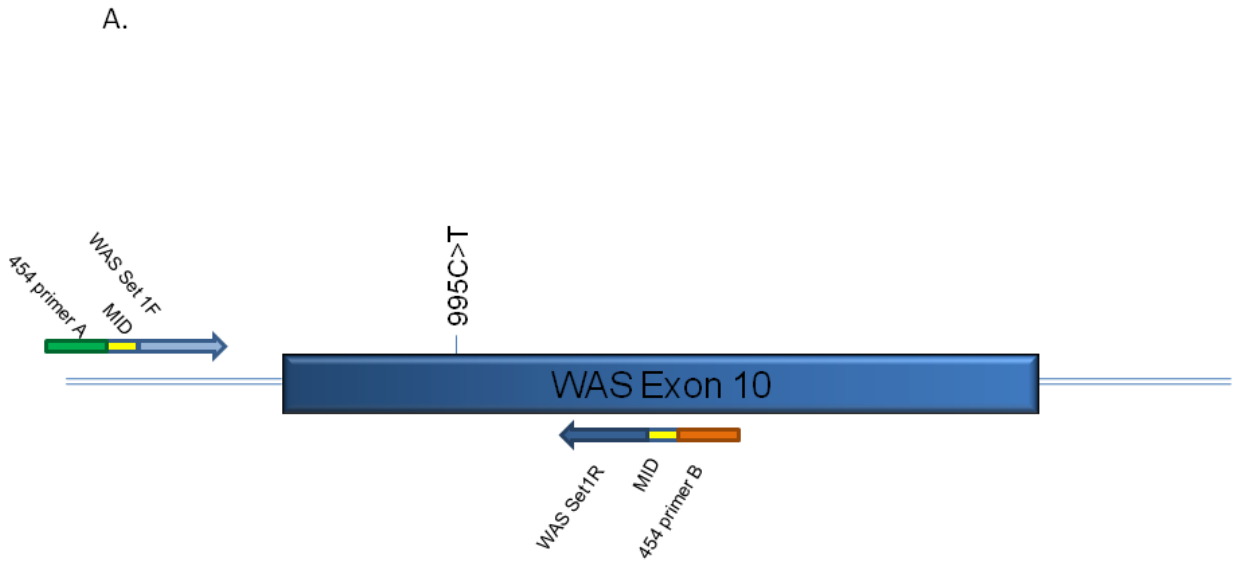

Figure 32: Schematic illustrating PCR strategy for amplification of material from individual cell populations of lymphocytes isolated from WAS-revertant patients. Primers contain identifier sequences attached at the 5' end which allow for labeling amplicons from each population.

Patient	Samples	MID-F	MID-R	MID sequence-F	MID sequence-R
WAS4	CD4+WASp+Ro+	13	13	CATAGTAGTG	CATAGTAGTG
WAS4	CD8+WASp+Ro+	16	16	TCACGTACTA	TCACGTACTA
WAS4	CD8+WASp+Ro-	14	14	CGAGAGATAC	CGAGAGATAC
WAS4	CD4+WASp+	5	1	ATCAGACACG	ACGAGTGCGT
WAS4	CD8+WASp+	5	15	ATCAGACACG	ATACGACGTA
WASJ	CD4+WASp+	9	19	TAGTATCAGC	TGTACTACTC
WASJ	CD8+WASp+	9	11	TAGTATCAGC	TGATACGTCT

Table 5: List of multiplex identifier sequences utilized for labeling of each lymphocyte population from WAS4 and WASJ patients.

3.9 Detection and Characterization of revertant genotypes in WASp$^+$ lymphocytes from WAS revertant patients

The emergence of WASp$^+$ lymphocytes in patients carrying deleterious WAS germ line mutations suggests that restoration of protein expression must have occurred by mechanisms that somehow overcame the original defect. Our goal was to investigate the molecular events (either site-specific reversion of original mutation or second-site mutations) that occurred in the revertant cells to provide restoration of protein expression.

With the advent of next generation sequencing (NGS) technology, obtaining large volumes of genomic sequence data is easily attainable. Moreover, this powerful technology allows for ultra-deep DNA analyses, able to detect even those events that appear at very low frequencies. Using the Roche 454 GS Titanium Amplicon NGS platform, we sequenced a 260-bp segment of the *WAS* gene encompassing the germline mutation (C→T at position 995 in exon 10) in 2 WAS-revertant patients, WAS4 and WASJ.

In order to generate purified material for NGS, we PCR-amplified each desired region from sorted WASp$^+$ cells for each patient, and, in some cases, also from WASp$^-$ cells as a control. Each different cell population was amplified with primers containing a unique multiplex identifier (MID) sequence (listed in table 4), and thus libraries from each population were generated. This feature allowed us to sequence several libraries together in a multiplex fashion, and later deconvolute the data in the analysis software using the MIDs as a tool for sorting amplicons from different

populations. Subsequent to amplification, samples were purified on Ampure beads and purity was assessed on a bioanalyzer. Sample quality and purity are crucial for efficient sequencing. Contamination with even slight amounts of residual primer dimer, for instance, can affect sequencing results significantly. Once samples were ready, we combined libraries for each patient, and following clonal amplification in microbeads in an oil emulsion, each library was bi-directionally sequenced using the Roche 454 Amplicon sequencing platform. Following comprehensive analysis of individual cell populations, we identified hundreds of revertant genotypes in our patient set. With ultra-deep sequencing analysis, we identified, in this study, over a hundred potential revertant genotypes in the sorted $WASp^{+}$ cells of both P1 and P2, some of which occurred at low frequencies and could only be detected with a more powerful approach such as NGS. In this report we will outline two classes of reversions identified: Class I reversions (base-pair changes occurring directly in the germline mutant codon), and Class II reversions (genotypic changes in intron 9 affecting splicing).

Following intracellular immunostaining and flow cytometric analysis, we identified WASp-expressing cells in T-lymphocytes from both patients. Because we had greater amount of sample from WAS4, we were able to also analyze memory and naïve T-cells subsets for this patient. We compared our findings for the memory and naïve populations, and observed that an Adenine at position 995 (replacing the stop codon with an arginine) was the most frequent class I genotype found in both $CD4^{+}$ memory T-cells and $CD8^{+}$ naïve T-cells. However, in the $CD8^{+}$

memory T-cell population, the predominating class I reversion was a 996G→C (replacing the premature stop codon with a serine amino acid) (Table 6).

		$CD4^+WASp^+RO^+$	$CD8^+WASp^+RO^+$	$CD8^+WASp^+RO^-$
995A	F	735	350	2086
	R	981	427	2591
	Total	1716	777	4677
	%	69.45	38.56	88.20
995C	F	124	3	0
	R	119	3	1
	Total	243	6	1
	%	9.83	0.30	0.02
995G	F	100	31	0
	R	120	25	1
	Total	220	56	1
	%	8.90	2.78	0.02
996A	F	0	0	0
	R	0	0	0
	Total	0	0	0
	%	0	0	0
996C	F	70	516	288
	R	98	601	336
	Total	168	1117	624
	%	6.80	55.43	11.77
996T	F	15	1	0
	R	17	4	0
	Total	32	5	0
	%	1.39	0.56	0.00
997C	F	9	23	0
	R	7	31	0
	Total	16	54	0
	%	0.70	6.05	0.00
997G	F	31	0	0
	R	37	0	0
	Total	68	0	0
	%	2.75	0	0
997T	F	4	0	0
	R	4	0	0
	Total	8	0	0
	%	0.32	0	0

Table 6: Summary of Class I revertant genotypes detected in memory and naïve T-cells from WAS4.

We also looked at the class II changes across memory and naïve T-cell populations from patient WAS4, and found a large number of base-pair changes present. As noted in table 6, a direct comparison between naïve and memory $CD8^+$ T-cells showed highest predominance of reversion in the memory population.

WAS 4		CD4:WASp:RO+			CD8:WASp:RO+			CD8:WASp:RO-		
Reversion	Position	F	R	% of Total	F2	R3	% of Total4	F5	R6	% of Total7
T>G	-30	2	1	0.00	0	0	0.00	0	0	0.00
A>C	-29	0	0	0.00	0	0	0.00	0	0	0.00
A>C	-28	0	0	0.00	0	0	0.00	0	0	0.00
A>G	-28	2	1	0.07	2	0	0.03	0	0	0.00
C>G	-27	2	14	0.36	0	0	0.00	0	0	0.00
C>T	-27	0	0	0.00	0	0	0.00	1	1	0.05
A>G	-26	0	0	0.00	0	0	0.00	0	0	0.00
C>G	-24	28	24	1.17	1	2	0.04	0	0	0.00
A>C	-22	0	0	0.00	0	0	0.00	0	0	0.00
T>G	-21	2	1	0.07	0	0	0.00	0	0	0.00
G>A	-20	0	0	0.00	0	3	0.04	0	0	0.00
T>A	-19	0	0	0.00	0	0	0.00	0	0	0.00
T>G	-19	4	2	0.13	5	11	0.22	0	0	0.00
T>C	-19	0	0	0.00	0	0	0.00	0	0	0.00
T>A	-17	4	2	0.13	0	0	0.00	0	0	0.00
T>G	-17	10	6	0.36	0	0	0.00	0	0	0.00
T>G	-16	0	0	0.00	0	0	0.00	0	0	0.00
A>G	-15	0	0	0.00	0	0	0.00	0	0	0.00
T>G	-14	7	6	0.29	2	1	0.04	0	0	0.00
T>C	-14	0	0	0.00	0	0	0.00	0	0	0.00
T>A	-14	0	0	0.00	0	0	0.00	0	0	0.00
A>G	-13	0	0	0.00	0	0	0.00	0	0	0.00
C>T	-12	0	0	0.00	0	0	0.00	0	0	0.00
C>G	-12	34	58	2.07	5	5	0.14	0	0	0.00
C>T	-11	0	0	0.00	0	0	0.00	0	0	0.00
C>A	-11	0	0	0.00	0	0	0.00	4	2	0.10
C>G	-9	5	5	0.22	0	0	0.00	0	0	0.00
C>T	-9	0	0	0.00	0	0	0.00	0	0	0.00
C>A	-8	0	0	0.00	0	0	0.00	0	0	0.00
C>T	-8	0	0	0.00	0	0	0.00	0	0	0.00
T>A	-7	4	6	0.22	2	1	0.04	0	0	0.00
T>G	-7	20	22	0.94	0	0	0.00	0	0	0.00
T>C	-7	0	0	0.00	0	0	0.00	0	0	0.00
C>A	-6	0	0	0.00	10	10	0.28	0	0	0.00
C>G	-6	15	7	0.49	1	6	0.10	0	0	0.00
C>A	-5	0	0	0.00	2	3	0.07	0	0	0.00
C>G	-5	4	9	0.29	3	3	0.08	0	0	0.00
A>C	-4	2	7	0.20	1	2	0.04	0	0	0.00
A>T	-4	0	0	0.00	0	0	0.00	0	0	0.00
C>A	-3	0	0	0.00	0	0	0.00	0	0	0.00
C>T	-3	28	34	1.39	186	178	5.08	13	45	0.97
C>G	-3	21	21	0.94	479	563	14.54	37	40	1.29
A>G	-2	17	16	0.74	25	15	0.56	27	34	1.02
A>C	-2	3	2	0.11	0	0	0.00	0	0	0.00
A>T	-2	0	0	0.00	0	0	0.00	0	0	0.00
G>A	-1	9	12	0.47	146	121	3.73	100	131	3.88
G>T	-1	3	3	0.13	0	0	0.00	0	0	0.00
G>C	-1	2	7	0.20	9	1	0.14	0	0	0.00
Total ClassI				11.04			25.17			7.32

Table 7: Summary of Class II reversions identified in memory and naïve T-cells from WAS4.

We also compared the pattern of reversions between WAS4 and WASJ. This analysis showed both patients possessed Class I and Class II reversions. Interestingly, for patient WAS4, in both total $CD4^+$ and total $CD8^+$ T-cells, the most common Class I reversion was 995T→A ,restoring the original Arginine amino acid, and thus encoding for wild-type WAS protein (Table 7, marked in red). However, in WASJ, though 995T→C (restoring original arginine) appeared at highest frequency among $CD4^+$ T-cells, the most predominant genetic change in $CD8^+$ T-cells was 997A→C, which replaces the stop codon with the amino acid Serine (Table 7 marked in blue). These observations may suggest that reversions originated earlier in lymphocyte development, irrespective of whether or not they fully restore wild-type protein, undergo positive selection and accumulate over time.

		995A			995C			995G			996A			996C			996T			997C			997G			997T		
		F	R	%	F	R	%	F	R	%	F	R	%	F	R	%	F	R	%	F	R	%	F	R	%	F	R	%
WAS 4	CD4+	1330	1186	72.7	109	118	6.6	129	133	7.6	3	6	0.3	116	194	9.0	7	10	0.49	28	16	1.3	20	20	1.2	15	22	1.1
WAS J	CD4+	755	854	20.8	2232	2563	62.0	3	3	0.1	1	0	0.0	594	671	16.4	17	29	0.60	0	1	0.0	0	0	0.0	3	2	0.1
WAS 4	CD8+	1028	1223	53.9	31	30	1.5	46	71	2.8	0	0	0.0	751	884	39.2	11	17	0.67	46	37	2.0	0	0	0.0	0	0	0.0
WAS J	CD8+	0	0	0.0	2	3	0.6	7	14	2.7	0	1	0.1	74	86	20.7	0	0	0.00	267	317	75.6	0	0	0.0	1	0	0.1

Table 8: Summary of Class I reversions identified in WAS 4 and WASJ. Red-enclosed data show predominant genotypic reversion in $CD8^+$ T-cells from both patients. Blue-enclosed data show predominant reversion in $CD4^+$ T-cells.

Evaluation of Class II reversions in total lymphocyte populations from both patients revealed a greater frequency of revert ants in the $CD8^+$ T-cells from WAS4 as well as WASJ (Table 8). Additionally, many of the more-common Class II reversions appeared in both patients, and in some cases, across all four lymphocyte populations (e.g. changing the original cytosine located in intron 9, 3 base pairs upstream of exon 10).

		WAS4 CD4+ T-cells				WAS J CD4+ T-cells				WAS 4 CD8+ T-cells				WAS J CD8+ T-cells			
Reversion	Position	F	R	Total	% of Total	F	R	Total	% of Total	F	R	Total	% of Total	F	R	Total	% of Total
T>G	-30	11	9	20	0.3	0	0	0	0	0	0	0	0	0	0	0	0
A>C	-29	0	0	0	0	0	0	0	0	0	0	0	0	0	0	0	0
A>C	-28	5	1	6	0.1	0	0	0	0	0	0	0	0	0	0	0	0
A>G	-28	0	0	0	0	0	2	2	0	0	0	0	0	0	0	0	0
C>G	-27	3	2	5	0.1	0	0	0	0	1	1	2	0	0	0	0	0
C>T	-27	0	0	0	0	0	0	0	0	0	0	0	0	0	0	0	0
A>G	-26	0	0	0	0	0	0	0	0	1	2	3	0	0	0	0	0
C>G	-24	21	26	47	0.7	0	0	0	0	0	0	0	0	0	0	0	0
A>C	-22	0	0	0	0	0	0	0	0	0	0	0	0	0	0	0	0
T>G	-21	2	2	4	0.1	0	0	0	0	0	0	0	0	0	0	0	0
G>A	-20	0	0	0	0	0	0	0	0	0	0	0	0	0	0	0	0
T>A	-19	2	1	3	0	0	0	0	0	0	0	0	0	0	0	0	0
T>G	-19	7	11	18	0.3	0	0	0	0	7	10	17	0.2	0	0	0	0
T>C	-19	0	0	0	0	0	0	0	0	0	0	0	0	1	1	2	0
T>A	-17	2	3	5	0.1	0	0	0	0	0	0	0	0	0	0	0	0
T>G	-17	15	22	37	0.6	0	0	0	0	1	2	3	0	19	16	35	0.5
T>G	-16	0	0	0	0	0	0	0	0	0	0	0	0	0	0	0	0
A>G	-15	0	0	0	0	0	0	0	0	0	0	0	0	0	0	0	0
T>G	-14	6	3	9	0.1	0	0	0	0	5	0	5	0.1	23	31	54	0.7
T>C	-14	0	0	0	0	0	0	0	0	0	0	0	0	0	0	0	0
T>A	-14	0	0	0	0	0	0	0	0	0	0	0	0	0	0	0	0
A>G	-13	0	0	0	0	0	0	0	0	0	0	0	0	0	0	0	0
C>T	-12	0	0	0	0	0	0	0	0	0	0	0	0	2	0	2	0
C>G	-12	26	32	58	0.9	3	3	6	0.1	8	12	20	0.2	0	2	2	0
C>T	-11	2	2	4	0.1	0	0	0	0	0	0	0	0	0	0	0	0
C>A	-11	0	0	0	0	0	0	0	0	0	0	0	0	0	0	0	0
C>G	-9	6	2	8	0.1	0	0	0	0	0	0	0	0	0	0	0	0
C>T	-9	0	0	0	0	0	0	0	0	0	0	0	0	0	4	4	0.1
C>A	-8	0	0	0	0	0	0	0	0	0	0	0	0	0	0	0	0
C>T	-8	0	0	0	0	0	0	0	0	0	0	0	0	0	37	37	0.5
T>A	-7	3	2	5	0.1	0	0	0	0	0	0	0	0	0	0	0	0
T>G	-7	22	34	56	0.8	0	0	0	0	0	0	0	0	0	0	0	0
T>C	-7	0	0	0	0	1	1	2	0	0	0	0	0	0	0	0	0
C>A	-6	1	1	2	0	0	0	0	0	4	4	8	0.1	16	22	38	0.5
C>G	-6	19	24	43	0.6	0	0	0	0	3	2	5	0.1	842	1056	1898	26.1
C>A	-5	0	0	0	0	0	0	0	0	0	0	0	0	0	0	0	0
C>G	-5	6	9	15	0.2	0	0	0	0	0	0	0	0	0	0	0	0
A>C	-4	5	12	17	0.3	0	0	0	0	0	4	4	0	0	0	0	0
A>T	-4	0	0	0	0	0	0	0	0	0	0	0	0	156	267	423	5.8
C>A	-3	7	7	14	0.2	0	0	0	0	4	4	8	0.1	11	24	35	0.5
C>T	-3	45	40	85	1.3	49	52	101	1.3	607	721	1328	15.2	104	126	230	3.2
C>G	-3	104	115	219	3.3	1	2	3	0	363	431	794	9.1	2	3	5	0.1
A>G	-2	13	7	20	0.3	0	3	3	0	34	44	78	0.9	0	0	0	0
A>C	-2	2	0	2	0	0	0	0	0	0	0	0	0	0	0	0	0
A>T	-2	0	0	0	0	0	0	0	0	4	8	12	0.1	0	0	0	0
G>A	-1	9	8	17	0.3	19	16	35	0.4	299	400	699	8	23	39	62	0.9
G>T	-1	6	4	10	0.1	0	0	0	0	0	0	0	0	0	0	0	0
G>C	-1	2	7	9	0.1	0	0	0	0	4	11	15	0.2	0	0	0	0
Total					11.1				1.8				34.3				38.9

Table 9: Summary of Class II reversions detected in T-cells from WAS4 and WASJ patients.

CHAPTER 4: DISCUSSION

4.1 Genome editing in iPSC for correction of Wiskott-Aldrich Syndrome

Primary immunedeficiencies such as Wiskott-Aldrich syndrome, typically result in very severe phenotypes. Until very recently, the only potential cure for patients with these disorders was an appropriately matched allogeneic hematopoietic stem cell transplant (HSCT) early in life. Despite the advancements in transplantation, the availability of a donor greatly impacts the success of this treatment. Gene therapy efforts are promising, but despite the good results reported in recent clinical trials with lentiviral vectors, the current virus-mediated methods still present a serious risk for insertional oncogenesis, due to the large number of randomly-integrated vector inserts per patient (approximately 10,000 -25,000) [46]. Site-specific gene correction is an attractive strategy that offers the benefit of targeting one locus on the genome, thereby minimizing the potential for deleterious insertional events.

We have pursued a patient-specific therapeutic approach consisting of first generating iPSC from skin from the patient, and subsequently correcting the disease-causing mutation *in vitro* by virus-free HDR-mediated targeted integration in the endogenous mutant WAS locus utilizing Zinc-finger nuclease technology. To date, successful nuclease-mediated gene correction studies have focused on repair of specific mutations by targeted substitution (which requires new reagents for each intended modification) [68, 86], or transgene integration in safe harbor loci, such as the AAVS1 locus on chromosome 19, as shown for correction of alpha-thalassemia

and X-linked Chronic Granulomatous Disease [60, 87]. Our work is the first to demonstrate the targeted insertion of a $WAS_{2\text{-}12}$ repair transgene in the endogenous DNA sequence. Targeted transgene integration offers significant advantages: 1) It is applicable to nearly all mutations in a given gene; and 2) it allows for endogenous regulation of transgene expression.

There are also significant potential advantages to correcting WAS-causing mutations in iPSC vs. primary HSC. First, the unlimited expansion potential of these cells ensures abundant sample availability. Second, the clonal property of iPSC growth facilitates assessment and detection of potential deleterious genetic changes in individual clonal populations. Lastly, although there is, at present, no protocol for generation of transplantable hematopoietic stem cells from human iPSC, in principle, transplantation of corrected iPSC-derived HSCs, would provide patients with a genetically homogenous population of corrected cells. In addition, our own studies of WAS-revertant patients suggest that restoration of WASp expression in T-cells alone, even at low frequencies, significantly reduces the severity of the disease, provided these cells encompass a sufficiently broad antigen-recognition immunological repertoire [23]. Therefore, iPSC-derived gene-corrected T-cell precursors could presumably also be utilized therapeutically for treatment of WAS patients.

Our gene correction study also highlights the importance of target site selection when designing an endogenous integration strategy. Because WAS patients may each have a different disease-causing mutation [5], with no single mutation being predominant among patients, proposing a correction approach that is applicable to

most patients is a challenging task. Our goal was to target the insertion of a full or partial WAS cDNA construct to the mutant WAS locus, at a site near the start of the *WAS* gene, and in this way cover almost all possible mutations, while allowing for endogenous control of transgene expression.

For our initial studies in K562, we tested two sets of ZFN, both of which cleaved a sequence early in the *WAS* gene, and therefore were suitable candidates for our strategy (Figure 9). We observed S4-ZFN targeting intron 1 offered two major advantages compared to S1-ZFN: higher targeting efficiency and low toxicity. Co-delivery of ZFN and donor to K562 cells resulted in targeted integration at the WAS locus, and even with significant increase in size of donor molecule, the integration efficiency did not reduce dramatically. When co-delivering a 1.6kb PGK-GFP donor, we detected sustained GFP expression over a period of 4 weeks. PCR-analysis showed correct targeting in 30% of the WAS alleles (Figure 10). It is possible that, because K562 are female cells (thus carrying two copies of the *WAS* gene), both alleles were targeted in specific cells. We, however, did not further investigate this possibility. We also analyzed DNA from GFP^+ cells transfected with the donor plasmid only. These cells, though stably expressing GFP, did not show integration in intron 1 of WAS, indicating expression arose from a random integration somewhere else in the genome. K562 are a tumor cell line [78] and, as such, intrinsic genomic instability likely results in random DSB which can facilitate integration of donor DNA.

Encouraged by our preliminary gene targeting data, we built our final donor construct comprised of WAS exons 2 through 12, preceded by a splice acceptor, in

order to allow proper splicing of our transgene. For the purpose of correction of WAS iPSC, we added a puro-TK selection cassette to the donor construct. Since pluripotent cells proliferate robustly in culture, the puromycin resistance facilitated identification of targeted clones. Though our overall targeting efficiency may initially seem low, with 7 clones (out of $2x10^6$ nucleofected cells) resulting after puromycin treatment (Figure 13), almost all of them (6 out of 7) had the desired insertion in intron 1. This observation suggested high specificity of ZFN activity, and indicated proper homology-directed repair of ZFN-induced DSB. We initially expanded clones 2 and 5 in culture and, over the course of several passages, observed close 5 was more stable in culture, maintaining a pluripotent, undifferentiated state over many passages. We selected this clone for Southern blot analysis. Utilizing a probe against the puromycin gene, we confirmed the presence of only the intended integration, at intron 1 of the WAS locus.

Zinc-Finger nuclease technology has been extensively studied, and various studies have shown successful targeting of genomic loci using ZFNs, some of which have already moved into clinical trials [91,88]. Though the efficacy of these reagents has been confirmed through these various studies, off-target effects of ZFN activity have been previously reported [59, 89-90, 92], with the extent of such effects varying depending on the ZFN and the target sequence. In order to analyze our cells for potential deleterious genomic effects due to ZFN activity, we performed comparative genomic hybridization array (aCGH) analysis of DNA from both mutant and corrected iPSC against a normal, diploid control. This analysis detected a total of thirty-two genomic changes in both the mutant and corrected iPSC lines, most of

which were small amplifications and deletions (Table 4). Twenty-five of these were found in both mutant and corrected cells, suggesting no association with the genetic manipulations we performed in the course of correction. Seven unique changes were reported between the two lines, mostly consisting of amplifications ranging from 54kb to 88kb. Four of them were found in the corrected iPSC, and three in the mutant. We have not examined in any detail the significance or potential consequences of the unique changes observed.

Since WASp is exclusively expressed in hematopoietic cells, we anticipated our ability to detect restoration of protein expression in corrected cells would first require that we derived hematopoietic cells from our cWAS iPSC. Various groups have reported successful in vitro generation of hematopoietic progenitors [75, 77, 94-96]. Guided by the principles established in these protocols, we derived $CD34^+CD43^+$ progenitor cells from both iPSC lines in a spin EB/OP9 co-culture, and from wild-type WA09 hES cells. Both WAS and cWAS iPSC generated high levels of hematopoietic progenitors in 10 separate experiments. We saw no evidence of impaired hematopoietic differentiation potential in WAS iPSC, when compared to both corrected iPSC and wild-type control WA09. Expression of our GFP reporter gene was observed in the corrected progenitors, reflecting both activation of the endogenous WAS promoter and correct splicing and expression of our transgene. This observation was further confirmed by performing RT-PCR analysis in total RNA harvested from WAS and cWAS progenitor cells. We detected GFP mRNA in only the cWAS-derived $CD34^+CD43^+$ cells. Furthermore, RT-PCR analysis revealed both mutant and corrected progenitors generated WAS mRNA, but sequencing analysis

of the RT-PCR product showed that cDNA generated from WAS progenitors carried the 1305insG mutation, while cWAS progenitors exclusively showed the correct WAS transgene exon 10 sequence. Furthermore, in the construction of our repair donor, we introduced a silent mutation at base-pair position 995 (310 bases upstream of 1305 insertion). This change was also present in mRNA from cWAS progenitors, providing additional confirmation of transgene expression. Western results validated WASp expression in corrected $CD34^{+}CD43^{+}$ cells, while no protein was detected in mutant cells, as expected. We anticipated WASp expressed from our transgene would have higher molecular weight. This is due to the use of 2A peptide to link both the WAS and GFP genes in the donor template. At the time of translation, ribosome skipping occurs near the end of the 2A sequence leaving 19 amino acids of the peptide attached to the upstream protein [80]. Thus, a shift in size of approximately 3kD is expected for the transgenic WASp. Indeed we observed the corrected $CD34^{+}CD43^{+}$ cells expressed a slightly larger WASp when compared to the wild-type WASp expressed from PBMC and from hESC-derived hematopoietic progenitor cells. Both Western Blot and FACS analysis of intracellular WASp showed corrected cells expressed a slightly lower level of WASp than that seen for hESC- derived progenitor cells. A possible explanation is that the presence of an additional 19 amino acids from the “2A tag” at the C-terminus may induce some level of premature degradation of protein. In addition, if the ribosome skipping at the 2A site is not 100% efficient, some of the translated WASp may be present as a WASp-2A-GFP fusion protein, and may, consequently, be degraded.

Our intracellular staining and FACS analysis results detected a small level of WASp in mutant progenitor cells. Western Blot analysis, on the contrary, does not show any detectable WAS protein in mutant progenitor cells or NK cells. At the RNA level, however, we do detect *WAS* RNA in both mutant and corrected progenitors (and the same is true for NK cells). Because the 1305insG mutation induces a frame-shift late in the gene, it is conceivable that an aberrant protein is formed, which is later degraded. However, Western Blot analysis shows no detectable WASp in either mutant progenitors or mutant NK cells. What is likely occurring is that the anti-WASp antibody used for intracellular staining exhibits a small level of non-specific binding, perhaps to N-WASp (close WASp family member that shares homology to WAS).

Having established the restoration of WASp expression in corrected cells, the next step was to evaluate whether *WAS* gene repair correlated with reinstatement of normal WASp-related function. Not much is known about the involvement of WASp in normal function of HSPCs. Some studies looking at $CD34^+$ HSPCs from obligate female carriers revealed non-random X-inactivation occurs in the progenitors found in the bone marrow, indicating a selective pressure against cells carrying the mutant copy [97,98]. Furthermore, Lacout et.al. observed that WASp-deficient mice display the same impairments in cell trafficking and chemotaxis reported in human $WASp^-$ cells. They attributed the non-random X-inactivation pattern reported in HSPC to a defect in migration ability which significantly affects the homing of these cells to the bone marrow [18]. WASp deficiency has also been linked to abnormal hematopoietic proliferation and differentiation in colony-forming

assays when primary bone marrow $CD34^+$ cells from WAS patients were compared to those from healthy controls [99].

We demonstrated proper progenitor function by in vitro differentiation of total $CD34^+$ hematopoietic progenitor cells in colony-forming assays. Day 14 spin EB-derived $CD34^+$ progenitor cells from both WAS and cWAS gave rise to macrophage (CFU-M), granulocyte (CFU-G) and granulocyte-macrophage (CFU-GM) colonies, however no erythrocyte lineages were observed in two separate experiments. Though our total numbers of colonies may appear low, they are consistent with values reported in similar work performed with *in vitro* hESC-derived progenitor cells [100]. cWAS-$CD34^+$ progenitors produced a higher number of colonies in two different experiments (each done in triplicate), perhaps suggesting a growth and differentiation advantage, though our numbers never reached statistical significance. All colonies derived from cWAS progenitors were GFP^+, demonstrating sustained transgene expression in progeny cells. We speculate the apparent lineage-restricted CFC potential (due to absence of erythromegakaryocytic colonies) observed in our iPSC- derived progenitors is an indicator of their stage in development. Our data show that most of the $CD34^+$ cells present in our day14 cultures (time of harvest) are also $CD43^+$, with a large number of those co-expressing CD45. Vodyanik and colleagues performed a detailed analysis of the CFC potential of different subsets of $CD43^+$ hematopoietic progenitors generated in WA09/OP9 co-cultures, and showed that $CD34^+CD43^+CD45^+$ cells expressed surface markers indicative of a more advanced, lineage-restricted specification.

Furthermore, they reported an association of these cells with a surge of CFC-GM/M colonies, which supports our CFC findings [96].

We subsequently took both WAS and cWAS-derived $CD34^+CD43^+$ progenitors through an NK-specific differentiation protocol, as previously described [101,102]. Within the first 10 days of culture, progenitor cells underwent substantial proliferation, with an average increase of approximately 20-fold observed for both mutant and corrected cells. Immunostaining analysis of day 16 cultures showed cWAS progenitors gave rise to a clearly identifiable population of $CD56^+$ NK cells, very similar to our control WA01/WA09 cells. Phenotypic analysis of corrected NK cells showed expression of NK-specific markers at levels comparable to those of normal control cells. Expression of CD16 (an NK-specific lysis receptor associated with NK cell cytotoxicity) was restored in cWAS-NK cells, whereas in mutant NK cells it was noticeably decreased, suggesting terminal maturation of these cells is impaired [104] Moreover, NK cells derived from cWAS progenitors expressed GFP, providing the first indication of stable expression of the integrated transgene. Western Blot analysis of NK cell lysates confirmed WASp was expressed in the corrected population, at a level similar to the wild-type WA09 control. Once again, the WASp from cWAS-derived NK cells was of slightly greater molecular weight than wild-type WASp, consistent with residual 2A peptide. The Western Blot did not include lysate from mutant NK cells, as the number of cells generated in the differentiation assay was not sufficient for this analysis. Because we did not investigate this observation further, we can only speculate that, perhaps the NK-

specific *in vitro* differentiation conditions required WASp expression at a certain point during development.

The extent of NK-cell functional abnormalities due to absence of WASp seems to vary between patients [17]. It is known, however, that the actin cytoskeleton plays a crucial role in activation of NK cells and T-cells [17]. The binding of NK cells to their targets, the lysis of these targets, and the subsequent recycling of NK cells are all events which require an intact cytoskeleton [94]. In addition, cytoskeletal reorganization is believed to be associated with cytokinetic movements required for polarization of the secretory machinery in the synaptic interface between the effector cells and their target [103]. As previously described, WASp is a known key regulator of actin cytoskeleton reorganization through its interaction with the Arp2/3 complex. Furthermore, Orange and colleagues [17] closely evaluated NK cells derived from two WAS patients, and demonstrated WASp is required for normal localization of F-actin to the activating immunologic synapse and the subsequent activation of NK-cell cytotoxic function.

Based on these reports that WASp plays a significant role in activation of NK cells, we investigated whether restoration of WASp expression in corrected cells correlated with restoration of function. When assayed for their functionality, WAS NK cells exhibited significant deficits in comparison to wild-type (WA01) hESC-derived NK cells. Upon stimulation with K562 cells, both WA01-derived NK cells and cWAS-derived NK cells upregulated production of interferon-γ (IFNγ) and tumor necrosis factor-α (TNFα). These pro-inflammatory cytokines are produced by NK cells upon activation by antigen, and are believed to be critical for NK-mediated

antiviral defense [105-107]. Moreover, the upregulation of interferon-γ is associated with normal NK activation and the subsequent induction of target-cell cytolysis [108, 109]. This response to stimulation was not exhibited by WAS-derived mutant NK cells, which is consistent with previous reports that NK cells from WAS patients show a significant reduction in their ability to bind K562 targets due to the insufficient accumulation of F-actin at the immunologic synapse [105]. The poor binding ability prevents proper stimulation of NK cells. Taken together, these data indicate correction of WAS restored NK cell functionality and cytokine production when exposed to K562 erythroleukemia cells.

During our NK differentiation work, we observed WAS-derived mutant progenitors displayed a remarkable deficiency in generating NK cells, whereas corrected progenitors produced NK cells robustly. This deficit in our mutant line remained until the end of the 30-day culture, suggesting a true defect, and not simply a delayed response to cytokine and feeder stimulation. Moreover, these results were seen in 6 of 6 experiments, utilizing either OP9-DL1 or OP9-DL4 stromal support.

This observation suggests correction of WAS may have conferred a selective advantage to these cells *in vitro.* To date, however, no data have yet reported a link between WASp deficiency and impaired NK cell development. In fact, a closer analysis of PBMC obtained from WAS-patients showed a significantly higher percentage of NK cells than seen in normal individuals [17], indicating no deficiency in NK cell generation. Interestingly, Zhang and colleagues [110] developed a mouse model engineered to express a 1305insG mutation in exon 10 of the *WAS*

gene. This mutation, like the one we have in our WAS-NK cells (1305insG), leads to the loss of the catalytic VCA domain necessary for normal function of WASp. They observed that, whereas humans and mice lacking WASp have modest T-cell deficits, the mice expressing the 1305insG mutant protein showed significant impairment in T-cell lymphopoiesis, with thymic cellularity at 12-16% of the normal levels of thymocytes seen in wild-type mice [111]. Upon analysis of thymocyte subpopulations, they traced this defect to a severe block occurring after TCRβ rearrangement during T-cell development.

Based on such pronounced phenotype, Zhang and colleages hypothesize that the 1305delG mutant WASp might have a dominant-negative effect by interfering with the compensatory function of a redundant protein such as N-WASp (a WASp family member, expressed ubiquitously). They believe that, in the absence of functional WASp, N-WASp is recruited via the N-terminal domains (which are conserved between the two proteins) to sites of activation and performs a redundant function, compensating for the lack of WASp. Because the 1305delG mutant protein still has an intact N-terminus, it interferes with the recruitment of N-WASp. Additional evidence reported in other studies of WASp-deficient mice substantiates the claim that N-WASp plays a role in murine lymphocyte development [112,113]. Similar studies have not been conducted in humans, and there is, at present, no clear evidence of the involvement of N-WASp in human lymphocyte development.

Remold-O'Donnel's group, through their study of two WAS-revertant patients carrying the same 1305delG mutation, proposed that human thymocytes expressing the mutant WASp encounter a block to differentiation at a similar time point to that

seen in mice, after TCRβ rearrangement, and that this block creates a selective advantage for cells which have restored WASp expression. Based on this notion, we speculate that perhaps NK cell development is also impaired at some stage during development in the case of our mutant cells, and that, by correcting the WAS defect, a functional protein is produced and restores the full NK differentiation potential.

We believe our work is innovative in many aspects. First, to our knowledge, this is the first report of modeling WAS disease in WAS iPSC. Moreover, our targeted endogenous integration approach for correction of a mutant gene in iPSC differs from the many reports published thus far, which comprise of safe-harbor integration or site-specific base-pair substitution strategies [71-73]. Lastly, by using an endogenous knock-in GFP reporter in our donor template, we generated a useful tool for tracking WASp expression during hematopoietic development.

4.2 Somatic Revertant Mosaicism in WAS patients

Somatic Revertant Mosaicism has been described in various hematological, as well as non-hematological disorders [114] Wiskott-Aldrich Syndrome is among the primary immunedeficiencies for which many revertant patients have been reported. A world-wide research study looking at 272 patients with WAS identified a total of 30 revertant patients, thus setting the frequency of WAS somatic revertants at 11% [115]. Occurring at this reasonably high frequency, this phenomenon has attracted

the interest of several investigators seeking to elucidate the extent of these reversions and how they influence disease phenotype.

Thus far, T-cells have been the most frequent subset of lymphocytes found to carry reversions [114]. Our group was one of the first to report the discovery of several revertant genotypes in a WAS patient [116]. The development of reversions in WAS patients has also been observed in B-cell and NK-cells, albeit to a lesser extent [117-119]. To date, these discoveries have resulted from Sanger sequencing assessment of the mutation region, which offers limited depth of analysis. Most studies have reported finding only one revertant genotype per patient. However, the few reports identifying multiple different reversions in a given patient has raised questions as to how diverse the revertant repertoire truly is, and whether there are reversions occurring at frequencies that are below the threshold detected by the current methods.

In order to address these questions, we analyzed lymphocyte populations from 3 WAS patients (previously described as revertant) using next-generation sequencing (NGS). This methodology provides the depth of coverage that allows detection of even low-frequency revertant genotypes. We hypothesized that our analysis would result in identification of many revertant genotypes in a given patient.

We previously reported our finding of over 30 different revertant genotypes in WAS4 revertant T-cells [116,119]. Those results were obtained from studies of clonal T-cell populations. In this new study, we analyzed sorted $WASp^{+}$ WAS4 T-cells, but this time using next generation sequencing analysis. With this

methodology, we identified a much larger number of genotypic changes, some occurring at very low frequency, which explained why they were not detected in the first analysis. These changes constituted a mixture of point mutations, splicing variants, as well as deletions and insertion, confirming the different classes of genotypes we observed in our first analysis [119]. In this report, we focus on two classes of reversions: Class I (genetic changes occurring directly in the mutant codon), and Class II (base-pair changes found in intron 9, upstream of mutant codon). The class I revertants likely restore a full-length WAS protein by replacing the mutant stop codon with various amino acids. Class II reversions, on the other hand, possibly restore expression by generating an internally-deleted or frame-shifted WASp through alternative splicing, skipping the mutant codon [26].

For patient WAS4, we were able to assay not only bulk T- and B-cells, but also memory and naïve T-cell subsets. When comparing these two populations, our analysis showed a greater diversity of revertant genotypes in the memory cells. We speculate this is indicative of cells that, because of restoration of WASp expression, were able to properly respond to antigen stimulation, and remained as part of the memory T-cell pool. It is well established that WASp plays a significant role in T-cell activation. Though WAS patients are capable of generating T-cells, these are unable to reach optimal levels of activation through the T-cell receptor (TCR), and do not respond well to IL-2 stimulation [15,16]. Restoration of WASp expression normalizes these responses, and therefore reestablishes T-cells function.

Analogous to WAS4, our observations were that patient WASJ, though not related to WAS4, also possessed a diverse revertant repertoire, sharing some of the same class I and class II reversions detected in WAS4. Interestingly, in a side-by-side comparison of T-cell populations from both patients, we observed that even though both patients showed a similar variety of class I genotypes, WAS 4 had an more diverse repertoire of class II reversions in both his $CD4^+$ and $CD8^+$ T-cells. We believe this can be explained by the difference in age between WAS 4 (45 years old) and WASJ (18 years old). Somatic reversions result from spontaneous mutations and thus, with time, newer revertant genotypes may arise, and their respective frequencies may increase, as it has been described previously [24].

At this time, we can only speculate regarding the mechanisms underlying the origination of such a diverse revertant repertoire in these patients. Possible suggested mechanisms may include DNA polymerase errors, DNA repair defect, or exposure to genotoxic agents. We currently do not have knowledge of potential contributions from any of these to the origination of reversions in these patients. However, analysis of mutation rate in the *PIG-A* gene in WAS4 revertant B-lymphocytes, showed no difference when compared to that observed in non-revertant WAS patients and normal individuals [23].

To our knowledge, this is the first study to report ultra-deep sequencing analysis of WAS-revertant patients. It provides an unprecedented view of spontaneous mutation in a human organism, made possible through the selective pressure for cells that have restored full or partial gene function.

BIBLIOGRAPHY

1. Ochs, H. D., A. H. Filipovich, P. Veys, M. J. Cowan and N. Kapoor (2009). "Wiskott-Aldrich syndrome: diagnosis, clinical and laboratory manifestations, and treatment." Biol Blood Marrow Transplant **15**(1 Suppl): 84-90.
2. Massaad, M. J., N. Ramesh and R. S. Geha (2013). "Wiskott-Aldrich syndrome: a comprehensive review." Ann N Y Acad Sci **1285**: 26-43
3. Aldrich, R. A., A. G. Steinberg and D. C. campbell (1954). "Pedigree demonstrating a sex-linked recessive condition characterized by draining ears, eczematoid dermatitis and bloody diarrhea." Pediatrics **13**(2): 133-139.
4. Derry, J. M., H. D. Ochs and U. Francke (1994). "Isolation of a novel gene mutated in Wiskott-Aldrich syndrome." Cell **79**(5): following 922.
5. Jin, Y., C. Mazza, J. R. Christie, S. Giliani, M. Fiorini, P. Mella, F. Gandellini, D. M. Stewart, Q. Zhu, D. L. Nelson, L. D. Notarangelo and H. D. Ochs (2004). "Mutations of the Wiskott-Aldrich Syndrome Protein (WASP): hotspots, effect on transcription, and translation and phenotype/genotype correlation." Blood **104**(13): 4010-4019.
6. Ochs, H. D. (2009). "Mutations of the Wiskott-Aldrich Syndrome Protein affect protein expression and dictate the clinical phenotypes." Immunol Res **44**(1-3): 84-88.
7. Ramesh, N. and R. Geha (2009). "Recent advances in the biology of WASP and WIP." Immunol Res **44**(1-3): 99-111.

8. Zhang, J., F. Shi, K. Badour, Y. Deng, M. K. McGavin and K. A. Siminovitch (2002). "WASp verprolin homology, cofilin homology, and acidic region domain-mediated actin polymerization is required for T cell development." Proc Natl Acad Sci U S A **99**(4): 2240-2245.
9. Badour, K., J. Zhang and K. A. Siminovitch (2004). "Involvement of the Wiskott-Aldrich syndrome protein and other actin regulatory adaptors in T cell activation." Semin Immunol **16**(6): 395-407.
10. Yarar, D., W. To, A. Abo and M. D. Welch (1999). "The Wiskott-Aldrich syndrome protein directs actin-based motility by stimulating actin nucleation with the Arp2/3 complex." Curr Biol **9**(10): 555-558.
11. Padrick, S. B., H. C. Cheng, A. M. Ismail, S. C. Panchal, L. K. Doolittle, S. Kim, B. M. Skehan, J. Umetani, C. A. Brautigam, J. M. Leong and M. K. Rosen (2008). "Hierarchical regulation of WASP/WAVE proteins." Mol Cell **32**(3): 426-438.
12. Thrasher, A. J. and S. O. Burns (2010). "WASP: a key immunological multitasker." Nat Rev Immunol **10**(3): 182-192.
13. Devriendt, K., A. S. Kim, G. Mathijs, S. G. Frints, M. Schwartz, J. J. Van Den Oord, G. E. Verhoef, M. A. Boogaerts, J. P. Fryns, D. You, M. K. Rosen and P. Vandenberghe (2001). "Constitutively activating mutation in WASP causes X-linked severe congenital neutropenia." Nat Genet **27**(3): 313-317.
14. Marangoni, F., M. Bosticardo, S. Charrier, E. Draghici, M. Locci, S. Scaramuzza, C. Panaroni, M. Ponzoni, F. Sanvito, C. Doglioni, M. Liabeuf, B. Gjata, M. Montus, K. Siminovitch, A. Aiuti, L. Naldini, L. Dupré, M. G.

Roncarolo, A. Galy and A. Villa (2009). "Evidence for long-term efficacy and safety of gene therapy for Wiskott-Aldrich syndrome in preclinical models." Mol Ther 17(6): 1073-1082.

15. Charrier, S., L. Dupré, S. Scaramuzza, L. Jeanson-Leh, M. P. Blundell, O. Danos, F. Cattaneo, A. Aiuti, R. Eckenberg, A. J. Thrasher, M. G. Roncarolo and A. Galy (2007). "Lentiviral vectors targeting WASp expression to hematopoietic cells, efficiently transduce and correct cells from WAS patients." Gene Ther 14(5): 415-428.
16. Dupré, L., S. Trifari, A. Follenzi, F. Marangoni, T. Lain de Lera, A. Bernad, S. Martino, S. Tsuchiya, C. Bordignon, L. Naldini, A. Aiuti and M. G. Roncarolo (2004). "Lentiviral vector-mediated gene transfer in T cells from Wiskott-Aldrich syndrome patients leads to functional correction." Mol Ther **10**(5): 903-915.
17. Orange, J. S., N. Ramesh, E. Remold-O'Donnell, Y. Sasahara, L. Koopman, M. Byrne, F. A. Bonilla, F. S. Rosen, R. S. Geha and J. L. Strominger (2002). "Wiskott-Aldrich syndrome protein is required for NK cell cytotoxicity and colocalizes with actin to NK cell-activating immunologic synapses." Proc Natl Acad Sci U S A **99**(17): 11351-11356.
18. Lacout, C., E. Haddad, S. Sabri, F. Svinarchouk, L. Garçon, C. Capron, A. Foudi, R. Mzali, S. B. Snapper, F. Louache, W. Vainchenker and D. Duménil (2003). "A defect in hematopoietic stem cell migration explains the nonrandom X-chromosome inactivation in carriers of Wiskott-Aldrich syndrome." Blood **102**(4): 1282-1289.

19. Filipovich, A. H., J. V. Stone, S. C. Tomany, M. Ireland, C. Kollman, C. J. Pelz, J. T. Casper, M. J. Cowan, J. R. Edwards, A. Fasth, R. P. Gale, A. Junker, N. R. Kamani, B. J. Loechelt, D. W. Pietryga, O. Ringdén, M. Vowels, J. Hegland, A. V. Williams, J. P. Klein, K. A. Sobocinski, P. A. Rowlings and M. M. Horowitz (2001). "Impact of donor type on outcome of bone marrow transplantation for Wiskott-Aldrich syndrome: collaborative study of the International Bone Marrow Transplant Registry and the National Marrow Donor Program." Blood **97**(6): 1598-1603.
20. Davis, B. R. and F. Candotti (2009). "Revertant somatic mosaicism in the Wiskott-Aldrich syndrome." Immunol Res **44**(1-3): 127-131.
21. Pasmooij, A. M., M. Garcia, M. J. Escamez, A. M. Nijenhuis, A. Azon, N. Cuadrado-Corrales, M. F. Jonkman and M. Del Rio (2010). "Revertant mosaicism due to a second-site mutation in COL7A1 in a patient with recessive dystrophic epidermolysis bullosa." J Invest Dermatol **130**(10): 2407-2411.
22. Pasmooij, A. M., H. H. Pas, M. C. Bolling and M. F. Jonkman (2007). "Revertant mosaicism in junctional epidermolysis bullosa due to multiple correcting second-site mutations in LAMB3." J Clin Invest **117**(5): 1240-1248.
23. Davis, B. R., Q. Yan, J. H. Bui, K. Felix, D. Moratto, L. M. Muul, N. L. Prokopishyn, R. M. Blaese and F. Candotti (2010). "Somatic mosaicism in the Wiskott-Aldrich syndrome: molecular and functional characterization of genotypic revertants." Clin Immunol **135**(1): 72-83.

24. Davis, B. R. and F. Candotti (2010). "Genetics. Mosaicism--switch or spectrum?" Science **330**(6000): 46-47.
25. Wada, T., A. Konno, S. H. Schurman, E. K. Garabedian, S. M. Anderson, M. Kirby, D. L. Nelson and F. Candotti (2003). "Second-site mutation in the Wiskott-Aldrich syndrome (WAS) protein gene causes somatic mosaicism in two WAS siblings." J Clin Invest **111**(9): 1389-1397.
26. Davis, B. R., M. J. Dicola, N. L. Prokopishyn, J. B. Rosenberg, D. Moratto, L. M. Muul, F. Candotti and R. Michael Blaese (2008). "Unprecedented diversity of genotypic revertants in lymphocytes of a patient with Wiskott-Aldrich syndrome." Blood **111**(10): 5064-5067.
27. Ariga, T., T. Kondoh, K. Yamaguchi, M. Yamada, S. Sasaki, D. L. Nelson, H. Ikeda, K. Kobayashi, H. Moriuchi and Y. Sakiyama (2001). "Spontaneous in vivo reversion of an inherited mutation in the Wiskott-Aldrich syndrome." J Immunol **166**(8): 5245-5249.
28. Mukherjee, S. and A. J. Thrasher (2013). "Gene therapy for PIDs: progress, pitfalls and prospects." Gene **525**(2): 174-181.
29. Kohn, D. B. (2010). "Update on gene therapy for immunodeficiencies." Clin Immunol **135**(2): 247-254.
30. Dick, J. E., M. C. Magli, D. Huszar, R. A. Phillips and A. Bernstein (1985). "Introduction of a selectable gene into primitive stem cells capable of long-term reconstitution of the hemopoietic system of W/Wv mice." Cell **42**(1): 71-79.

31. Williams, D. A., I. R. Lemischka, D. G. Nathan and R. C. Mulligan (1984). "Introduction of new genetic material into pluripotent haematopoietic stem cells of the mouse." Nature **310**(5977): 476-480.
32. Blaese, R. M. (1993). "Development of gene therapy for immunodeficiency: adenosine deaminase deficiency." Pediatr Res **33**(1 Suppl): S49-53; discussion S53-45.
33. Hacein-Bey-Abina, S., C. von Kalle, M. Schmidt, F. Le Deist, N. Wulffraat, E. McIntyre, I. Radford, J. L. Villeval, C. C. Fraser, M. Cavazzana-Calvo and A. Fischer (2003). "A serious adverse event after successful gene therapy for X-linked severe combined immunodeficiency." N Engl J Med **348**(3): 255-256.
34. Hacein-Bey-Abina, S., C. Von Kalle, M. Schmidt, M. P. McCormack, N. Wulffraat, P. Leboulch, A. Lim, C. S. Osborne, R. Pawliuk, E. Morillon, R. Sorensen, A. Forster, P. Fraser, J. I. Cohen, G. de Saint Basile, I. Alexander, U. Wintergerst, T. Frebourg, A. Aurias, D. Stoppa-Lyonnet, S. Romana, I. Radford-Weiss, F. Gross, F. Valensi, E. Delabesse, E. Macintyre, F. Sigaux, J. Soulier, L. E. Leiva, M. Wissler, C. Prinz, T. H. Rabbitts, F. Le Deist, A. Fischer and M. Cavazzana-Calvo (2003). "LMO2-associated clonal T cell proliferation in two patients after gene therapy for SCID-X1." Science **302**(5644): 415-419.
35. Biasco, L., C. Baricordi and A. Aiuti (2012). "Retroviral integrations in gene therapy trials." Mol Ther **20**(4): 709-716.
36. Gabriel, R., M. Schmidt and C. von Kalle (2012). "Integration of retroviral vectors." Curr Opin Immunol **24**(5): 592-597.

37. Fischer, A., S. Hacein-Bey-Abina and M. Cavazzana-Calvo (2004). "[Gene therapy of children with X-linked severe combined immune deficiency: efficiency and complications]." Med Sci (Paris) **20**(1): 115-117.
38. Hacein-Bey-Abina, S., A. Garrigue, G. P. Wang, J. Soulier, A. Lim, E. Morillon, E. Clappier, L. Caccavelli, E. Delabesse, K. Beldjord, V. Asnafi, E. MacIntyre, L. Dal Cortivo, I. Radford, N. Brousse, F. Sigaux, D. Moshous, J. Hauer, A. Borkhardt, B. H. Belohradsky, U. Wintergerst, M. C. Velez, L. Leiva, R. Sorensen, N. Wulffraat, S. Blanche, F. D. Bushman, A. Fischer and M. Cavazzana-Calvo (2008). "Insertional oncogenesis in 4 patients after retrovirus-mediated gene therapy of SCID-X1." J Clin Invest **118**(9): 3132-3142.
39. Tiscornia, G., O. Singer and I. M. Verma (2006). "Production and purification of lentiviral vectors." Nat Protoc **1**(1): 241-245.
40. Fischer, A., S. Hacein-Bey-Abina and M. Cavazzana-Calvo (2013). "Gene therapy of primary T cell immunodeficiencies." Gene **525**(2): 170-173.
41. Cavazzana-Calvo, M., A. Fischer, S. Hacein-Bey-Abina and A. Aiuti (2012). "Gene therapy for primary immunodeficiencies: Part 1." Curr Opin Immunol **24**(5): 580-584.
42. Avedillo Díez, I., D. Zychlinski, E. G. Coci, M. Galla, U. Modlich, R. A. Dewey, A. Schwarzer, T. Maetzig, N. Mpofu, E. Jaeckel, K. Boztug, C. Baum, C. Klein and A. Schambach (2011). "Development of novel efficient SIN vectors with improved safety features for Wiskott-Aldrich syndrome stem cell based gene therapy." Mol Pharm **8**(5): 1525-1537.

43. Schambach, A., D. Mueller, M. Galla, M. M. Verstegen, G. Wagemaker, R. Loew, C. Baum and J. Bohne (2006). "Overcoming promoter competition in packaging cells improves production of self-inactivating retroviral vectors." Gene Ther **13**(21): 1524-1533.
44. Cornils, K., C. C. Bartholomae, L. Thielecke, C. Lange, A. Arens, I. Glauche, U. Mock, K. Riecken, S. Gerdes, C. von Kalle, M. Schmidt, I. Roeder and B. Fehse (2013). "Comparative clonal analysis of reconstitution kinetics after transplantation of hematopoietic stem cells gene marked with a lentiviral SIN or a γ-retroviral LTR vector." Exp Hematol **41**(1): 28-38.e23.
45. Cartier, N., S. Hacein-Bey-Abina, C. Von Kalle, P. Bougnères, A. Fischer, M. Cavazzana-Calvo and P. Aubourg (2010). "[Gene therapy of x-linked adrenoleukodystrophy using hematopoietic stem cells and a lentiviral vector]." Bull Acad Natl Med **194**(2): 255-264; discussion 264-258.
46. Aiuti, A., L. Biasco, S. Scaramuzza, F. Ferrua, M. P. Cicalese, C. Baricordi, F. Dionisio, A. Calabria, S. Giannelli, M. C. Castiello, M. Bosticardo, C. Evangelio, A. Assanelli, M. Casiraghi, S. Di Nunzio, L. Callegaro, C. Benati, P. Rizzardi, D. Pellin, C. Di Serio, M. Schmidt, C. Von Kalle, J. Gardner, N. Mehta, V. Neduva, D. J. Dow, A. Galy, R. Miniero, A. Finocchi, A. Metin, P. P. Banerjee, J. S. Orange, S. Galimberti, M. G. Valsecchi, A. Biffi, E. Montini, A. Villa, F. Ciceri, M. G. Roncarolo and L. Naldini (2013). "Lentiviral hematopoietic stem cell gene therapy in patients with Wiskott-Aldrich syndrome." Science **341**(6148): 1233151

47. Moehle, E. A., J. M. Rock, Y. L. Lee, Y. Jouvenot, R. C. DeKelver, R. C. Dekelver, P. D. Gregory, F. D. Urnov and M. C. Holmes (2007). "Targeted gene addition into a specified location in the human genome using designed zinc finger nucleases." Proc Natl Acad Sci U S A 104(9): 3055-3060.
48. Cathomen, T. and J. K. Joung (2008). "Zinc-finger nucleases: the next generation emerges." Mol Ther **16**(7): 1200-1207.
49. Carroll, D. (2004). "Using nucleases to stimulate homologous recombination." Methods Mol Biol **262**: 195-207.
50. Li, M., K. Suzuki, N. Y. Kim, G. H. Liu and J. C. Izpisua Belmonte (2014). "A Cut above the Rest: Targeted Genome Editing Technologies in Human Pluripotent Stem Cells." J Biol Chem **289**(8): 4594-4599.
51. Urnov, F. D., J. C. Miller, Y. L. Lee, C. M. Beausejour, J. M. Rock, S. Augustus, A. C. Jamieson, M. H. Porteus, P. D. Gregory and M. C. Holmes (2005). "Highly efficient endogenous human gene correction using designed zinc-finger nucleases." Nature **435**(7042): 646-651
52. Gaj, T., C. A. Gersbach and C. F. Barbas (2013). "ZFN, TALEN, and CRISPR/Cas-based methods for genome engineering." Trends Biotechnol **31**(7): 397-405.
53. Wiedenheft, B., S. H. Sternberg and J. A. Doudna (2012). "RNA-guided genetic silencing systems in bacteria and archaea." Nature **482**(7385): 331-338.

54. Urnov, F. D., E. J. Rebar, M. C. Holmes, H. S. Zhang and P. D. Gregory (2010). "Genome editing with engineered zinc finger nucleases." Nat Rev Genet 11(9): 636-646.
55. Cathomen, T. and C. Söllü (2010). "In vitro assessment of zinc finger nuclease activity." Methods Mol Biol 649: 227-235.
56. Händel, E. M. and T. Cathomen (2011). "Zinc-finger nuclease based genome surgery: it's all about specificity." Curr Gene Ther 11(1): 28-37.
57. Klug, A. (2005). "Towards therapeutic applications of engineered zinc finger proteins." FEBS Lett 579(4): 892-894.
58. Klug, A. (2010). "The discovery of zinc fingers and their applications in gene regulation and genome manipulation." Annu Rev Biochem 79: 213-231.
59. Perez, E. E., J. Wang, J. C. Miller, Y. Jouvenot, K. A. Kim, O. Liu, N. Wang, G. Lee, V. V. Bartsevich, Y. L. Lee, D. Y. Guschin, I. Rupniewski, A. J. Waite, C. Carpenito, R. G. Carroll, J. S. Orange, F. D. Urnov, E. J. Rebar, D. Ando, P. D. Gregory, J. L. Riley, M. C. Holmes and C. H. June (2008). "Establishment of HIV-1 resistance in CD4+ T cells by genome editing using zinc-finger nucleases." Nat Biotechnol 26(7): 808-816.
60. Zou, J., C. L. Sweeney, B. K. Chou, U. Choi, J. Pan, H. Wang, S. N. Dowey, L. Cheng and H. L. Malech (2011). "Oxidase-deficient neutrophils from X-linked chronic granulomatous disease iPS cells: functional correction by zinc finger nuclease-mediated safe harbor targeting." Blood 117(21): 5561-5572.
61. Santiago, Y., E. Chan, P. Q. Liu, S. Orlando, L. Zhang, F. D. Urnov, M. C. Holmes, D. Guschin, A. Waite, J. C. Miller, E. J. Rebar, P. D. Gregory, A. Klug

and T. N. Collingwood (2008). "Targeted gene knockout in mammalian cells by using engineered zinc-finger nucleases." Proc Natl Acad Sci U S A **105**(15): 5809-5814.

62. Holt, N., J. Wang, K. Kim, G. Friedman, X. Wang, V. Taupin, G. M. Crooks, D. B. Kohn, P. D. Gregory, M. C. Holmes and P. M. Cannon (2010). "Human hematopoietic stem/progenitor cells modified by zinc-finger nucleases targeted to CCR5 control HIV-1 in vivo." Nat Biotechnol 28(8): 839-847.
63. Takahashi, K. and S. Yamanaka (2006). "Induction of pluripotent stem cells from mouse embryonic and adult fibroblast cultures by defined factors." Cell **126**(4): 663-676.
64. Yu, J., M. A. Vodyanik, K. Smuga-Otto, J. Antosiewicz-Bourget, J. L. Frane, S. Tian, J. Nie, G. A. Jonsdottir, V. Ruotti, R. Stewart, I. I. Slukvin and J. A. Thomson (2007). "Induced pluripotent stem cell lines derived from human somatic cells." Science **318**(5858): 1917-1920.
65. Cheng, L. T., L. T. Sun and T. Tada (2012). "Genome editing in induced pluripotent stem cells." Genes Cells **17**(6): 431-438.
66. Mali, P. and L. Cheng (2012). "Concise review: Human cell engineering: cellular reprogramming and genome editing." Stem Cells **30**(1): 75-81.
67. Hockemeyer, D. and R. Jaenisch (2010). "Gene targeting in human pluripotent cells." Cold Spring Harb Symp Quant Biol **75**: 201-209.
68. Wang, Y., C. G. Zheng, Y. Jiang, J. Zhang, J. Chen, C. Yao, Q. Zhao, S. Liu, K. Chen, J. Du, Z. Yang and S. Gao (2012). "Genetic correction of β-

thalassemia patient-specific iPS cells and its use in improving hemoglobin production in irradiated SCID mice." Cell Res **22**(4): 637-648.

69. Hockemeyer, D., F. Soldner, C. Beard, Q. Gao, M. Mitalipova, R. C. DeKelver, G. E. Katibah, R. Amora, E. A. Boydston, B. Zeitler, X. Meng, J. C. Miller, L. Zhang, E. J. Rebar, P. D. Gregory, F. D. Urnov and R. Jaenisch (2009). "Efficient targeting of expressed and silent genes in human ESCs and iPSCs using zinc-finger nucleases." Nat Biotechnol 27(9): 851-857.
70. Raya, A., I. Rodríguez-Pizà, G. Guenechea, R. Vassena, S. Navarro, M. J. Barrero, A. Consiglio, M. Castellà, P. Río, E. Sleep, F. González, G. Tiscornia, E. Garreta, T. Aasen, A. Veiga, I. M. Verma, J. Surrallés, J. Bueren and J. C. Izpisúa Belmonte (2009). "Disease-corrected haematopoietic progenitors from Fanconi anaemia induced pluripotent stem cells." Nature **460**(7251): 53-59.
71. Wang, Y., C. G. Zheng, Y. Jiang, J. Zhang, J. Chen, C. Yao, Q. Zhao, S. Liu, K. Chen, J. Du, Z. Yang and S. Gao (2012). "Genetic correction of β-thalassemia patient-specific iPS cells and its use in improving hemoglobin production in irradiated SCID mice." Cell Res **22**(4): 637-648.
72. Zou, J., P. Mali, X. Huang, S. N. Dowey and L. Cheng (2011). "Site-specific gene correction of a point mutation in human iPS cells derived from an adult patient with sickle cell disease." Blood **118**(17): 4599-4608.
73. Lombardo, A., P. Genovese, C. M. Beausejour, S. Colleoni, Y. L. Lee, K. A. Kim, D. Ando, F. D. Urnov, C. Galli, P. D. Gregory, M. C. Holmes and L. Naldini (2007). "Gene editing in human stem cells using zinc finger nucleases

and integrase-defective lentiviral vector delivery." Nat Biotechnol **25**(11): 1298-1306.

74. Park, I.-H., and Daley, G. Q. (2009) Human iPS cell derivation/reprogramming, *Curr Protoc Stem Cell Biol Chapter 4*, Unit 4A.1.
75. Ng, E. S., R. P. Davis, T. Hatzistavrou, E. G. Stanley and A. G. Elefanty (2008). "Directed differentiation of human embryonic stem cells as spin embryoid bodies and a description of the hematopoietic blast colony forming assay." Curr Protoc Stem Cell Biol **Chapter 1**: Unit 1D.3.
76. Ni, Z., D. A. Knorr, C. L. Clouser, M. K. Hexum, P. Southern, L. M. Mansky, I. H. Park and D. S. Kaufman (2011). "Human pluripotent stem cells produce natural killer cells that mediate anti-HIV-1 activity by utilizing diverse cellular mechanisms." J Virol **85**(1): 43-50.
77. Timmermans, F., I. Velghe, L. Vanwalleghem, M. De Smedt, S. Van Coppernolle, T. Taghon, H. D. Moore, G. Leclercq, A. W. Langerak, T. Kerre, J. Plum and B. Vandekerckhove (2009). "Generation of T cells from human embryonic stem cell-derived hematopoietic zones." J Immunol **182**(11): 6879-6888.
78. Klein, E., H. Ben-Bassat, H. Neumann, P. Ralph, J. Zeuthen, A. Polliack and F. Vánky (1976). "Properties of the K562 cell line, derived from a patient with chronic myeloid leukemia." Int J Cancer **18**(4): 421-431.
79. Trichas, G., J. Begbie and S. Srinivas (2008). "Use of the viral 2A peptide for bicistronic expression in transgenic mice." BMC Biol **6**: 40.

80. Szymczak-Workman, A. L., K. M. Vignali and D. A. Vignali (2012). "Design and construction of 2A peptide-linked multicistronic vectors." Cold Spring Harb Protoc **2012**(2): 199-204.
81. Carpén, O., I. Virtanen, V. P. Lehto and E. Saksela (1983). "Polarization of NK cell cytoskeleton upon conjugation with sensitive target cells." J Immunol **131**(6): 2695-2698.
82. Miller, J. S. (2001). "The biology of natural killer cells in cancer, infection, and pregnancy." Exp Hematol **29**(10): 1157-1168.
83. Orange, J. S. and Z. K. Ballas (2006). "Natural killer cells in human health and disease." Clin Immunol **118**(1): 1-10.
84. Woll, P. S., C. H. Martin, J. S. Miller and D. S. Kaufman (2005). "Human embryonic stem cell-derived NK cells acquire functional receptors and cytolytic activity." J Immunol **175**(8): 5095-5103.
85. Woll, P. S., B. Grzywacz, X. Tian, R. K. Marcus, D. A. Knorr, M. R. Verneris and D. S. Kaufman (2009). "Human embryonic stem cells differentiate into a homogeneous population of natural killer cells with potent in vivo antitumor activity." Blood **113**(24): 6094-6101.
86. Soldner, F., J. Laganière, A. W. Cheng, D. Hockemeyer, Q. Gao, R. Alagappan, V. Khurana, L. I. Golbe, R. H. Myers, S. Lindquist, L. Zhang, D. Guschin, L. K. Fong, B. J. Vu, X. Meng, F. D. Urnov, E. J. Rebar, P. D. Gregory, H. S. Zhang and R. Jaenisch (2011). "Generation of isogenic pluripotent stem cells differing exclusively at two early onset Parkinson point mutations." Cell **146**(2): 318-331.

87. Chang, C. J. and E. E. Bouhassira (2012). "Zinc-finger nuclease-mediated correction of α-thalassemia in iPS cells." Blood **120**(19): 3906-3914.
88. Tebas, P., D. Stein, W. W. Tang, I. Frank, S. Q. Wang, G. Lee, S. K. Spratt, R. T. Surosky, M. A. Giedlin, G. Nichol, M. C. Holmes, P. D. Gregory, D. G. Ando, M. Kalos, R. G. Collman, G. Binder-Scholl, G. Plesa, W. T. Hwang, B. L. Levine and C. H. June (2014). "Gene editing of CCR5 in autologous CD4 T cells of persons infected with HIV." N Engl J Med **370**(10): 901-910.
89. Radecke, S., F. Radecke, T. Cathomen and K. Schwarz (2010). "Zinc-finger nuclease-induced gene repair with oligodeoxynucleotides: wanted and unwanted target locus modifications." Mol Ther **18**(4): 743-753.
90. Do, T. U., B. Ho, S. J. Shih and A. Vaughan (2012). "Zinc Finger Nuclease induced DNA double stranded breaks and rearrangements in MLL." Mutat Res **740**(1-2): 34-42.
91. Yusa, K., S. T. Rashid, H. Strick-Marchand, I. Varela, P. Q. Liu, D. E. Paschon, E. Miranda, A. Ordóñez, N. R. Hannan, F. J. Rouhani, S. Darche, G. Alexander, S. J. Marciniak, N. Fusaki, M. Hasegawa, M. C. Holmes, J. P. Di Santo, D. A. Lomas, A. Bradley and L. Vallier (2011). "Targeted gene correction of α1-antitrypsin deficiency in induced pluripotent stem cells." Nature **478**(7369): 391-394.
92. Laurent, L. C., I. Ulitsky, I. Slavin, H. Tran, A. Schork, R. Morey, C. Lynch, J. V. Harness, S. Lee, M. J. Barrero, S. Ku, M. Martynova, R. Semechkin, V. Galat, J. Gottesfeld, J. C. Izpisua Belmonte, C. Murry, H. S. Keirstead, H. S. Park, U. Schmidt, A. L. Laslett, F. J. Muller, C. M. Nievergelt, R. Shamir and J.

F. Loring (2011). "Dynamic changes in the copy number of pluripotency and cell proliferation genes in human ESCs and iPSCs during reprogramming and time in culture." Cell Stem Cell **8**(1): 106-118.

93. Hill, K. L. and D. S. Kaufman (2008). "Hematopoietic differentiation of human embryonic stem cells by cocultivation with stromal layers." Curr Protoc Stem Cell Biol **Chapter 1**: Unit 1F.6.

94. Ng, E. S., R. P. Davis, L. Azzola, E. G. Stanley and A. G. Elefanty (2005). "Forced aggregation of defined numbers of human embryonic stem cells into embryoid bodies fosters robust, reproducible hematopoietic differentiation." Blood **106**(5): 1601-1603.

95. Ng, E. S., R. Davis, E. G. Stanley and A. G. Elefanty (2008). "A protocol describing the use of a recombinant protein-based, animal product-free medium (APEL) for human embryonic stem cell differentiation as spin embryoid bodies." Nat Protoc **3**(5): 768-776.

96. Vodyanik, M. A., J. A. Thomson and I. I. Slukvin (2006). "Leukosialin (CD43) defines hematopoietic progenitors in human embryonic stem cell differentiation cultures." Blood **108**(6): 2095-2105.

97. Wengler, G., J. B. Gorlin, J. M. Williamson, F. S. Rosen and D. H. Bing (1995). "Nonrandom inactivation of the X chromosome in early lineage hematopoietic cells in carriers of Wiskott-Aldrich syndrome." Blood **85**(9): 2471-2477.

98. Gealy, W. J., J. M. Dwyer and J. B. Harley (1980). "Allelic exclusion of glucose-6-phosphate dehydrogenase in platelets and T lymphocytes from a Wiskott-Aldrich syndrome carrier." Lancet **1**(8159): 63-65.

99. Kajiwara, M., S. Nonoyama, M. Eguchi, T. Morio, K. Imai, H. Okawa, M. Kaneko, M. Sako, S. Ohga, M. Maeda, S. Hibi, H. Hashimito, A. Shibuya, H. D. Ochs, T. Nakahata and J. I. Yata (1999). "WASP is involved in proliferation and differentiation of human haemopoietic progenitors in vitro." Br J Haematol **107**(2): 254-262.

100. Kaufman, D. S., E. T. Hanson, R. L. Lewis, R. Auerbach and J. A. Thomson (2001). "Hematopoietic colony-forming cells derived from human embryonic stem cells." Proc Natl Acad Sci U S A **98**(19): 10716-10721.

101. Bock, A. M., D. Knorr and D. S. Kaufman (2013). "Development, expansion, and in vivo monitoring of human NK cells from human embryonic stem cells (hESCs) and and induced pluripotent stem cells (iPSCs)." J Vis Exp(74): e50337.

102. Knorr, D. A., A. Bock, R. J. Brentjens and D. S. Kaufman (2013). "Engineered human embryonic stem cell-derived lymphocytes to study in vivo trafficking and immunotherapy." Stem Cells Dev **22**(13): 1861-1869.

103. Messina, C., D. Kirkpatrick, P. A. Fitzgerald, R. J. O'Reilly, F. P. Siegal, C. Cunningham-Rundles, M. Blaese, J. Oleske, S. Pahwa and C. Lopez (1986). "Natural killer cell function and interferon generation in patients with primary immunodeficiencies." Clin Immunol Immunopathol **39**(3): 394-404.

104. Mandelboim, O., P. Malik, D. M. Davis, C. H. Jo, J. E. Boyson and J. L. Strominger (1999). "Human CD16 as a lysis receptor mediating direct natural killer cell cytotoxicity." Proc Natl Acad Sci U S A **96**(10): 5640-5644.

105. Wang, R., J. J. Jaw, N. C. Stutzman, Z. Zou and P. D. Sun (2012). "Natural killer cell-produced IFN-γ and TNF-α induce target cell cytolysis through up-regulation of ICAM-1." J Leukoc Biol **91**(2): 299-309.

106. Marshall, J. D., D. S. Heeke, C. Abbate, P. Yee and G. Van Nest (2006). "Induction of interferon-gamma from natural killer cells by immunostimulatory CpG DNA is mediated through plasmacytoid-dendritic-cell-produced interferon-alpha and tumour necrosis factor-alpha." Immunology **117**(1): 38-46.

107. Lutskiy, M. I., J. Y. Park, S. K. Remold and E. Remold-O'Donnell (2008). "Evolution of highly polymorphic T cell populations in siblings with the Wiskott-Aldrich Syndrome." PLoS One **3**(10): e3444.

108. Zhang, J., F. Shi, K. Badour, Y. Deng, M. K. McGavin and K. A. Siminovitch (2002). "WASp verprolin homology, cofilin homology, and acidic region domain-mediated actin polymerization is required for T cell development." Proc Natl Acad Sci U S A **99**(4): 2240-2245.

109. Marshall, J. D., D. S. Heeke, C. Abbate, P. Yee and G. Van Nest (2006). "Induction of interferon-gamma from natural killer cells by immunostimulatory CpG DNA is mediated through plasmacytoid-dendritic-cell-produced interferon-alpha and tumour necrosis factor-alpha." Immunology **117**(1): 38-46.

110. Zhang, J., F. Shi, K. Badour, Y. Deng, M. K. McGavin and K. A. Siminovitch (2002). "WASp verprolin homology, cofilin homology, and acidic region domain-mediated actin polymerization is required for T cell development." Proc Natl Acad Sci U S A **99**(4): 2240-2245

111. Lutskiy, M. I., J. Y. Park, S. K. Remold and E. Remold-O'Donnell (2008). "Evolution of highly polymorphic T cell populations in siblings with the Wiskott-Aldrich Syndrome." PLoS One **3**(10): e3444.

112. Cotta-de-Almeida, V., L. Westerberg, M. H. Maillard, D. Onaldi, H. Wachtel, P. Meelu, U. I. Chung, R. Xavier, F. W. Alt and S. B. Snapper (2007). "Wiskott Aldrich syndrome protein (WASP) and N-WASP are critical for T cell development." Proc Natl Acad Sci U S A **104**(39): 15424-15429.

113. Westerberg, L. S., C. Dahlberg, M. Baptista, C. J. Moran, C. Detre, M. Keszei, M. A. Eston, F. W. Alt, C. Terhorst, L. D. Notarangelo and S. B. Snapper (2012). "Wiskott-Aldrich syndrome protein (WASP) and N-WASP are critical for peripheral B-cell development and function." Blood **119**(17): 3966-3974.

114. Wada, T. and F. Candotti (2008). "Somatic mosaicism in primary immune deficiencies." Curr Opin Allergy Clin Immunol **8**(6): 510-514.

115. Stewart, D. M., F. Candotti and D. L. Nelson (2007). "The phenomenon of spontaneous genetic reversions in the Wiskott-Aldrich syndrome: a report of the workshop of the ESID Genetics Working Party at the XIIth Meeting of the European Society for Immunodeficiencies (ESID). Budapest, Hungary October 4-7, 2006." J Clin Immunol **27**(6): 634-639.

116. Davis, B. R., M. J. Dicola, N. L. Prokopishyn, J. B. Rosenberg, D. Moratto, L. M. Muul, F. Candotti and R. Michael Blaese (2008). "Unprecedented diversity of genotypic revertants in lymphocytes of a patient with Wiskott-Aldrich syndrome." Blood **111**(10): 5064-5067.

117. Boztug, K., M. Germeshausen, I. Avedillo Díez, V. Gulacsy, J. Diestelhorst, M. Ballmaier, K. Welte, L. Maródi, L. Chernyshova and C. Klein (2008). "Multiple independent second-site mutations in two siblings with somatic mosaicism for Wiskott-Aldrich syndrome." Clin Genet **74**(1): 68-74.

118. Davis, B. R., Q. Yan, J. H. Bui, K. Felix, D. Moratto, L. M. Muul, N. L. Prokopishyn, R. M. Blaese and F. Candotti (2010). "Somatic mosaicism in the Wiskott-Aldrich syndrome: molecular and functional characterization of genotypic revertants." Clin Immunol **135**(1): 72-83.

119. Wada, T., S. H. Schurman, M. Otsu, E. K. Garabedian, H. D. Ochs, D. L. Nelson and F. Candotti (2001). "Somatic mosaicism in Wiskott--Aldrich syndrome suggests in vivo reversion by a DNA slippage mechanism." Proc Natl Acad Sci U S A **98**(15): 8697-8702.

120. Wilmut, I. (2007). "The first direct reprogramming of adult human fibroblasts." Cell Stem Cell **1**(6): 593-594.

VITA

Tamara Jatoba Laskowski was born in Rio de Janeiro, Brazil, daughter of Manoel Azevedo Jatoba and Marcia Oliveira Jatoba. She completed High School at Anglo Campinas School in the city of Americana, Brazil, and moved to Waco, Texas where she started her undergraduate studies at Baylor University in the Pre-med program. She received the degree of Bachelor of Science with a major in Biology in August of 2003. She remained at Baylor University one more semester where she took additional classes. For the next two and half years, she worked as a Research Assistant in the Department of Pediatrics and the Department of Rheumatology at The University of Texas Health Science Center at Houston Medical School. In August of 2007, she entered The University of Texas Graduate School of Biomedical Sciences at Houston where she pursued the PhD degree.